Universitetet i Stavanger

FACULTY OF SCIENCE AND TECHNOLOGY

MASTER'S THESIS

Study programme/specialisation: **MSc Petroleum Engineering/ Drilling Technology**	Spring semester, 2017 **Confidential**
Author: **Iris Sok Yee Kam**	…… (signature of author)
Programme coordinator: **n/a** Supervisor(s): **Mesfin Belayneh Agonafir**	
Title of master's thesis: **Nano-based Elastomer Swelling Agent**	
Credits: **30 ECTS**	
Keywords: **Nano-based Swelling Agent** **Swell Packer** **Nanoparticles** **Elastomer** **Nitrile** **Swelling** **TiO_2**	Number of pages: **107** + Supplemental material/other: **9** Stavanger,**14 June 2017**

Acknowledgement

The author would like to take this opportunity to thank the many people who have been involved in this entire process. From ideas brainstorming, experimental execution, Matlab modeling to the actual writing of thesis, these people have shown great help towards the author.

The first person which the author would like to show gratitude towards is Professor Mesfin Belayneh, the supervisor of this thesis work. Professor Mesfin's encouragement and dedication were unwavering despite the setbacks from early experimentations during the proof of concept stage. His keenness in taking on a new and previously unknown topic to him showed his deep devotion in the art of teaching.

The author would also like to thank the lab engineers who provided assistance during the experimentation works. In addition to that, the many friends who have provided guidance along the way from tips on software usages to verbal encouragements. Last but not least, the author would like to thank the entire staff of IPT department for providing the support needed administratively to ensure the success of this thesis.

Abstract

With multistage hydraulic fracturing and extended reach wells becoming increasingly common, the need for effective annular zonal isolation has become paramount. In such wells, swell packers are being preferred over traditional options such as mechanical packers and cementing. Significant cost savings due to reduction in rig time and all expenditures associated with cementing, perforating and coiled tubing operations have been a strong reason behind swell packers' success. However, premature expansion of these packers along with a lack of precise control of the swelling behavior have continued to be disadvantages associated with this technology.

To tackle these limitations, a novel idea was conceptualized to develop a TiO_2 nanoparticle-based trigger mechanism to activate swellable elastomers. These nano-based swelling agents (abbreviated as NSA) are designed to provide accurate control of when the downhole expansion of the swell packers is initiated, thereby, preventing problems associated with premature expansion.

Suitable nano-based swelling agents (NSA) were developed and tested with different elastomers to characterize their swelling performance. After six stages of experimentation, 4 systems were identified as the optimal combinations of elastomer and nano-based swelling agents (NSA). The extent of swelling volume and the rate of swelling were identified as key metrics in this narrowing down process. Additionally, performance of the systems under varying operational factors such as the wellbore fluid type, temperature and pH of the downhole environment were also important considerations.

The data gathered from all the experiments was then used to generate a predictive model to determine the performance for different NSA-rubber systems as a function of operating temperature and exposure time. The equations for the different systems generated was a variation of the power law form. In the final part of the thesis, a selection chart was developed to aid users in choosing the optimal nano-based swelling system depending on operational and budgetary constraints.

Table of Contents

List of Figures

List of Tables

Nomenclature

°F	Degree Fahrenheit
°C	Degree Celsius
%wt	Percentage Weight
g	grams
ΔM	Change in Mass
ΔV	Change in Volume
$\frac{d\Delta V}{dt}$	Rate of Change of Elastomer Swelling
ΔV_{ss}	Final Steady State Increase in Volume
$	Cost of Nano-based Swelling Agent

Abbreviations

ACN	Acrylonitrile
BOP	Blow Out Preventer
CNT	Carbon Nano Tubes
CoMo	Cobalt Molybdenum
CuO	Copper Oxide
ECD	Equivalent Circulating Density
EOR	Enhanced Oil Recovery
EPDM	Ethylene Propylene Diene Monomer
Fe_2O_3	Iron Oxide
HNBR	Hydrogenated Nitrile Butadiene Rubber
HP	High Pressure
HPHT	High Pressure High Temperature
HSE	Health Safety and Environment
NaOH	Sodium Hydroxide
NBR	Nitrile Butadiene Rubber
NiO	Nickel Oxide
NPT	Non-Productive Time
NSA	Nano-based Swelling Agent
OBM	Oil-based Mud
OD	Outside Diameter
PdO	Palladium Oxide
SEM	Scanning Electron Microscope
TiO_2	Titanium Dioxide
WBM	Water-based Mud
ZnO	Zinc Oxide

1 Introduction

In horizontal and extended reach wells, there has been a growing preference for the use of swell packers in lieu of traditional methods such as mechanical packers and cementing attributable to the simplicity in operations and significant cost savings. This thesis aims to provide an overview of swell packers, the current challenges with using them and subsequently, conduct experimental investigations into the potential of using nanoparticle-based swelling agents to address some of these limitations. The effects of controlling factors such as temperature, pH of wellbore fluid, concentration and costs have been analyzed to aid in the selection of an optimal solution.

1.1 Background and Research Motivation

As multi-stage fracturing, horizontal drilling and extended reach drilling have started becoming a common occurrence in several regions, the need for effective annular zonal isolation has become paramount. There are several reasons why zonal isolation is important - to prevent unwanted cross-flow from higher to lower pressure sections within reservoirs, allowing for isolation during well shut-ins and avoiding injecting fluids into unintended zones [1].

Traditionally, cementing is the natural option and has been for many decades in all types of wells. However, for unconventional reservoirs which require hydraulic fracturing (aka fracking) in horizontal wells, this would require an expensive and complex pumping system to force fracture treatments through perforations. In addition, the skin effect from cementing has been proven to be very damaging to sensitive formations and the ECD requirements in depleted zones and extended reach wells often restrict the safe application of cement [1]. This technology void was temporarily filled with the creation of open-hole packer which can be set hydraulically or mechanically downhole. However, a new set of problems sprung up in cases where the well configurations hinder the activation mechanism such as slotted liners.

Elastomers are an essential component in oilfield equipment and they exists in the form of conventional packer elements, seal stacks, O-rings and seals in BOP stack, to name a few. For the longest time in the oil and gas industry, swelling of elastomer was considered to be a disadvantage as it significantly reduced the performance of sealing elastomers used in downhole equipment where dimensional stability and material integrity were key to holding high pressures [2]. A lot of

resources and efforts had been allocated to ensure that elastomers swell as little as possible when exposed to wellbore fluids.

The increased popularity of swelling elastomers in other industries such as mining inspired the oil and gas industry to revisit the potential use of swelling rubber polymers [2]. The swell packer was invented and introduced in the early 2000s. Significant cost savings due to reduction in rig time and expenditures associated with cementing, perforating and coiled tubing operations have all been major reasons behind the swell packers' success. Swell packers have also been proven to be more effective in isolating gas and water than conventional cemented wells and is a viable option for HPHT reservoirs where it could increase the recovery factor for challenging fields [3, 4].

The mechanically simple swell packers are easy to run but they certainly have their disadvantages. Most of the commercially available swell packers require several days, even weeks for wellbore fluids to diffuse into the elastomer and cause enough swelling to sufficiently form a viable seal [1]. The duration of the swelling period is critical and must be closely monitored. The biggest risk with using swell packers is that the packer can prematurely swell resulting in a stuck pipe scenario before the lower completion string is in place causing serious well complications. Since the swelling process is typically not reversible, it leads to additional rig-time which inflates the cost. To counter this problem, certain varieties of high end swell packers contain a proprietary shell which is designed to delay the contact reaction. This, however, is a fine balancing act as the operation time will be further prolonged [2].

In certain other operations, there is an advantage to being able to delay the swelling as it buys time to allow incorporating other operations to be run during this deferment period [2]. Therefore, the ideal scenario would be the ability to run the swell packer in depth, perform other desired downhole operations without the fear of untimely swelling and when needed, initiate the swelling process which is able to provide a seal in a rapid rate.

1.2 Thesis Concept and Problem Formulation

A novel idea was conceptualized in this thesis with inspiration drawn from the work of Vinches et al. [5]. The aforementioned paper investigated the swelling of elastomeric gloves when exposed to TiO_2 colloidal solutions. The isolated swelling effect was proven to be detrimental to the functionality of protective gloves. However, in this thesis, it was recognized that this effect could be potentially valuable for initiating the swelling of reactive elastomers using targeted triggers consisting of nanoparticles. Identifying these Nano-based Swelling Agents (henceforth referred to in this work as NSA) and verifying their suitability for oilfield applications is the crux of this thesis.

Nanotechnology has created a great deal of advancements in many application areas such as biomedical, information, aerospace, pharmaceutical and many more for a significant period of time. The relevance of this technology has proven to be a game changer in the short amount of time since its introduction in the oil and gas industry [6]. The many application of nanoparticles in the energy industry are explored in further detail as part of the literature studies (Section 2.3). Nonetheless, at present, no existing literature has been found on using nanoparticles for the specific purpose of elastomer swelling for oilfield applications. Therefore, the main objective of this study is to investigate the potential behind the possible applications of NSA to initiate the swelling of oilfield elastomers. Such a swelling agent can be used to precisely determine the point in time when the swell packer will begin to expand. This would provide more control of the swelling process and therefore, address issues related to premature swelling. This work is a pivotal step towards creating an original and innovative solution to address the challenges encountered during the usage of swell packers.

The following are the research questions that this thesis aims to answer:

i. Can nanoparticle (TiO_2) based solutions be used to cause sufficient swelling of oilfield elastomers in a controlled manner?
ii. What would be the main constituents of these potential possible Nano-based Swelling Agents?
iii. What types of elastomers would the above NSAs have sufficient swelling effects on?

iv. What would be the concentrations and proportions of the ingredients that make up the NSA and how would this affect the swelling performance?
v. What is the effect of acidic or basic environment on the NSA elastomer systems?
vi. How would temperature affect the swelling process?
vii. Would the presence of oil-based mud or water-based mud affect the elastomer specimens?
viii. Is it possible to predict the swelling performance of a given elastomer-NSA system under different conditions by modelling the experimental data?
ix. What are the selection criteria and methodologies based on which an appropriate elastomer-NSA combination may be chosen from the available options in order to obtain the desired swelling performances?

1.3 Thesis Objectives

In order to plan and develop the experiments necessary to ensure proper execution of the thesis, it is important to define clear objectives which shall answer the aforementioned research questions. The objectives to be achieved are summarized below:

i. Using TiO_2 nanoparticles to create an innovative solution for controlled swelling of elastomers as well as tackle other challenges that are faced by traditional swell packer faces
ii. The new swelling system shall have reduced reaction times relative to current market options
iii. Investigate the targeted swelling capability of the NSA on different elastomers
iv. Refine the constituents or individual components of the NSA to optimize results
v. Study the effects on the systems' swelling performance caused by variations in nanoparticle solution's concentration, pH of the environment and temperature
vi. Evaluate the performance of elastomer swelling in conventional technology fluids such as OBM and WBM
vii. Examine the results from different stages to narrow down the optimal systems based on performance, efficiency and cost.
viii. Develop a predictive model using the experimental results obtained for varying temperature and exposure duration
ix. Generate a selection chart to select the most suitable NSA systems based on operational and planning requirements

1.4 Thesis Structure

There are three main parts to this thesis work. The first part is a comprehensive literature review (Chapter 2) to look at what the industry current practices are with regards to swell packers, the popular types of elastomers in use, types of nanoparticles and the application of nanoparticles in the industry and elsewhere.

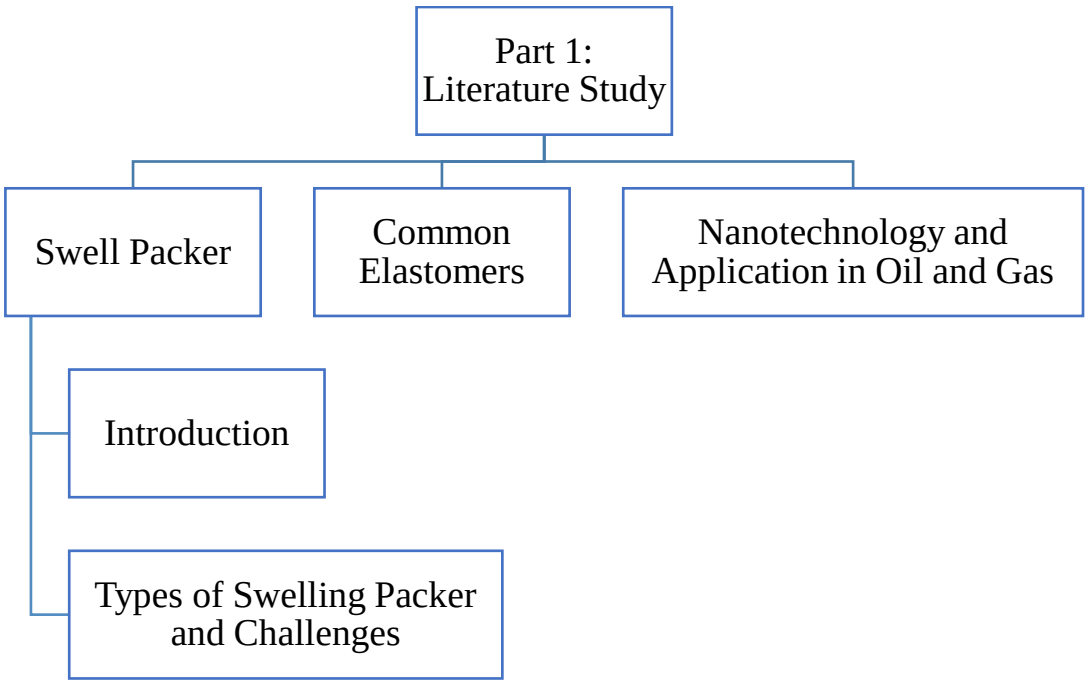

Figure 1-1: Part 1 of literature review structure breakdown

The second part of the thesis delves into the experimental work with the aim of reaching conclusions on the potential swelling capability of elastomers when triggered by Nano-based Swelling Agent (NSA). This part spans across Chapter 3 and 4 of this thesis. The experiments in part two are divided into different stages with each stage addressing a vital component of the optimization process. The different stages serve as performance evaluation rounds to identify the NSA systems and elastomers which yield the best results. The evaluation criteria for the best systems are primarily based on the final swelling volume, rate of swelling, cost involved and functionality in different operating environments.

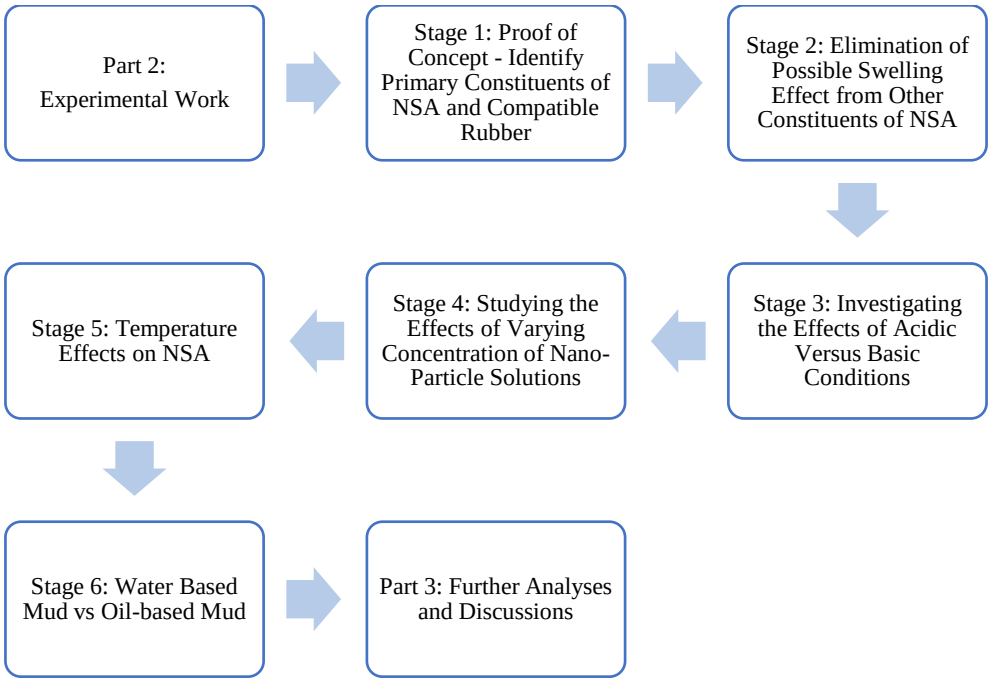

Figure 1-2: Experimental work structure breakdown for part 2

The last part of this thesis attempts to develop a predictive model using regression methods based on the experimental data. The third part also includes development of a NSA system selection chart to aid users in choosing the optimal swelling solution for their operational needs as well as cost considerations.

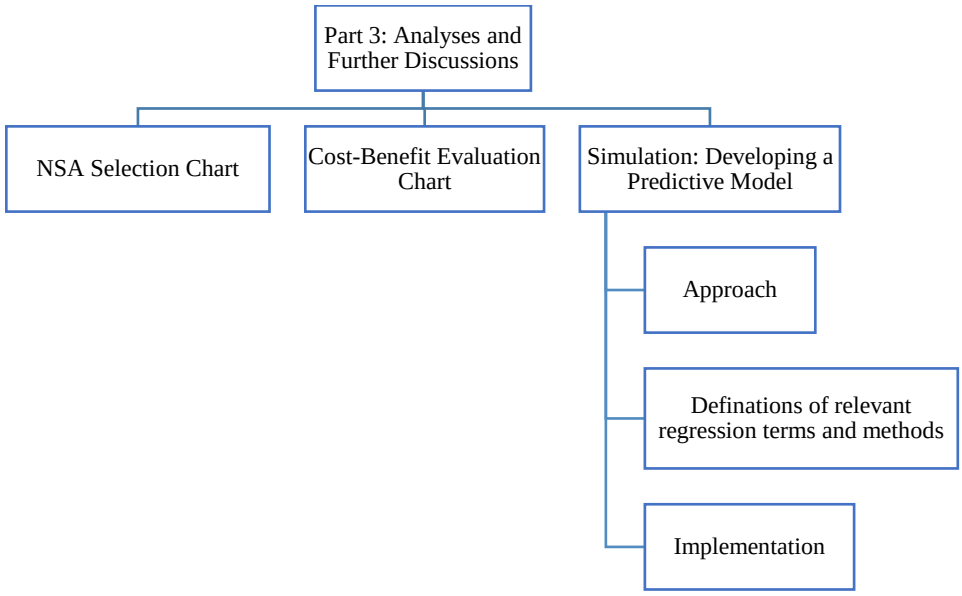

Figure 1-3: Structural breakdown of part 3

2 Literature Study

It is imperative to have a strong understanding of the basic workings of the topic of interest before proceeding to the core experimental investigation and results. In this section, the swell packer technology is examined closely including introduction, types and current industry practices. In addition, various applications of nanoparticles in oil and gas industry are also discussed along with the benefits and challenges.

2.1 Swell Packer

2.1.1 Introduction

Annular isolation is more important than ever as the world competes with longer and deeper well drilling and completions. New age swelling packers which require no activation mechanism and based only on elastomer swelling have been gaining popularity amongst operators to replace the traditional open hole packer as well as cementing due to the ever increasing demand for higher production of hydrocarbons and the need to reduce cost [3, 7]. Swell packers are capable of providing critical zonal isolation to avoid the challenges associated with cementing and placement as it has proven to be difficult to qualify, and measure the success of any cement job [3]. Other potential issues such as the pump-ability due to immediate hydration process beginning for the cement slurry as well as the need to protect the well while waiting on cement can also be avoided [8]. In some well cases, using cement could even compromise the entire completion operation as cement filtrate would result in irreversible formation damage [9].

Not having proper zonal isolation translates to lacking the ability to control each zonal flow independently. This could lead to problems such as loss of productivity, sand production and unintended gas migration resulting in expensive remedial actions [7]. For operations such as hydraulic fracturing, a regular and common occurrence for most wells these day, a good zonal isolation is vital for well success as it inhibits mechanical issues which includes potential casing collapse. Casing collapse is regarded as one of the worst well bore problems with very limited remedial actions available. It leads to expensive non-productive down time and hence should be avoided at all cost.

The open-hole traditional packer was once a very popular choice in completion when cementing is simply not deployable. However, as well's trajectory became more complicated, the setting mechanism for conventional packers proves to be problematic as it typically requires a tubing to run the tool in position or a separate tool for hydraulic activation to set. The packer setting process for an extended horizontal well would involve multiple trips in and out of the well which would add to the rig time extremely unfavorably.

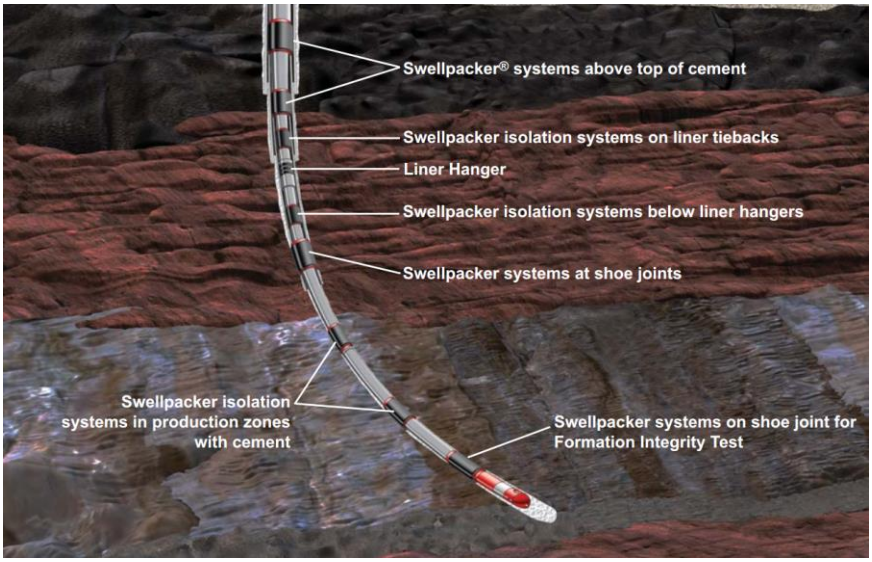

Figure 2-1: Typical well schematic for operations involving the use of swell packers [10]

Swell packers are usually run in tandem with other operational tools as seen in Figure 2-2, where the swell packers were used in a multistage stimulation service which increases efficiency in extended reach lateral wells. Figure 2-1 and Figure 2-2 illustrate the typical positioning of swell packers in different operation's purposes.

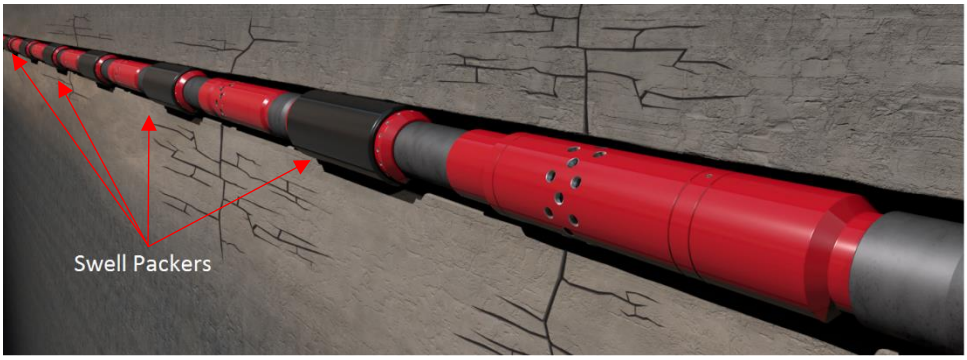

Figure 2-2: Close-up depiction of swell packer used in an unconventional completion operation [11]

The swell packer comes in the form of simple mechanism with no moving parts, it requires no running tools, no special trip and negates the need of a specialized trained personnel to be presence [7]. It simply swells when in contact with a fluid medium and eliminates complicated operation sequences which quantifies into cost savings due to reduced rig time as well as material. A typical swell packer can be of any length or diameter and it is designed to be modular with layered of rubber bonded and cured around a joint of tubing.

Figure 2-3: Typical Swell Packer [12]

One of the benefits swell packer has over conventional external open hole packer is the maximum OD of the tool. This smaller profile allows a wider range of drift and tools can be run at higher speed with significantly lesser risk of surge and swab effects [2]. This also means the tools can pass through much tighter restrictions without the worries of a well hang-up. The tradeoff between the run in clearance and swelling capability should be cautiously considered with regards to the OD selection for the tool. Large OD will risk tight run in clearance and small OD risks sealing effectiveness [7]. The base pipe diameter of the packer also known as the packer mandrel is often chosen to replicate the mechanical properties such as tensile, yield strength and the threaded connection of the liner string used for the well [7]. This ensures the weak point will never be at the swell packer during operations. The simple yet robust build of this packer also allows customization for intelligent completion solutions - the spliceless cable feed-through option is a popular option for intelligent well completion [9].

Other advantages of using swell packer includes its ability to adapt to any type of borehole and form an effective seal regardless of borehole eccentricity. This feature is especially important for long horizontal wells as decentralized tools during cementing operations can lead to a poor cement job done which ultimately results in failed isolation [13]. Conventional compression set packer are also not an ideal solution in this scenario as it can run into difficulties while trying to seal off non-centered or irregular boreholes.

The lower running friction for swell packer during trip in equates to shorter operation time [9]. Not only do traditional set packers take longer to run in hole, care also has to be taken not to damage any packing elements on these packer during run in as it affects the pressure sealing capability. The swell packer has the ability to repair any scratched surface on the element package, molds and seals itself onto any surface including tubulars which suffers from corrosion, an unwanted side effect of production [2]. Each of these principal advantages and unique characteristics of swell packer are important in ensuring an overall reduction in well costs and increase of the uptime.

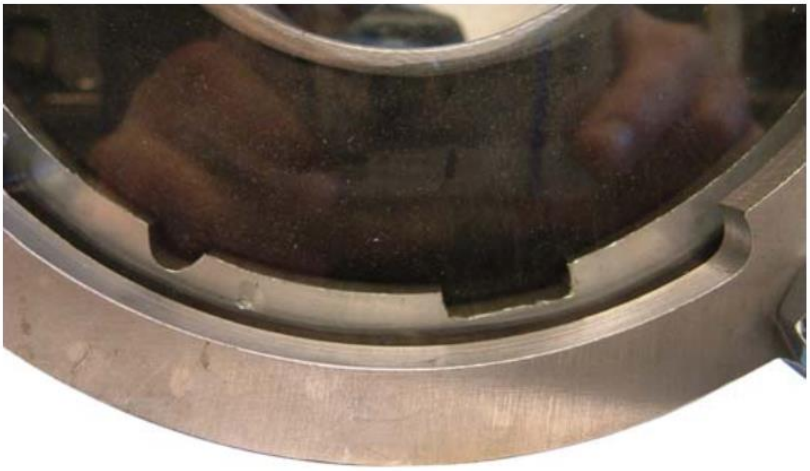

Figure 2-4: A picture showing the swelling rubber forming a pressure seal with a variety of geometry shaped containers (groves and rectangular cut out) [2]

The length of a swell packer is typically governed only by the length of a casing joint due to the limitation of handling equipment on the rig floor. This length allowance tips the advantage scale further towards swell packer over traditional packers as the longer sealing packer statistically has a better chance at landing correctly in the pre-planned section of the hole which increases the isolation effectiveness [7]. As the purpose of a well typically changes throughout the lifetime -

such as converting from production to injection well - the borehole conditions could alter as a result. The use of swellable packers negates potential problems due to these dynamic borehole conditions.

Traditional packers which seal through compression sets or zonal isolation from cements could come undone while the swell packer has the capability to reseal the annulus with its ability to autonomously swell multiple times as long as the activation fluid is present [2]. This one of a kind feature of swell packer is crucial in preventing casing collapse in fracturing operation where frac pressure coupled with fluid hydrostatic pressure often exceeds the safety margin of casing yield strength [9].

Extensive research and testing has been done on the expansion properties of swellable packer technology in order to accurately predict the expansion ratio, differential pressure sealing capability and the swelling time taken for effective annulus sealing for any given OD of a packer element [3]. This allows for correct sizing of tool to minimize unwanted down time and concerns for any risk events such as surging, torque and drag can be correctly modeled. Its proven track record in the many case studies available has documented significant cost savings and success in highly laminated and complex reservoirs [2, 3]. In summary, although swelling packer technology is relatively new in the oil and gas industry, the applications are far and wide reaching. This includes stimulation placement, replacing cementing and perforation, smart wells, open and closed hole straddles, water control, multi-lateral wells as well as expandables [9].

2.1.2 Types of Swell Packer

There are two kinds of swell packer currently in existence in the industry - an oil-based fluid reactive rubber and a water-based fluid reactive rubber. Oil-based rubber can be either man-made or naturally occurring whereas water-based reactive rubber is man-made only. The most common type of reacting solution is hydrocarbon in liquid form for the oil-based rubber and the mechanism is determined by interactions at a molecular level between the rubber polymer and swelling media [2]. This is a thermodynamic absorption time-dependent process where the molecules stretch to allow the hydrocarbon to enter the structure [3]. When polymers are submerged into a medium with a solubility parameter which is close to the polymer’s own solubility parameter, there exists

a strong affinity between the two and coupled with the flexible network of polymer, results in swelling [14].

Water-based rubber swells through a process called osmosis, which allows the rubber to expand under certain conditions and reversible under specific conditions [2]. The swelling of rubber alters certain mechanical properties negatively such as tear strength, hardness and tensile but it does not degrade the structural integrity. It instead could positively improve other properties such as resilience, low temperature properties as well as sealing pressure [14]. The presence of any contamination in fluids for traditional swell packers can severely alter the effect of the swelling rate for the worst. In water-based completion, various salts which can be added to the drilling fluid or naturally occurring in the well could negatively affect the rate of swelling to a point where the tool can be deemed ineffective [7]. Lighter oil tends to activate the swelling faster than heavier oil for oil-based rubber and certain fluids may even allow a higher percentage swelling rate compared to others. Care has to be taken in swelling fluid selection to ensure proper sealing of the annulus.

A tiny amount of hydrocarbons exposure is sufficient to initiate the thermodynamic absorption swelling process [15]. Therefore depending on the downhole conditions, different layering system of rubbers is used in the manufacturing process to ensure the operation runs as smoothly as possible since premature swelling could result in non-productive time on well site. For example in oil-based drilling fluid system, a packer with multi-layered elastomer bonding is used to deter the early onset swelling of the packer while it is being run to depth. A high swelling inner core surrounded by a low swelling outer layer along with a diffusive barrier is used to delay the onset of swelling by 72 hours or more [3, 15]. On the other hand in a water-based drilling fluid system, the most common type of swell packer is a single layer of rubber bonded simply around the tubular as the accidental swelling could be reversed due to osmosis process and therefore not as dire as oil-based swell packer. Although the water reactive swell packer's reaction can be reversed under specific condition, it would still incur unnecessary cost and unwanted downtime. As the activation fluids for both types of swell packer are widely accessible on site as well as down in well bore, the operation sequence has to include clean up trips prior to run in and allocate quarantine zones on site to isolate the packers from possible contamination.

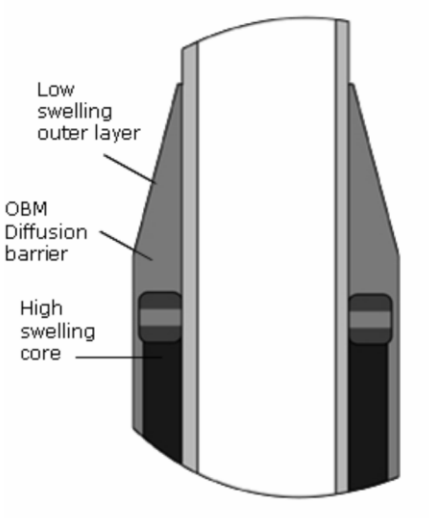

Figure 2-5: Oil-based fluid reactive packer [3]

As the swelling rate is dependent on the type of elastomer used, bottom hole temperatures and the viscosity of the activation fluids, it is a delicate balance effort to delay the swelling time just enough to accomplish all operations but not cause too much delay to the production [2]. Another challenge also lies in finding the right combination of chemicals and thermal ageing stability with the appropriate elastomer of choice in order to optimize the mechanical properties in both pre-swollen and swollen stage [14]. In some cases, the swelling time required for an effective seal can be as much as 5 to 100 days depending on the swell packer used [9, 16]. With such a large range of activation time, most operators try to plan the operation sequences to utilize this swelling time for other tasks as much as possible.

2.2 Types of Common Elastomer Used in Oil and Gas Industry

According to Bellarby's book on Well Completion Design [17], elastomers are long chained cross-linked polymers that can be easily deformed but virtually incompressible. They can be divided into two groups, thermoplastics (partially crystalline) and thermosetting plastics (cross-linked by curing). Thermoplastics soften and melt when exposed to high temperature while thermosetting plastics such as epoxy resins characteristically decompose at high temperature [17]. Elastomers matrix which have a tendency to swell when exposed to fuel are basically a complex mixtures of

polymers, antioxidants, curing agents, fillers, oil, plasticizer, antizonants, stabilizers and processing aids [18]. In this section, some of the most commonly used elastomer or rubber in traditional packer and swell packer will be discussed.

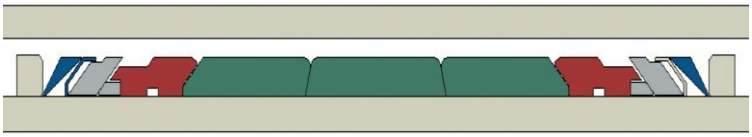

Figure 2-6: Common configuration of a packer's element

The swell packer elements, as mentioned in previous section, are rather simple compared to the traditional packer's element. Figure 2-6 above shows the typical configurations of the element system in a conventional packer. The element system can consist of elastomers of different types which forms an annular seal when activated through compression delivered in the form of hydraulics or mechanically. Some of the more sophisticated element system in high end packer's technology will have multiple back-up systems made of stronger rubbers to prevent possible extrusion or it can be made of metal support as well depending on the operational needs. The choice of elastomer in both swell packer and traditional packer can be customized based on well service requirement as well as budget allocation as some options are more expensive than others.

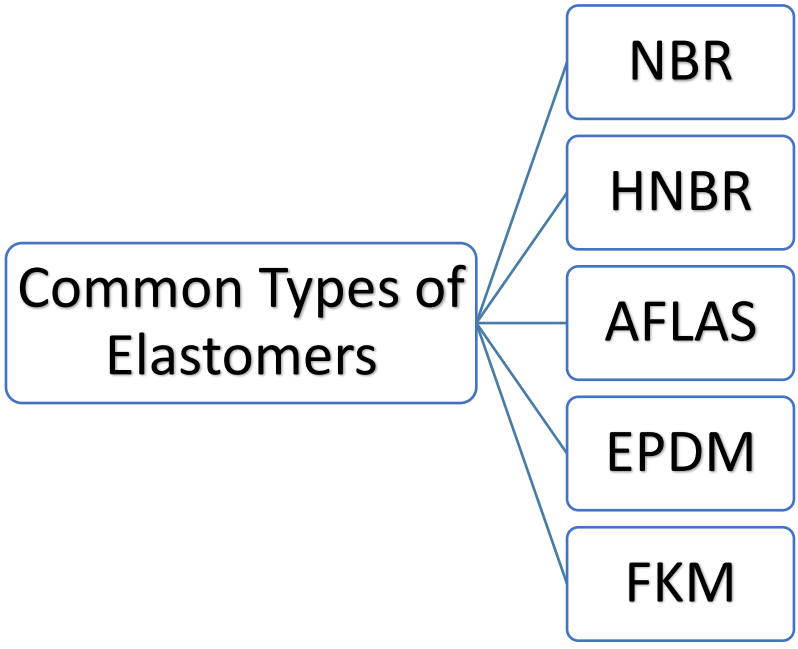

Figure 2-7: List of commonly used elastomers in oil and gas packer products

NBR or nitrile butadiene rubber is a complex family of unsaturated copolymers of acrylonitrile (ACN) and butadiene which generally has a good resistance towards oil and has low gas permeability [19]. The higher acrylonitrile content in NBR, the lower percentage of swelling it will experience in fuels as the crosslinks in polymer backbone increases [18]. The higher amount of acrylonitrile content also helps with influencing properties such as solvent resistance, increasing tensile strength and hardness [20]. NBR is the oldest and most common material in oil and gas applications such as blow out preventers, packers and seals [21]. It is also found quite often used as O-rings in fuels application due to its resistance to swell [22]. A typical nitrile rubber O-ring has approximately 30% acrylonitrile. Butadiene is largely nonpolar and is held together by weak van der Waals forces whereas acrylonitrile are attracted to each other by strong dipole-dipole bonds [23]. This unique characteristic is the reason behind NBR's softness and malleability (due to butadiene) and lack of reaction with fuels (acrylonitrile). For the reasons above, while researching for topic of interests the paper on investigating the swelling effects on NBR gloves with nanoparticles really stood out amongst other potentials and inspired the following thesis work as NBR is such a versatile and inexpensive seal material.

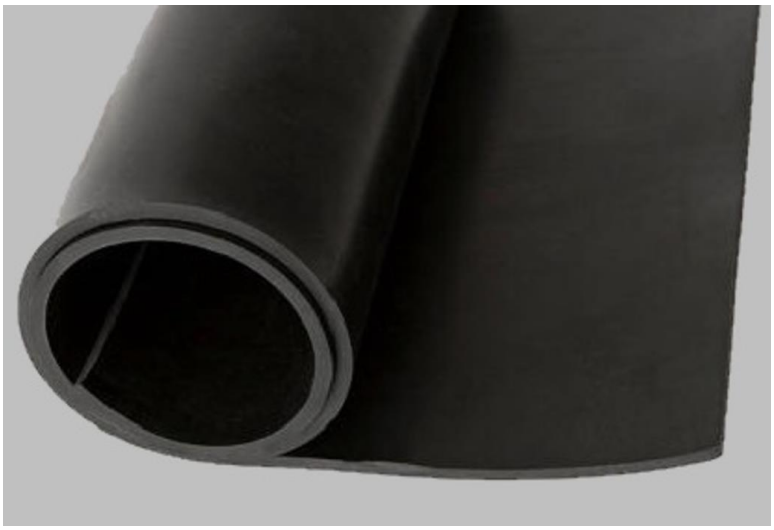

Figure 2-8: Typical NBR sheets [24]

Hydrogenated nitrile butadiene rubber or better known as HNBR is also a common choice for the use in packer's element due to its improved properties from regular NBR. The reason behind the increased temperature range and ozone resistance comes from selective hydrogenation of butadiene group in the NBR family [21]. Although both NBR and HNBR are thermosets with

similar chemical properties, HNBR has a superior wear and tear resistance as well as more compatible in sour service, making it the obvious choice in wells which required higher temperature rating and sour well service grade even though it is more expensive than NBR. However, HNBR has been proven in development tests to be more prone to extrusions than NBR and hence need a more advance element back-up systems when used as packer elements. Extrusions are a bad phenomenon during the setting of tool as it means the structure of elastomer is not stable and could risk leaks in the seals formed.

AFLAS is the trade name for copolymer of tetraflouroethylene and propylene which has good oil sealing capability at high temperature up to 400°F but not at lower temperature. It is also known to have excellent chemical resistance to a wide range of aggressive reactant which makes it a perfect choice for HPHT scenarios. Though this elastomer is often chosen when high temperature service range is required, care should be taken as certain operations during the life cycle of a well such as water injection could push the well environment into lower temperature and render this elastomer useless in sealing.

Ethylene propylene diene monomer or more commonly known as EPDM is created when a non-conjugated diene is grafted onto the main polymer chain EPM [21]. This material has superior resistance to water, steam, glycol, alcohols, similar polar fluids and most importantly electrical. This unique properties of EPDM is extremely useful in high voltage cable covers which sometimes is part of the packer's component in intelligent well operations. The temperature service range of EPDM is lower than of AFLAS and HNBR and it is considered to be a poor seal in the presence of hydrocarbon.

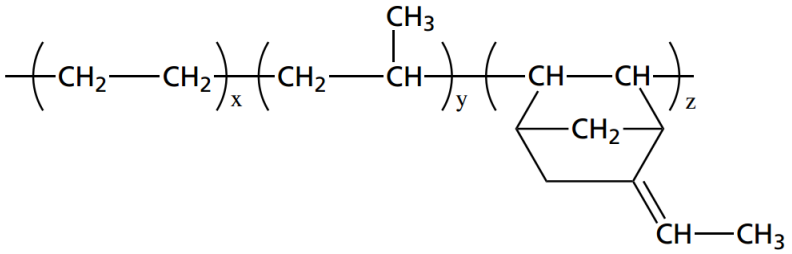

Figure 2-9: Chemical structure of EPDM [21]

FKM or fluorocarbon rubber is more known under its trade name, Viton. Just like AFLAS rubber, FKM also has excellent high temperature resistance which can be distinguish from other rubbers by its green or brown colour. It is more often used in o-rings material rather than packer's element due to its poor extrusion resistance which is an important characteristic to have to ensure good annular isolation [17]. FKM has a unique feature in that when exposed to flames, it has the ability to self-extinguish while other elastomers have the tendency to burn totally out of control until the source is removed. This is a huge plus point for HSE considerations in well planning and executions especially for critical barrier tools such as BOP and X-mas trees. Nevertheless, certain chemicals should be used with caution when in the presence of FKM such as amines and alkalis as the elastomer tends to harden, embrittle and can even crack at very high temperature [21].

2.3 Nanotechnology and Application in the Oil and Gas Industry

Nanotechnology has been around for many years and while many initially thought it is only a hype which would eventually peter out, recent innovations and developments on more ways nanotechnology inclusion can improve products and processes have brought about a revolution. With the rapid progression of nanoscience, it is rather curious that there exists many available definition of a nanomaterial [25]. However, the general consensus of nanotechnology is that it represents the development and application of materials, process, and devices in which the nanomaterial critical length is between 1 to 100nm [6].

Many of the modern technologies such as chlorine free refrigeration, cancer treating medication, high strength polymers etc. would not be possible without the existence of nano-catalysts. The majority of these industrial catalysts which are fundamental to the processes are high surface area solids onto which an active component is disseminated in the form of very fine particles. These particles are more commonly known as nanoparticles [26]. The difference between bulk materials and nanoparticles are the number of atoms at the surface of the material. Important properties such as thermal resistance, optical behavior, chemical and physical activities are modified whenever the size of a particle is reduced close to the standard wavelength of conducting electrons. This change is due to the extreme increase in surface to volume ratio which renders the number of atoms at the surface of the material more significant when compared to the average bulk [27].

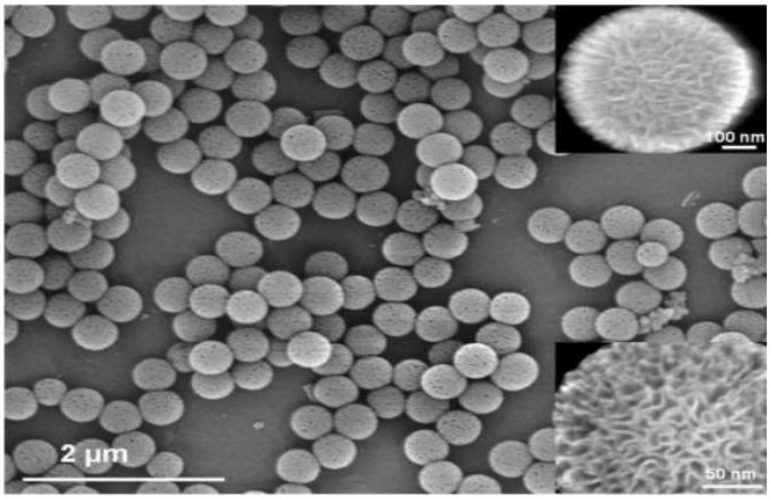

Figure 2-10: Nanosilica image from Scanning Electron Microscopy [28]

Since the initial discovery of nanoparticles, the types of nanoparticles available have multiplied exponentially with the invention of more synthesis techniques. They range from the typical graphene, which is a thin layer of hexagonal carbon structure to carbon nano-tubes (CNT) and nanosilica, as well as metallic nanoparticles such as alumina, nickel, cobalt. In an effort to narrow down the many nanoparticle options available and stay true to the work of Vinches et al. [5] which inspired this thesis work, TiO_2 nanoparticles shall be the main constituent of interest for this thesis. However, to appreciate the role of nanotechnology in several industries including oil and gas, a brief summary of their applications is featured below.

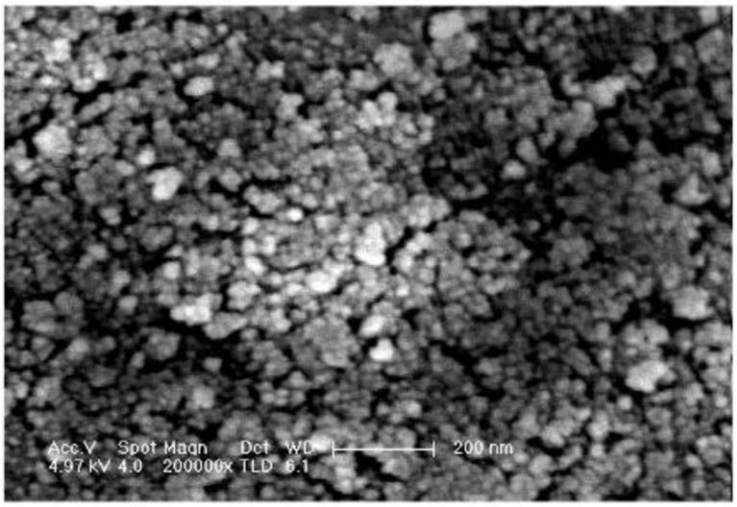

Figure 2-11: Pure TiO2 nanoparticles [29]

Typical Application of Nanotechnology in Oil and Gas Industry

With the constant increase in demand for fossil fuels and new energy resources to feed the global energy consumption, scientists are forced to look at new classes of materials such as nanoparticles to solve many current challenges within the industry [30]. Development of nanotechnology has allowed fabrication of various unique materials and tools which have important ramifications for fields of aerospace, medical, manufacturing, electronics and etc. [31, 32].

There are different challenges which lie in the petroleum lifecycle from as early as reservoir mapping in exploration stage to drilling operations, completing the well, managing the reservoir as well as post production processes such as refining. Exploration activity is considered a high-risk and expensive process as each site is unique with unexpected terrain and geology. Drilling provides critical access to reservoir and hence, it is crucial to optimize drilling with as little reservoir damage as possible to ensure high recovery factors.

The next stages, cementation and completion are often credited with ensuring well integrity for the entire life of the well. As exploration shifts to unconventional wells such as shale and heavy oil, production and methods of recovery have to be improvised as the traditional options no longer suffice. The earliest applications of nanoscience in the industry which is still ongoing is in downstream refinery practices where nano-based catalysts are a common sight. The table below summarizes the contributions of nanotechnology at the different stages ranging from detecting cruel oil to usable consumables.

Exploration	• Nano-based sensor as reservoir probes to gain valuable information and solve complex structure to reduce risky operations [30]. • Metallic nanoparticles used to aid geochemical exploration in delineating ore deposition [33]. • Applying magnetic nanoparticles for high resolution reservoir mapping with electromagnetic characterization [34].
Drilling	• Coating drilling equipment with special nanoparticles to ensure better resistance for corrosion and wear [27]. • Reducing fluid loss to formation and formation damages to as high as 56% during drilling with nanosilica [35]. • Improving fluid rheology, electrical as well as thermal properties with CuO and ZnO nanoparticles when used along with xanthan gum for WBM in HPHT scenario [36].
Cementing and Completion	• Several metal oxide nanoparticles such as TiO_2, Fe_2O_3, CuO and etc. are added to cement slurry to improve crucial properties such as strength, water penetration prevention and hydration reaction control [30]. • Multi-walled carbon nano-tubes have proven to help in areas such as impact toughness, durability and permeability resistance [37]. • Improved elastomer by combining nanoparticles with existing rubber materials to use in downhole tools for HPHT reservoir conditions [38].
Reservoir Management	• Nanosilica helped to stabilize formation with CO_2 foam injection for EOR process which aid in improvement of oil production [39]. • Nanomembranes are able to improve sand exclusion and increase the mobility of injectant [27]. • Nano-catalyst with iron oxide are used for in-situ aquathermolysis in order to improve the quality and productivity of heavy oil [40].
Production	• Nano-catalysts such as Nickel nanoparticles are capable of reducing the viscosity of heavy oil which eases production [41].

	• Hydraulic fracturing fluid with the addition of nanoparticles are able to develop better filter cake on the face of porous media to increase fluid loss resistance [30].
Refining	• Metal oxide nanoparticles such as NiO and PdO along with nanosilica used in hydrocarbon processing which helps in lowering the reaction activation energy [30]. • CoMo with multi-walled carbon nano-tubes are able to perform the desulfurization process better than just pure CoMo catalyst [42].

Table 2-1: Summary of nanoparticle applications in oil and gas industry

Seeing the many benefits nanoparticles has brought to several applications in oil and gas, the current investigation aims to explore the potential advantages of nanoparticle-triggered swell packer systems. The eventual goal is to create a nano-based swelling agent (NSA) which provides superior performance and better control compared to existing swell packer systems.

3 Experimental Work

The swelling effect of TiO_2 nanoparticles on protective gloves was considered a negative phenomenon by Vinches et al. [5]. In order to transform this into a positive effect for the swell packer application, different elastomer candidates have been examined to determine the viability of inducing elastomer swelling due to TiO_2 nanoparticles. Since nitrile rubbers gloves had experienced the largest amount of swelling with the TiO_2 nanoparticles-based colloidal solutions in [5], industrial grade base elastomers with no additional additives were used as the starting point in the following experimental study.

The heart of this experimental work lies within understanding the properties of nano-based swelling agent (NSA) and identifying the factors that affect their performance. Several NSA solutions were explored and options were refined during subsequent stages of the investigation to obtain the best possible swelling system. The elastomers and the NSA chosen for the experimental investigation are detailed in sections 3.1.1 and 3.1.2 respectively.

3.1 Materials Used

3.1.1 Elastomers Specimen

For the main study, five different types of elastomers were acquired from Scientific Polymer Product Inc., USA. The elastomers were used straight out of the packaging without any further modification.

As previously mentioned in Section 2.2, with the increase in acrylonitrile content, properties such as tensile strength, hardness, heat and abrasion resistance also increase. Therefore, elastomers with different ranges of acrylonitrile contents were used to compare the possible swelling reactive outcomes [21]. In addition, Styrene and Butadiene copolymer was also ordered due to the close relationship between SBR and NBR have.

The elastomers ordered have been tabulated below along with their CAS and CAT numbers for reference. The elastomers ordered came in the form of slabs and were cut and prepared into smaller

pieces in order to fit into the containers used for experiments which will be discussed further in following sections.

	Elastomer Specimen Abbreviation	Elastomer Specimen Full Name	CAS Number	CAT Number
1	21ACN	21% Acrylonitrile/Butadiene copolymer	9003-18-3	523
2	31ACN	31% Acrylonitrile/Butadiene copolymer	9003-18-3	055
3	41ACN	41% Acrylonitrile/Butadiene copolymer	9003-18-3	532
4	5STY	5% Styrene/Butadiene copolymer with 1.25% stabilizer added	9003-55-8	199
5	45STY	45% Styrene/Butadiene copolymer with 1.25% stabilizer added	9003-55-8	201

Table 3-1: Elastomer List

Figure 3-1: 21ACN elastomer

Figure 3-2: 31ACN elastomer

Figure 3-3: 41ACN elastomer

Figure 3-4: 5STY elastomer

Figure 3-5: 45STY elastomer

3.1.2 NSA Constituents

The most important material used in the experimental work are the Nano-based Swelling Agents (NSA). The basic properties of the important elements used in the NSA shall be broken down in this sub section. The NSA comprises of 3 main parts:

NSA = Primary Constituent (Constituent A) + Nanoparticle Solution (Constituent B) + Emulsifier (Constituent C)

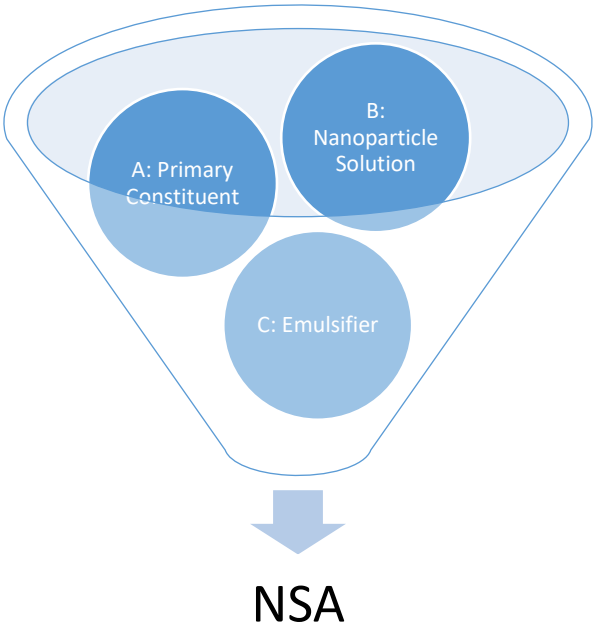

Figure 3-6: The 3 main parts of the nano-based swelling agent

A: Primary Constituent

Table 3-2 summarizes the properties for the possible candidates for primary constituents in NSA mixtures.

	Acetone	Heptane	Toluene	Xylene
Boiling Point	56.05°C	98.38°C	111°C	139.5°C
Melting Point	-94.7°C	-90.549°C	-95°C	-47.4°C
Chemical Formula	$(CH_3)_2CO$	C_7H_{16}	C_7H_8	C_8H_{10}
Typical Application	Typically used in different cleaning purposes. Good solvent for plastics.	Used in laboratories as non-polar solvent	Typically used as solvent for paints and industrial feedstock.	Common component in ink, rubber, also used in leather industry
Miscibility with water	Yes	0.0003% only	0.52g/L	No
Appearance and Odor	Colourless liquid with a pungent and irritating smell	Colourless liquid with a petrolic smell	Colourless liquid with paint thinners smell	Colourless and slightly greasy liquid and sweet smelling

Table 3-2: Properties summary for primary constituents

B: Nanoparticle Solution

As the name NSA suggests, nanoparticle is one of the main elements and it serves as a catalyst for this research work. Anatase Titanium Oxide (TiO_2) dispersed in water (Stock number: 7011WJWA, CAS: 1317-70-0) was purchased from the company Nanostructured & Amorphous Materials Inc., USA to mimic the type used in the paper which inspired this thesis. The nanoparticles are between the sizes 5nm to 30nm with a naturally occurring pH of 1 to 5. It has a milky white translucent colour.

The concentration ordered was 15wt%. It was important to have a clear definition of concentration since different sources have varied explanations. It is imperative the same method as the original solution is used for the dilution needed in subsequent experiments. In some context, the concentration of a dispersed solution is defined as weight of the solid to be dispersed divided by

the total weight of the solution after dispersion. After clarifying with the company which manufactured the solution, they define concentration as total weight of the solid (in this case the TiO_2 nanoparticle powder) divided by the total weight of the dispersant (water) before mixture. This calculation method will hence be used in all experiments to ensure consistency when diluting solution to achieve different concentration is required.

$$\%\, Wt.Concentration = \frac{Total\ weight\ of\ TiO_2\ (gms)}{Total\ Weight\ of\ the\ solvent, water\ (gms)} x\ 100$$

C: Emulsifier

An emulsifier is a substance which can stabilize an emulsion when added. An emulsion refers to a mixture of two or more liquids which generally are not mixable when combined. In the nano-based swelling agent, some of the primary constituent used are not soluble in water as indicated in Table 3-2 and since the nanoparticle solutions used in this case is a water dispersed solution, an emulsifier is required to bind the two. The emulsifier used in all experiments is ONE-MUL which is a liquid emulsifier commonly used in drilling fluids.

3.1.3 Oil-based Mud and Water-based Mud

In stage 6 of the experiment (Section 3.3.6), the correlation of the swelling effect of OBM and WBM on elastomers was investigated. The constituents of the oil-based mud (OBM) and water-based mud (WBM) used in this experiment are tabulated below.

Oil-based Mud (500ml)	Water Based Mud (500ml)
• Base oil - 221.55g • Emulsifier (One Mul) - 12.5g • Clay - 3.5g • Alkalinity - 12.5g • Filter Loss Control - 5g • Fresh Water - 68.2g • Salt - 21g • Barite - 530.57g	• Bentonite - 25g • Fresh Water - 475g

Figure 3-7: Ingredients list for OBM and WBM

The Hamilton Beach mixer was used to combine all the ingredients as listed in Figure 3-7 for OBM and WBM in the laboratory. The blending process was done in batches until the solutions were rid of any presence of chunks and a homogeneous solution was achieved. Gloves were used to ensure safe handling and any extra solutions were disposed at the designated area.

Figure 3-8: Hamilton Beach mixers used in the making of OBM and WBM

3.2 Methods of Measurement

- Change in Mass

  The elastomer specimens was prepared and weighed in air and the reading was recorded as M_1 in grams. Specimen was then immersed into glass tube containing reactive NSA solution for a specified amount of time. After specified durations, elastomer specimen was retrieved from the solution and rinsed using distilled water to ensure no external precipitation contributes to the weight measurement. Specimen was then patted dry using laboratory napkins before it was weighed again. The result is recorded as M_2 in grams. The percentage mass change is then calculated with the following formula:

$$\Delta M, \% \, Swell = \frac{M_2 - M_1}{M_1} \, x \, 100$$

- Change in Volume

  Elastomer specimen was cut into cuboid forms and measured using a digital vernier caliper for accuracy. The three different lengths were recorded as L_1, L_2 and L_3 in mm. Specimen was then immersed into glass tube containing reactive solution for a specified amount of time. After the stated time was up, specimen was retrieved from the solution and rinsed with distilled water and dried using laboratory paper towel. Specimen dimensions were again measured carefully to ensure no pressure is exerted on the elastomer which could alter or affect the reading. The readings were recorded as L_4, L_5, L_6 in the millimeters.

Figure 3-9: Digital Vernier caliper used for dimensional measurement

The total volume change or percentage of swelling is calculated with the following formula:

$$\Delta V, \%\, Swell = \frac{(L_4\ x\ L_5\ x\ L_6) - (L_1\ x\ L_2\ x\ L_3)}{L_1\ x\ L_2\ x\ L_3}\ x\ 100$$

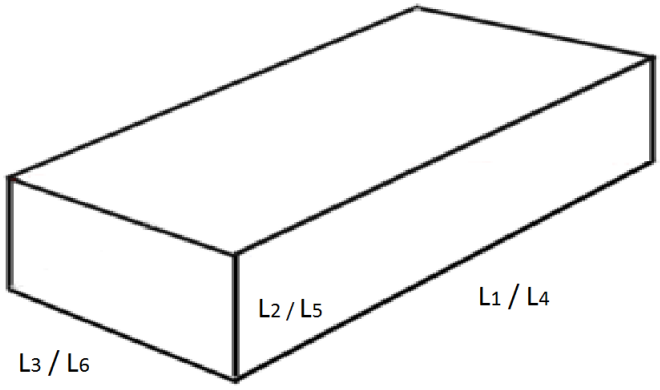

Figure 3-10: An example of how the measurement was done on the cuboid where L1, L2, and L3 are measurements before and L4, L5 and L6 are measurements after

3.3 Experimental Procedures

This section will discuss the methods that were used during the entire experimental planning and execution of the thesis. The experiments were broken down into six different stages. Different experiments were conducted in a multitude of laboratories in University of Stavanger (UiS) in order to determine the effect of different parameters as listed in the objectives on the swelling of elastomer.

The methods of measurement were adopted from ASTM D471, which is a standard test method for rubber properties. This standard provides procedures for exposing elastomer specimens to test liquids under defined conditions of temperature and time. The changes in physical properties were measured with methods such as changes in mass, volume and dimensions as described in the previous section.

The exposure time can also be varied to be continuous or intermittent in order to simulate realistic downhole conditions. The recommended testing period per ASTM D471 is 24 hours, 168 hours or 672 hours. Due to time limitation, 24 hours was the most ideal option for this experimental work. Specimen changes were charted in hourly intervals to quantify the different rate of change among the reactive solutions, if any. In some procedures, the experiments were allowed to run to the point where the specimens no longer have any reaction with the solutions and were deemed to have achieved a stable equilibrium condition. Glass tubes with caps were used to contain the specimens to avoid any possible reaction between the container and solutions. When possible, specimens were kept in a condition devoid of light as per ASTM D471 recommendation.

One of the goals of this work was to identify the best system in which the swelling of the elastomer is the greatest. With this in mind, the experiment methodologies were planned such that the systems displaying promising results were selected for further testing in subsequent stages whereas those systems with poor results were eliminated at the end each stage. This allowed for a more focused approach in gradually narrowing down to the optimal systems while efficiently managing time and resources.

3.3.1 Stage 1: Proof of Concept – Identification of Primary NSA Constituents and Compatible Rubbers

In this initial stage, all five of the elastomers, 21ACN, 31ACN, 41ACN, 5STY and 45STY were first subjected to solutions with different stand-alone primary constituents and a mixture of primary constituents with TiO_2 nanoparticles catalyst in order to examine the individual swelling effect. The elastomers were tested in controlled room temperature of 16°C. The nanoparticles solution used in this stage was 15 wt% Anatase Titanium Oxide in water. The measurements for all elastomers were taken once every hour for 7 hours and also at the 24 hour mark.

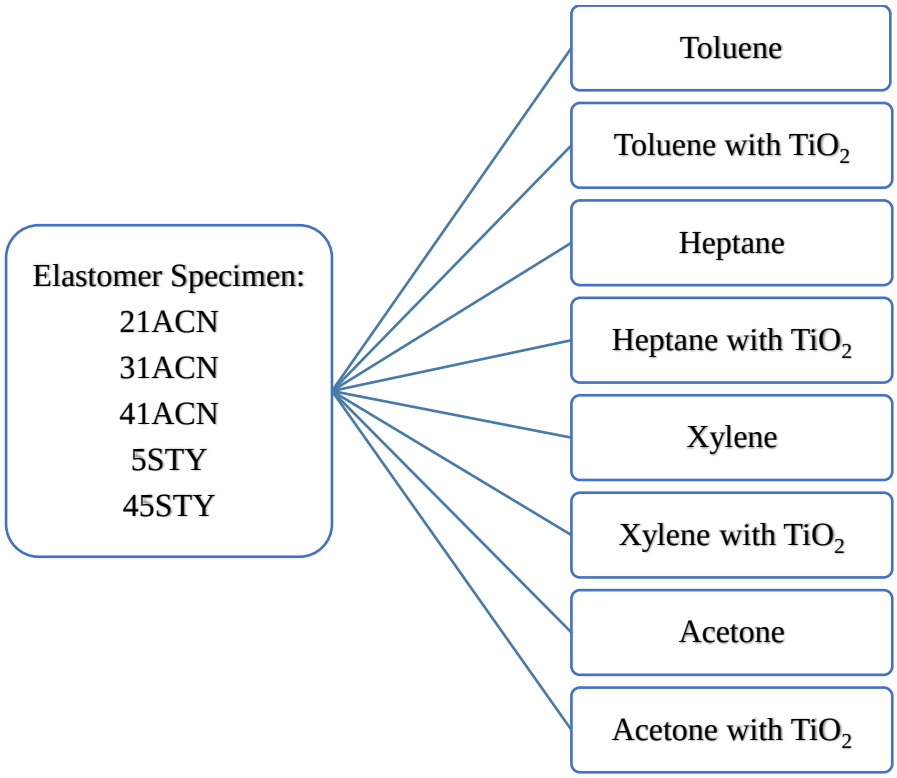

Figure 3-11: Chart on stage 1 experiment 1 arrangements

For swelling agents with TiO_2 nanoparticles, a small amount of emulsifier was added to the concoction in order to bind the primary constituent and the nanoparticle colloidal solution. The amount of emulsifier added to all solutions was controlled to be the same amount. The mixture ratio chosen for the first experiment batch was 1:1 ratio, where 1 part of primary constituent was

added to 1 part of TiO_2 nanoparticles solution to form the NSA. The goal of experiment 1 in stage 1 was to narrow down the potential elastomers and identify nano-based swelling agent (NSA) which amplified the swelling effect when compared to pure primary constituents only.

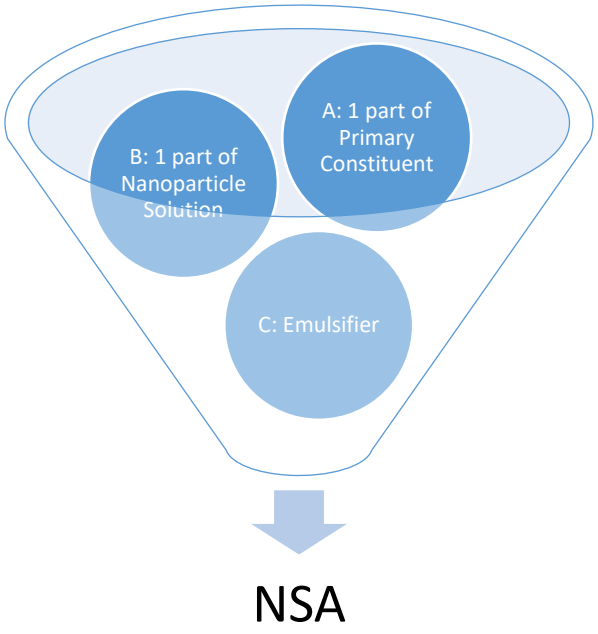

Figure 3-12: Mixture ratio for NSA in stage 1 experiment 1

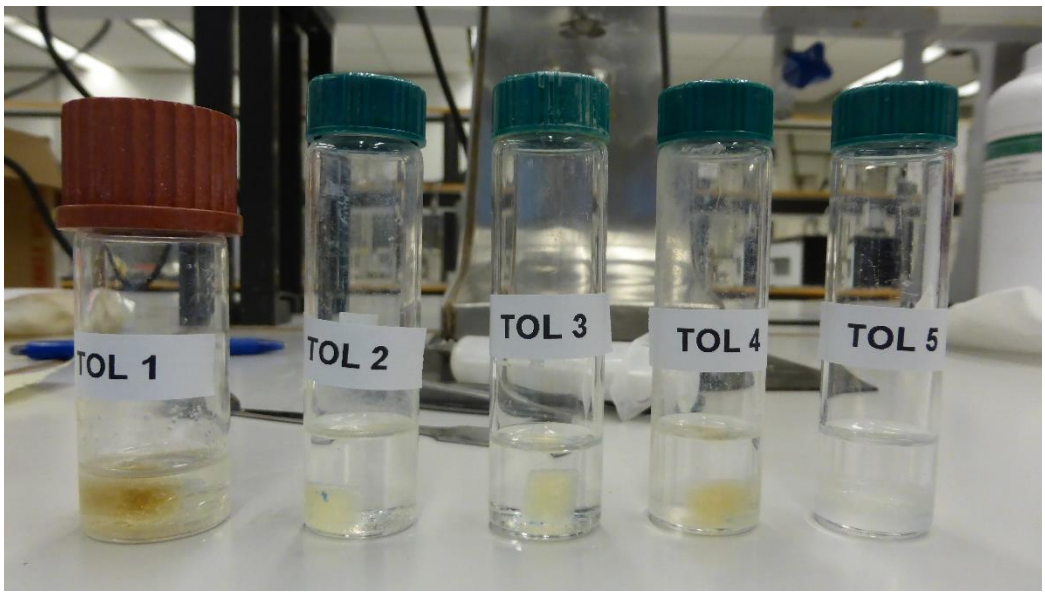

Figure 3-13: Labelled samples for Toluene only experiment, where 1 - 21ACN, 2 - 31ACN, 3 – 41ACN, 4 – 5STY, 5 – 45STY

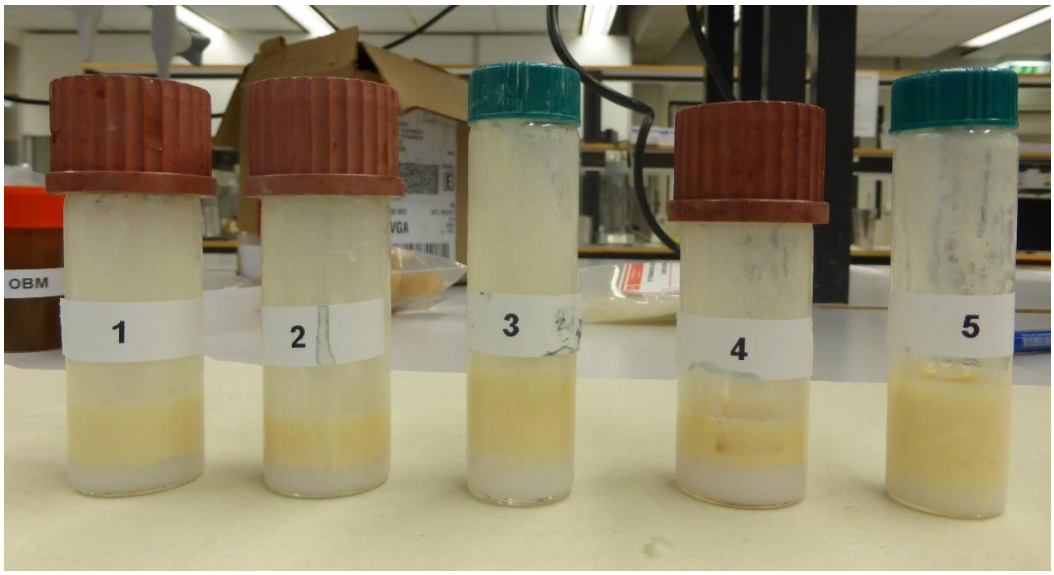

Figure 3-14: Labelled samples for the mixture of Toluene with TiO_2 nanoparticles solutions, where 1 – 21ACN, 2 - 31ACN, 3 – 41ACN, 4 – 5STY, 5 – 45STY

After the first experiment, the nano-based swelling agent (NSA) systems with most promising results were then subjected to a subsequent experimental batch, where different ratios of solution mixtures were tested. The ratio tested were 1:2, 1:3, 1:4 and 1:5. For example, the ratio 1:5 refers to one part primary constituent is mixed with 5 parts of TiO_2 nanoparticles solution. The goal of this stage 1 experiment 2 was to observe the effect different ratio of mixture had on the swelling rate.

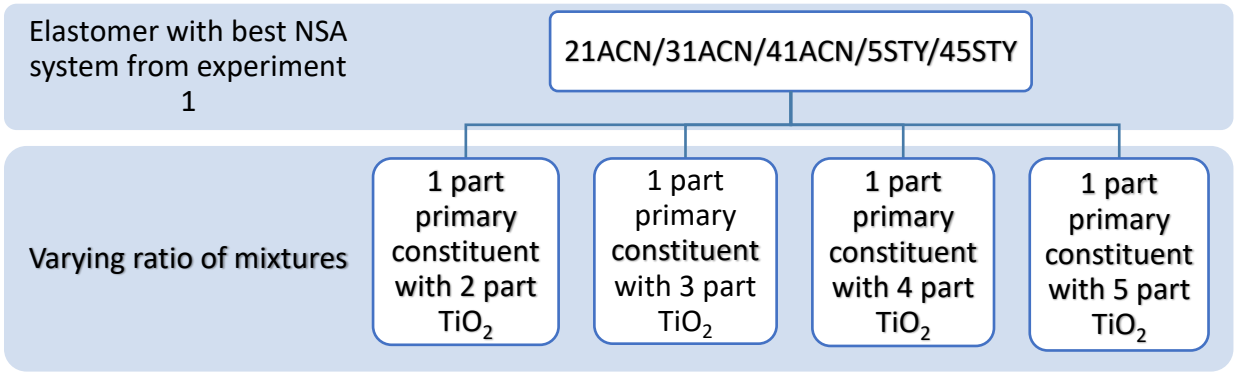

Figure 3-15: Chart for stage 1, experiment 2 arrangements

3.3.2 Stage 2: Elimination of Possible Swelling Effect from Other Constituents of NSA

At the end of stage 1 experiments, several NSA systems were identified as effective and yielded good swelling results. Before proceeding any further with optimizing the NSA systems, Stage 2 experiments were conducted with the sole purpose of investigating whether the individual components of the NSA – water, TiO_2 nanoparticles solution and the emulsifier, caused any swelling on the elastomers. If there were evidences of assist in swelling due to other constituents, this had to be taken into account in the end results.

Stage 2 Experiment 1 examined the swelling effects of pure water. Should elastomers swell in this condition, it imitates a water-based swelling packer environment which strays from the objective of this work. As per practice of ASTM D471, the water used in the experiment to determine the effect of water on the various elastomer samples was distilled water. Elastomers were soaked inside a glass tube for 24 hours in the absence of light and measurements were taken before and after the immersion to calculate volume and mass changes, if any.

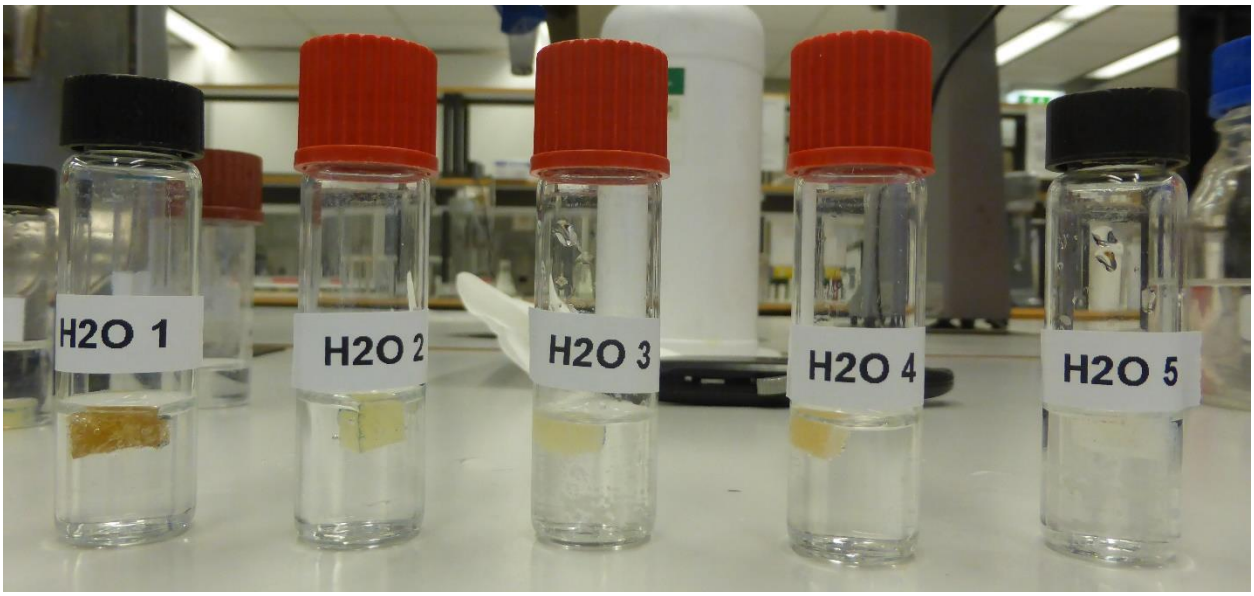

Figure 3-16: Elastomers immersed in distilled water. From left to right: 21ACN, 31ACN, 41ACN, 5STY and 45STY

Stage 2 Experiment 2 concentrated on the effect of pure TiO_2 nanoparticle solutions – constituent B of NSA (refer to section 3.1.2) when exposed to the elastomers. The TiO_2 nanoparticle solution

used were 15wt% Anatase with 5-30 nm sizing purchased with no additional handling. If this pure nano-based system was able to induce reasonable amount of swelling in the elastomers, it would have been a beneficial outcome as the end solution would have been a simpler one. Specimens were measured before the immersion for dimensions as well as mass and cleaned using distilled water to get rid of any residues on the surface before measured again after 24 hours.

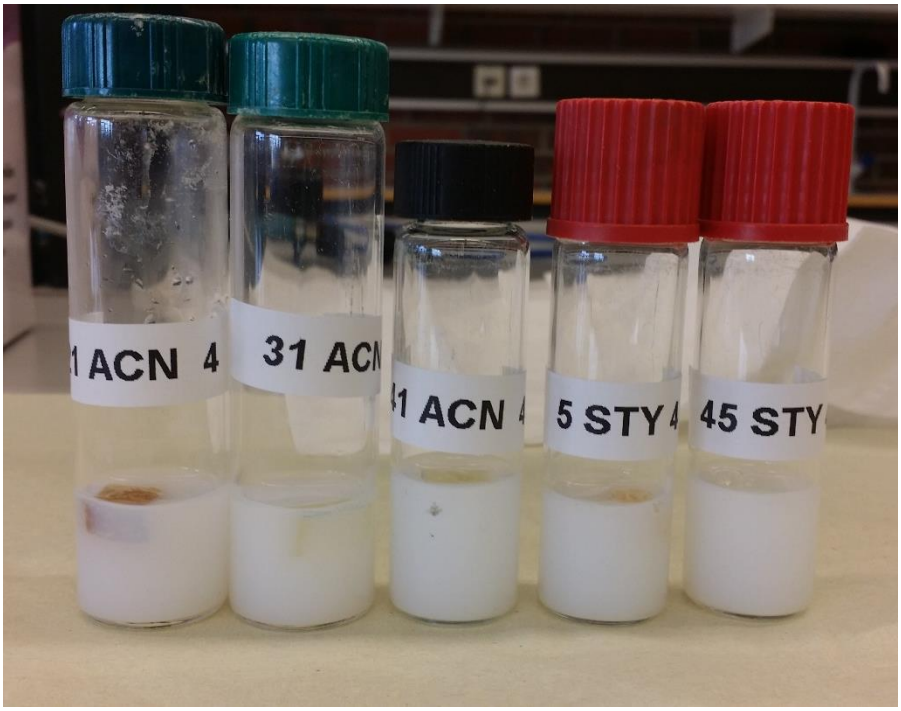

Figure 3-17: Elastomers immersed in TiO_2 15wt% nanoparticles solution. From left to right: 21ACN, 31ACN, 41ACN, 5STY and 45STY

In **Stage 2 Experiment 3**, the investigation focused on the emulsifier – constituent C in NSA (refer to section 3.1.2) used in binding the NSA mixtures. Although a bare minimal and controlled amount was used in creating the NSA concoction, it was imperative to determine if the emulsifier had any influence in the swelling process. Sufficient emulsifiers were used to ensure total coverage of the elastomers in a glass tube. In this experiment, volume or dimensional measurements were used solely to assess the results as it was difficult to remove all residues off the surface of specimens. Experiment ran for 24 hours and results were recorded accordingly.

All results are documented in section 4 with discussions for each individual experiments conducted in stage 2.

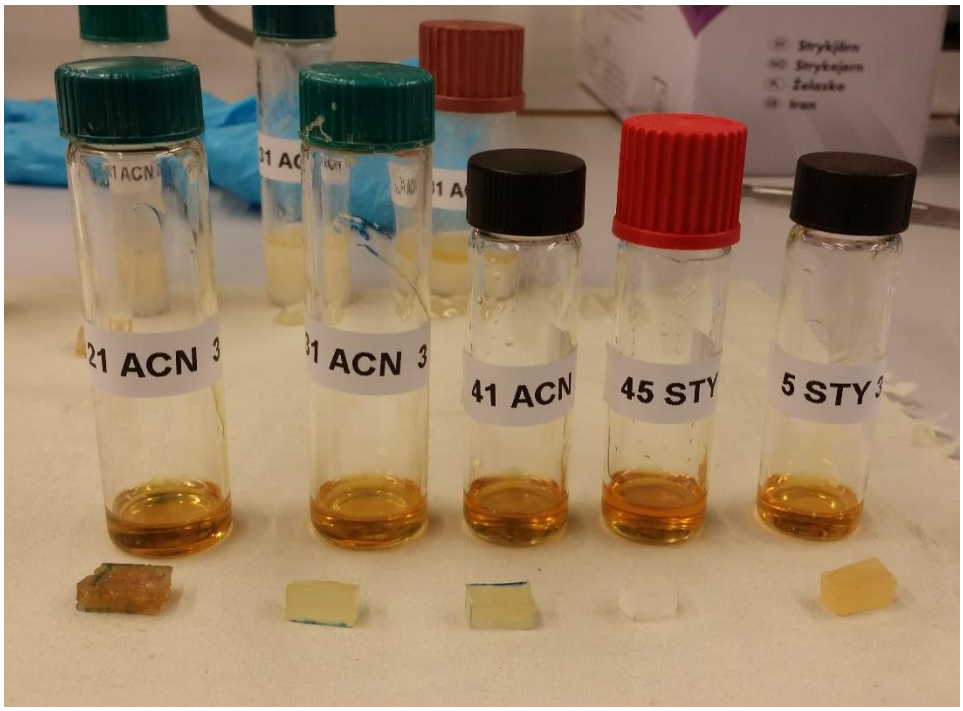

Figure 3-18: Elastomers before immersion in emulsifier used in binding of a two phase liquid

3.3.3 Stage 3: Investigating the Effects of Acidic Versus Basic Conditions

As the potential NSA systems were identified in stage 1 and the likelihood of possible swelling effect from other constituents of NSA eliminated in stage 2, the next stage was to investigate the effects of pH on the swelling reactions. Depending on the operations type, wellbore conditions could be low pH due to activities such as acid stimulation or acid fracturing while other wellbores could be high pH to tackle near-wellbore calcite and silica problems. High pH could also help to avoid corrosion problems which comes with an overly acidic well.

Considering that the range of pH can be high or low for a wellbore, it is crucial to study the effects of acidity and basic conditions for the NSAs. The type of systems chosen for the wellbore conditions could then be optimize based on the swelling rate desired. From stage 1, three potential elastomer candidates in two NSA systems were narrowed down. In this experiment, all three of the shortlisted elastomers were subjected to both acidic and basic conditions. Figure 3-19 shows two test tubes of the same elastomer specimen. The left glass tube (sample 1) is acidic with a pH of 1.3 which is the original pH of the NSA solutions without any adjustments. Sample 2 in Figure 3-19 is basic with a pH of 8.2. Droplets from a 5% Sodium Hydroxide (NaOH) solution were used to alter the pH.

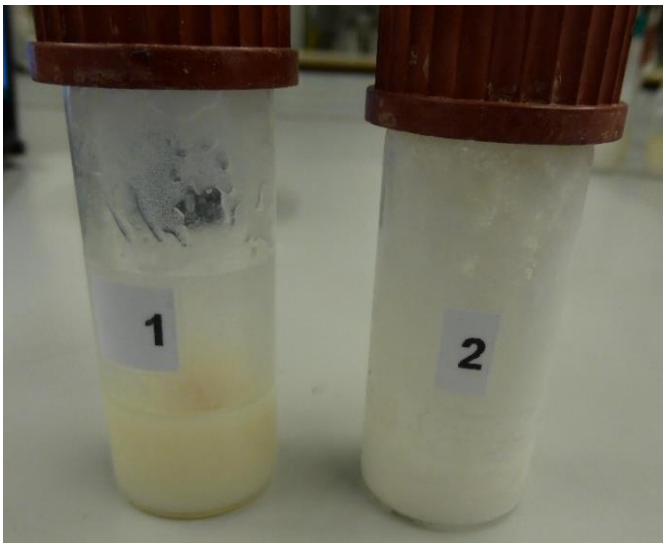

Figure 3-19: Elastomer specimen in Toluene NSA, left is acidic and right is basic

The Orion Research digital pH meter was used to determine the pH for all mixtures in this stage. The pH meter was always calibrated with a known buffer solution of pH 7 before dipping into the NSA mixtures. After each measurement, the sensor probe was rinsed thoroughly with distilled water before performing the next measurement. Care was taken to ensure that the pH reading stabilized before recording was done.

Figure 3-20: Orion Research digital pH meter

As per previous procedures, the specimens were immersed in respective solutions for a 24 hour period in the absence of light and dimensions were recorded before and after the experiments. The pH number for all the solutions, their implications and stage 3 results and discussions are captured in section 4.3.

3.3.4 Stage 4: Studying the Effects of Varying Concentration of Nano-Particle Solutions

Up to this point, the 15wt% concentration of TiO_2 nanoparticles solution (Constituent B of NSA) which was purchased and used as is have been taking center stage in all of the previous stages' experiments as part of the main constituents. In this stage, the possibility of using a lower concentration of TiO_2 nanoparticle solutions and its swelling reaction will be examined. As the world's energy crisis pressure mounts up, it is imperative that there be a viable lower cost option available especially when oil and gas industry is constantly challenged to keep the expenses in check. Reducing the concentration of TiO_2 nanoparticle solutions in the NSA mixtures but keeping the volume increase percentages constant is a much desirable effect.

At the end of Stage 3, three potential systems were identified and these systems were selected for further investigation in stage 4. In each these selected systems, 3 different concentrations of TiO_2 nanoparticle solutions were used to create a total of 9 variations. The three different TiO_2 nanoparticle solution concentrations used were 1wt%, 5wt% and 10wt%.

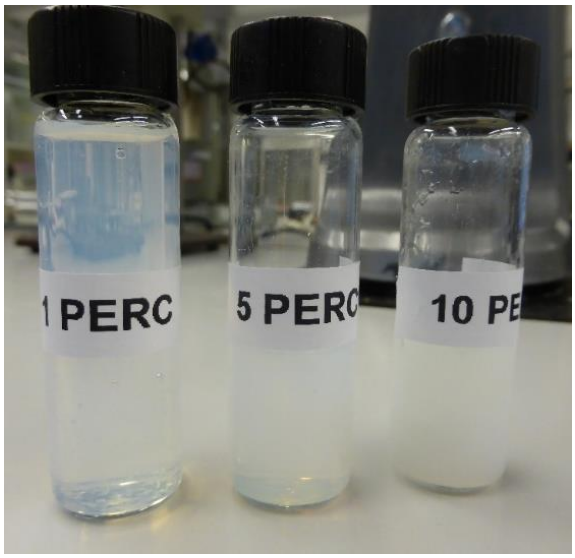

Figure 3-21: TiO_2 Nanoparticles Solutions in 1wt%, 5wt% and 10wt%

From section 3.1.2, it is understood that the way weight percentage (wt%) for the default TiO_2 nanoparticle solution bought is calculated as 15% of the total weight of dispersion.

$$\%\ Wt.Concentration = \frac{Total\ weight\ of\ TiO_2\ (gms)}{Total\ Weight\ of\ the\ solvent, water\ (gms)}$$

This means that 150g of TiO_2 nanoparticles in 850g of water. This understanding is important for proper dilution technique in this stage's experiments. Figure 3-21 shows the diluted TiO_2 nanoparticles solutions in concentration of 1wt%, 5wt% and 10wt%. The solutions were diluted with distilled water and homogenously dispersed in a single phase liquid.

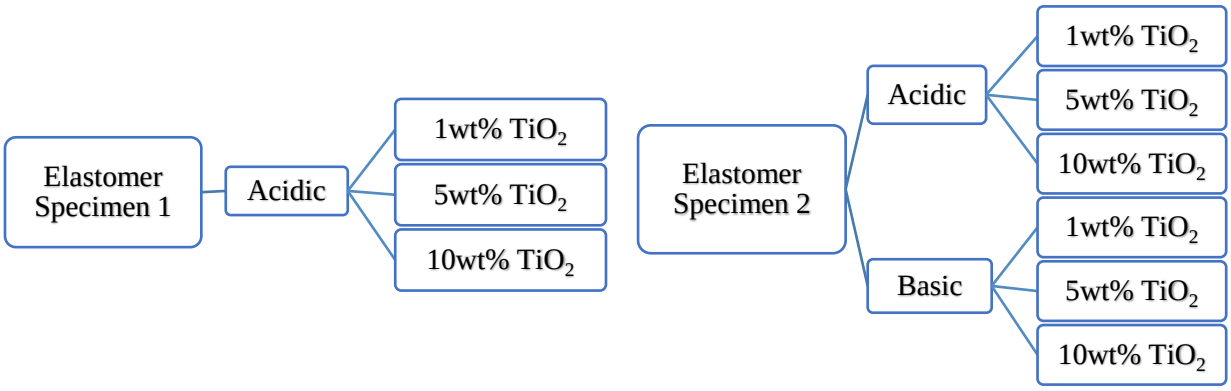

Figure 3-22: Stage 4 experimental chart arrangements

Nine experiments were run in total for stage 4 as illustrated in Figure 3-22, where elastomer specimens 1 and 2 were the best performing from stage 3. The procedures in preparing the specimens in Figure 3-23 and Figure 3-24 were the same previous stages with the exception of the TiO_2 nanoparticles solutions concentration. Specimens were immersed into NSA mixtures for a period of 24 hours in the absence of light and measurements of mass and dimensions were recorded before and after.

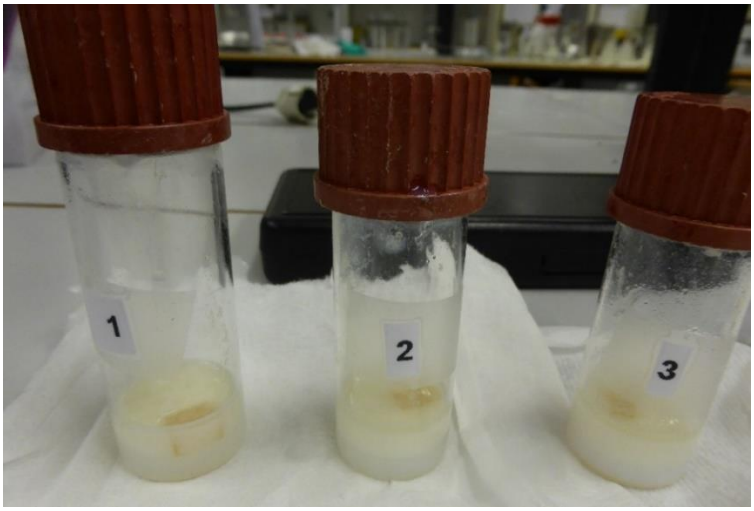

Figure 3-23: Elastomer specimen 1 in acidic NSA in an array of TiO_2 nanoparticles solution concentration. From left to right, 1wt%, 5wt%, 10wt%

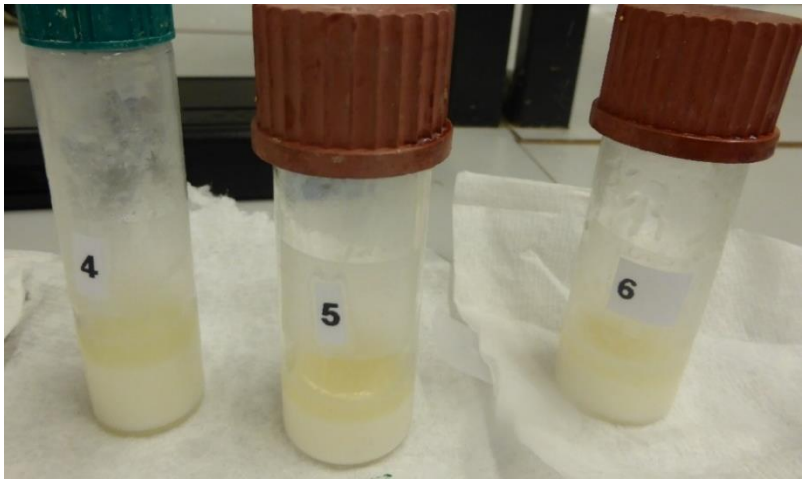

Figure 3-24: Elastomer specimen 2 in acidic NSA in an array of TiO_2 nanoparticles solution concentration. From left to right, 1wt%, 5wt%, 10wt%

NSA mixtures with 1wt%, 5wt% and 10wt% do not differ much from 15wt% in terms of physical handling and visual inspection. Similar to stage 3, droplets of 5% Sodium Hydroxide was added to the test tubes in Figure 3-25 to modify the pH from acidic to basic. The pH of the solutions were kept as close to each other as possible and the same off white coloration was observed for the basic solutions as per stage 3. The most ideal systems from this stage will be the final line-up for possible elastomer swelling in NSA for intended swell packer commercialization use.

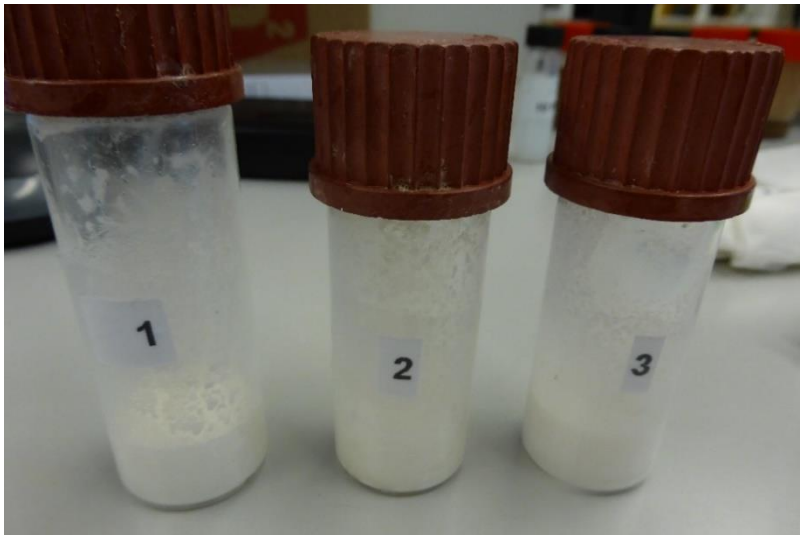

Figure 3-25: Elastomer specimen 2 in basic NSA in an array of TiO_2 nanoparticles solution concentration. From left to right, 1wt%, 5wt%, 10wt%

3.3.5 Stage 5: Temperature Effects on NSA

Before the start of the experimental work for this thesis, the hypothesis developed was that only one optimal elastomeric NSA system would emerge as the best system to use for potential commercialization while the rest would be filtered out. However from the experiments in previous stages, this premise had to be revised due to the unexpectedly good outcomes of the investigation with several systems displaying exceptional performance. Different factors such as swelling rate, potential wellbore pH condition, operation time and cost savings all played a role in the reason for revision.

Wellbore temperature increases as the depth of the well increases and it is known to have an effect on a variety of things such as fluid density, ECD as well as swelling rate for elastomer. It could also potentially affect the integrity of elastomer used which is why all elastomers used in oil and gas application tends to come with a temperature range for functional use. From stage 4, a total of four best elastomeric NSA systems were narrowed down and this stage will explore the effects of temperature on these systems as illustrated in Figure 3-26. This stage is not meant to be a conclusive experiment on the functionality of the elastomeric NSA in temperature but rather for a glimpse of the potential relationship between swelling performance and temperature variation.

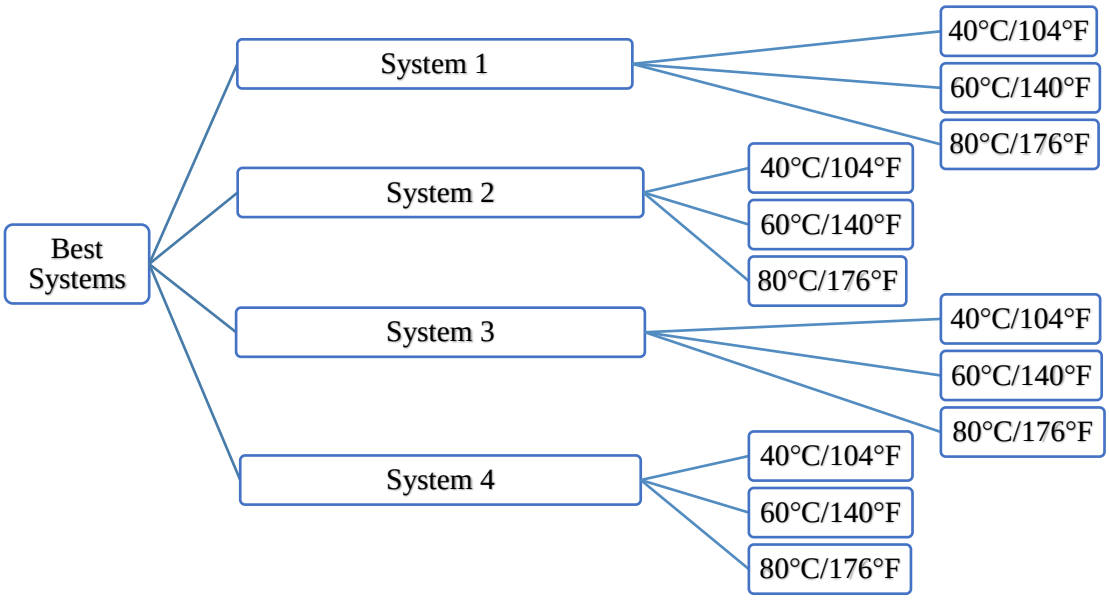

Figure 3-26: Stage 5 experimental arrangements

The details of each systems in Figure 3-26 are presented in results chapter (Section 4.5). The numbers in Figure 3-26 before the four best systems correspond to the numbers on the tube cap in Figure 3-27, Figure 3-29, Figure 3-30 and Figure 3-31 for ease of understanding.

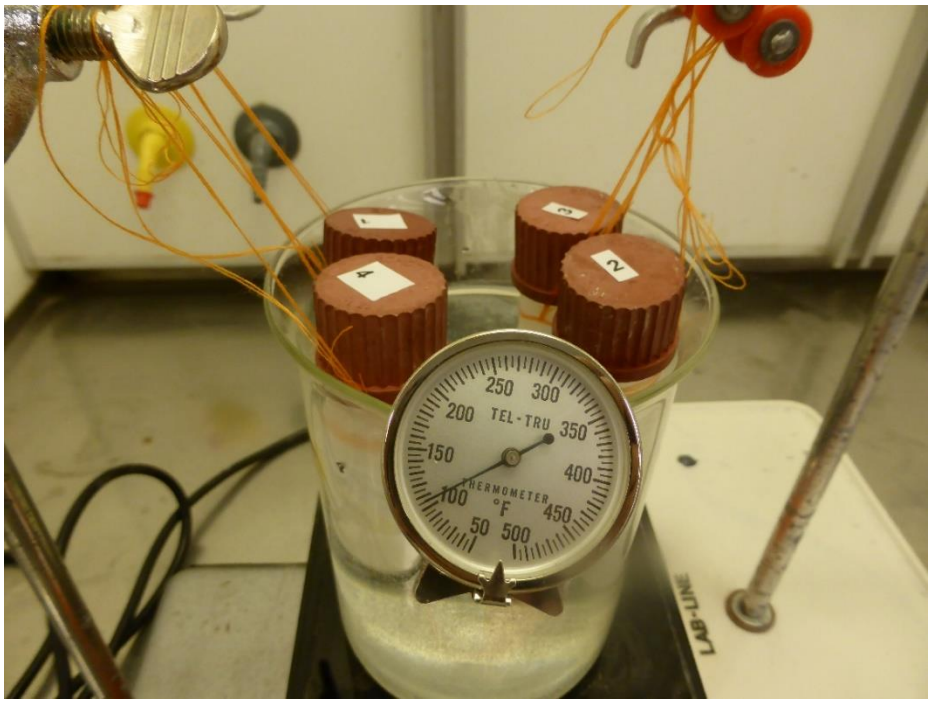

Figure 3-27: Specimens in glass tube submerged in a water bath heated to 40°C/104°F

The controlled temperature for all previous stages had been 16°C/60°F which was room temperature in the laboratories. To investigate the effects of temperature, the specimens from all four systems were submerged into a water bath with temperature 40°C/104°F, 60°C/140°F and 80°C/176°F. Water bath was chosen to ensure a uniform and safe heat transfer process with a Framo Geratetechnik M21/1 machine. Figure 3-28 shows a picture of the machine used. Though it is more commonly used as a magnetic stirrer for mixtures, it also has an automatic temperature regulator which is ideal for the intended use in this experiment.

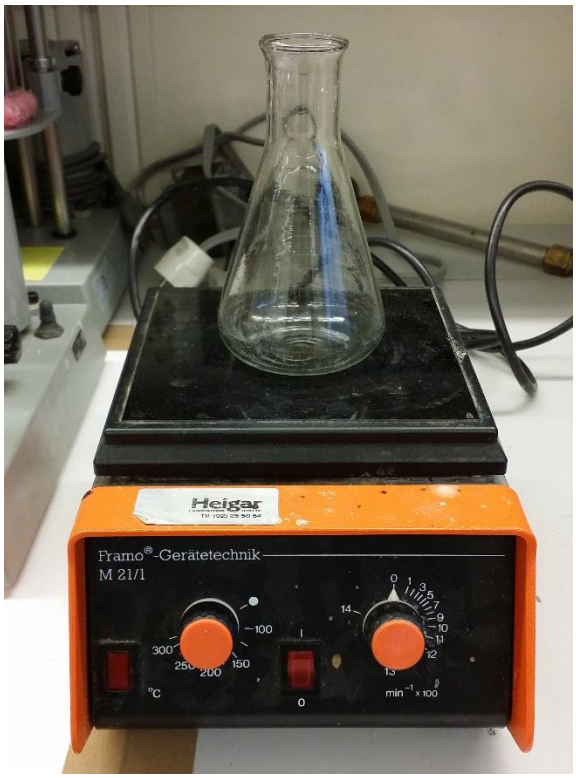

Figure 3-28: Framo Geratetechnik M21/1 hotplat magnetic stirrer machine was to provide heat to water bath

A recording thermometer was placed in the middle of the water bath near to the glass tubes in order to obtain an accurate reading. A thermometer was also placed inside the glass tubes with the solution prior to initiating the experiment to ensure proper thermodynamics has taken place. Desired temperature was stable for 15 minutes before experiment began for all experiments in this stage. See Figure 3-29 for the experimental setup. Glass tubes which contained specimens and NSA mixtures were suspended in the water bath to just below the tube cap to avoid water from entering the systems and diluting the NSA mixtures. Care was taken to ensure the NSA mixture liquid and specimens were well below the water bath liquid line for the entire duration of the experiment in order to keep the temperature constant.

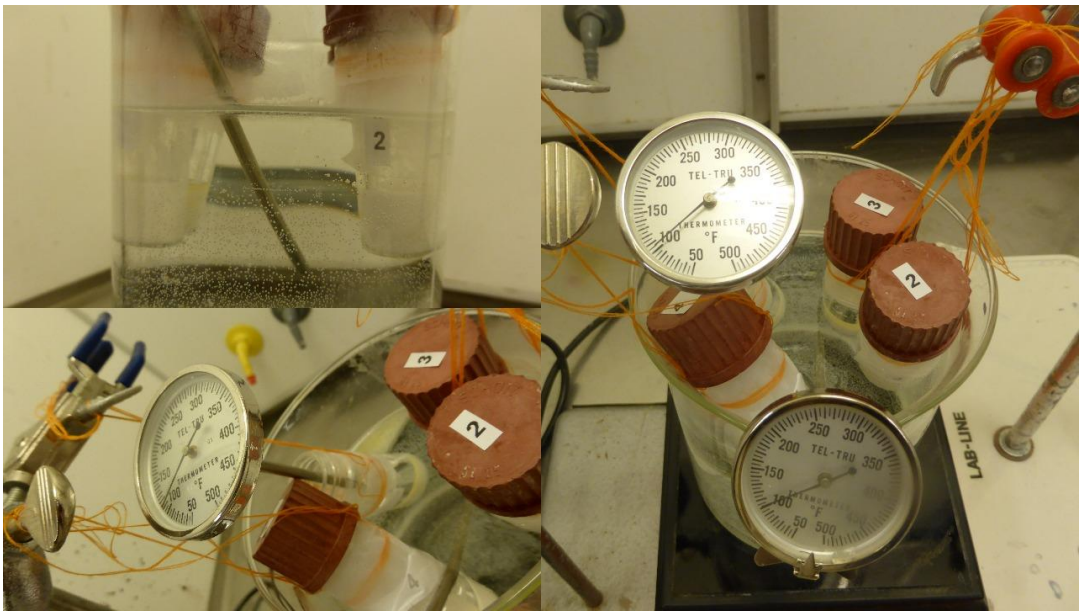

Figure 3-29: Experimental setup for water bath heating of specimens

Specimens and their respective NSA mixtures were prepared as per previous experiments and measurements were taken before and after. The measurements were done as fast as possible to circumvent losing too much heat. One difference in the experiments in this stage was the presence of light, since the water bath setup had to be placed inside a ventilated enclosure the total absence of light is not possible. Though when permitted, light sources were kept to a minimal. Figure 3-30 shows that similar setup was used for testing in 60°C/140°F.

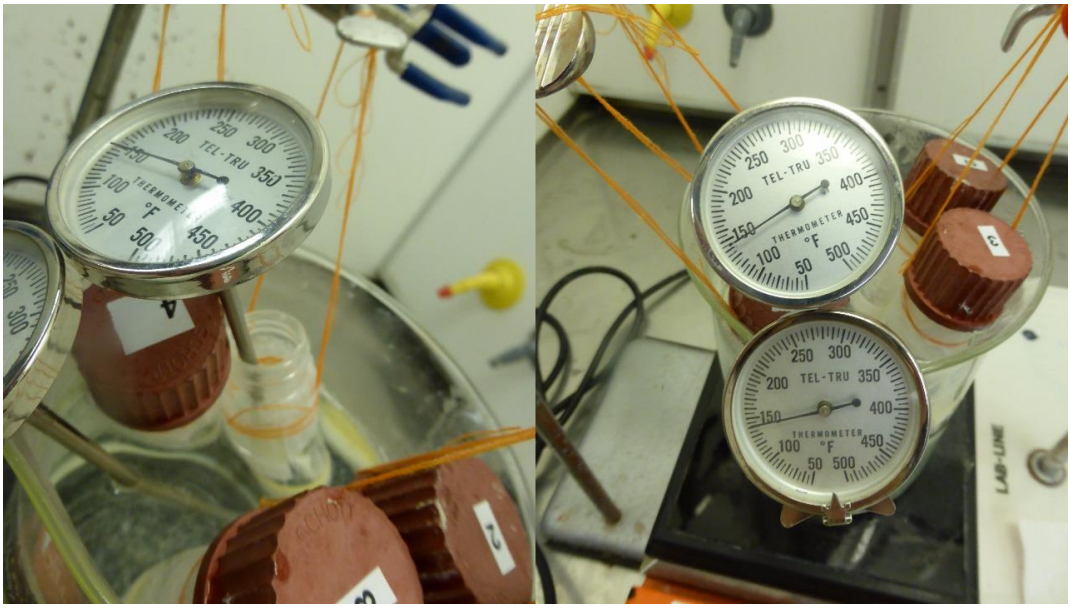

Figure 3-30: Experimental setup for 60°C/140°F

Since the glass tubes were exposed to higher temperature, thicker gloves were used in handling and water bath level was kept as consistent as possible despite rapid evaporations. Hot water was constantly added in small amount to maintain the desired temperature throughout the experiment. The experimental data obtained from this stage was used in developing a regression based predictive model as function of temperature and exposure time. This is discussed further in section 5.4.

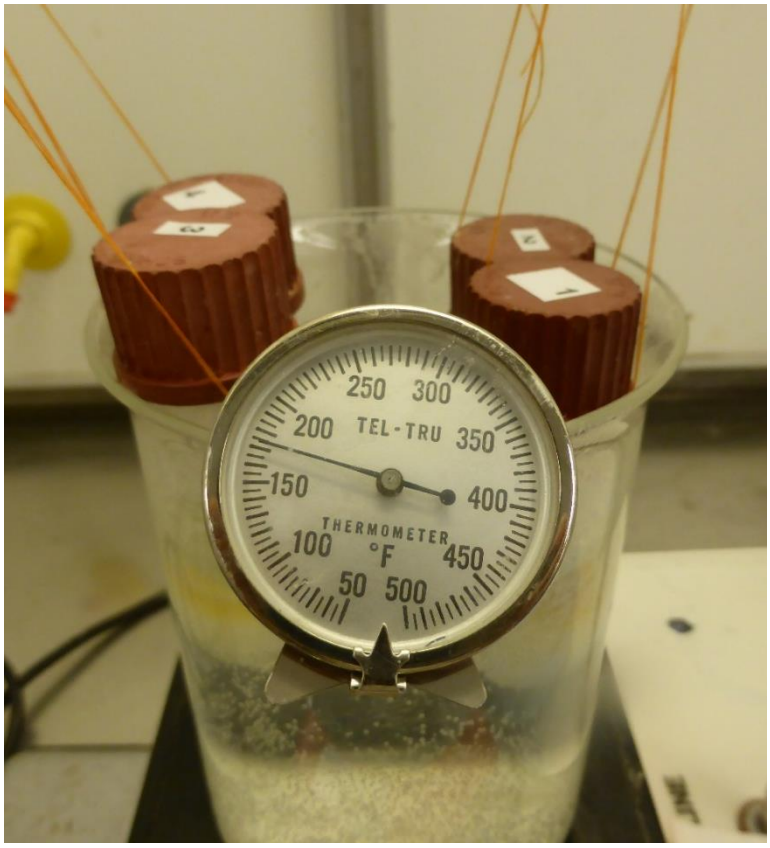

Figure 3-31: Specimens in glass tube with heated water bath in temperature 80°C/176°F

3.3.6 Stage 6: Water-based Mud vs Oil-based Mud

This last stage aims to examine the effects water-based mud (WBM) and oil-based mud (OBM) has on the two shortlisted elastomers from previous stages. One of the discussion at the beginning of this thesis was the driving factor on why NSA would be more superior to swell packer triggered by OBM or WBM. OBM and WBM induced swell packers always have the risk of well hang up and premature swelling if care was not taken to avoid contact between the tool and its reactant. This can result in stuck completion strings resulting in severe economic ramifications in terms of NPTs. This experiment is important to ensure the swelling of the potential elastomeric systems are due to only NSA and no contaminants easily available on rig site such as WBM or OBM could affect the outcome of the volume expansion.

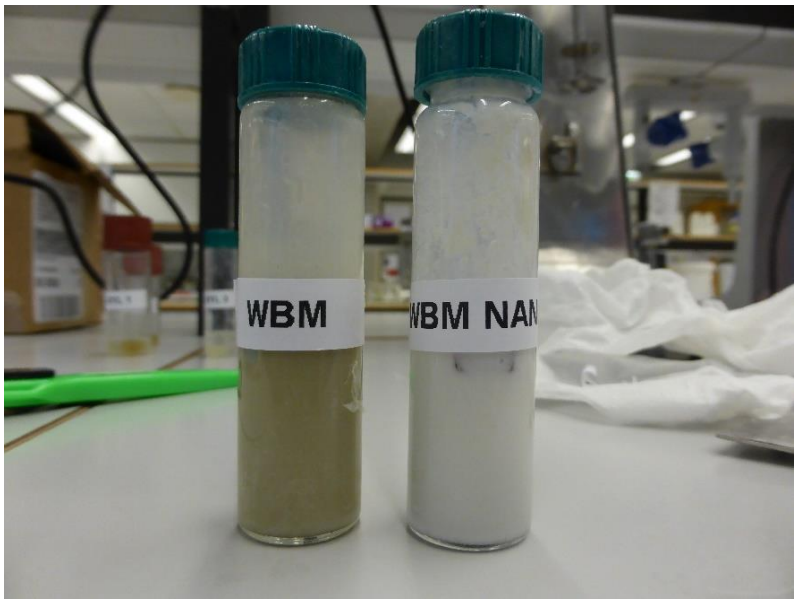

Figure 3-32: Water-based mud and water-based mud with TiO_2 nanoparticles solution

In the spirit of exploring new possible ventures, 15wt% TiO_2 nanoparticles solution was also added to WBM and OBM to investigate the consequence of these solution mixtures on the two elastomer specimens. The properties of OBM and WBM used in this stage have been listed out in section 3.1.3. The elastomer specimens samples were prepared and measured before the experiment and after. The experiment was run for a period of 24 hours in the absence of light.

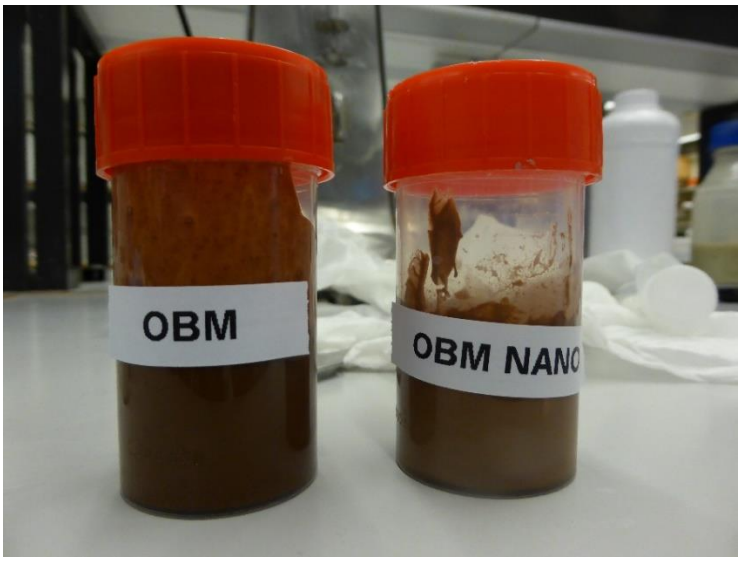

Figure 3-33: Oil-based mud and oil-based mud with TiO_2 nanoparticles solution

4 Results

In this section, the different experimental results in terms of change in mass or change in volume have been recorded and analyzed. In all instances, as per normal practice in the swell packer research, change of volume measurements are considered to be the most important parameter as ultimately the change in volume dictates the effectiveness in annular sealing capacity. The change in volume measurement is also vital in the determination of packer OD relative to the borehole sizes. Although change of mass measurement was also taken for all the experiments, it is not the preferred method of analysis in most experiments. This is because in some instances there were heavy precipitation on the elastomer specimens' surface which was difficult to rinse off entirely. This thin layer of precipitation did not affect the change of volume measurements but it could influence the weight taken. Hence the analysis would be based on change of volume as it is the most effective method of measurement.

An elimination method was used to filter out the best elastomer-NSA combinations in a gradual stage-wise manner and these systems were then subjected to further experimentation and variations. This section presents the discussions for each of the specific method chosen and the philosophy behind selection of optimal NSA.

4.1 Stage 1 Results and Discussions: Proof of Concept – Identification of Primary Constituents of NSA and Compatible Rubber

4.1.1 Stage 1 Experiment 1

In stage 1 experiment 1, all five of the elastomer specimens were tested with four primary constituents and a NSA solution mixture of both primary constituents and TiO_2 nanoparticles. Please refer to Figure 3-11 for a clear picture. This proof of concept in stage 1 turned out to be very encouraging as two out of the five elastomers showed promising results. Table 4-1 details the results from stage 1 experiment 1, where 1:1 ratio of NSA mixtures were administered for all the elastomer candidates.

	21ACN	31ACN	41ACN	5STY	45STY
Toluene	Results not effective				
Toluene with 15wt% TiO_2	Swelled better that pure Toluene, see Stage 1 Experiment 2 (Refer to section 4.1.2 for details)				
Heptane	Swelled less than 5%				
Heptane with 15wt% TiO_2	Swelled the same as pure Heptane				
Xylene	Result effective but not ideal due to softness	Result not effective	Swelled about 55%	Result not effective	Result not effective
Xylene with 15wt% TiO_2	Swelled good but structure too soft	Swelled but no structural integrity	Swelled about 185%	Swelled but no structural integrity	Swelled but no structural integrity
Acetone	Swelled about 70%				
Acetone with 15wt% TiO_2	Swell 35% only, worse than pure Acetone				

Table 4-1: Results from experiment 1 in stage 1, green box indicates potential

For all five elastomers in Toluene only solution, structural integrity was a concern since after 2 hours of immersion, most of the elastomers had partially dissolved into the solution. Some specimens were very soft to handle while others were extremely sticky to touch (see Figure 4-1). The experiments were stopped as it was difficult to obtain proper measurements of the elastomers. On the other hand, all five elastomers in Toluene with TiO_2 nanoparticles solution mixtures (Toluene NSA) performed better than pure Toluene in terms of volume percentage increase. However the rate of increase was too fast to capture and although the swelling rate was high, the

elastomers were starting to feel too soft before we could have a conclusive outcome. Hence this spawned the stage 1 experiment 2 discussed in 4.1.2.

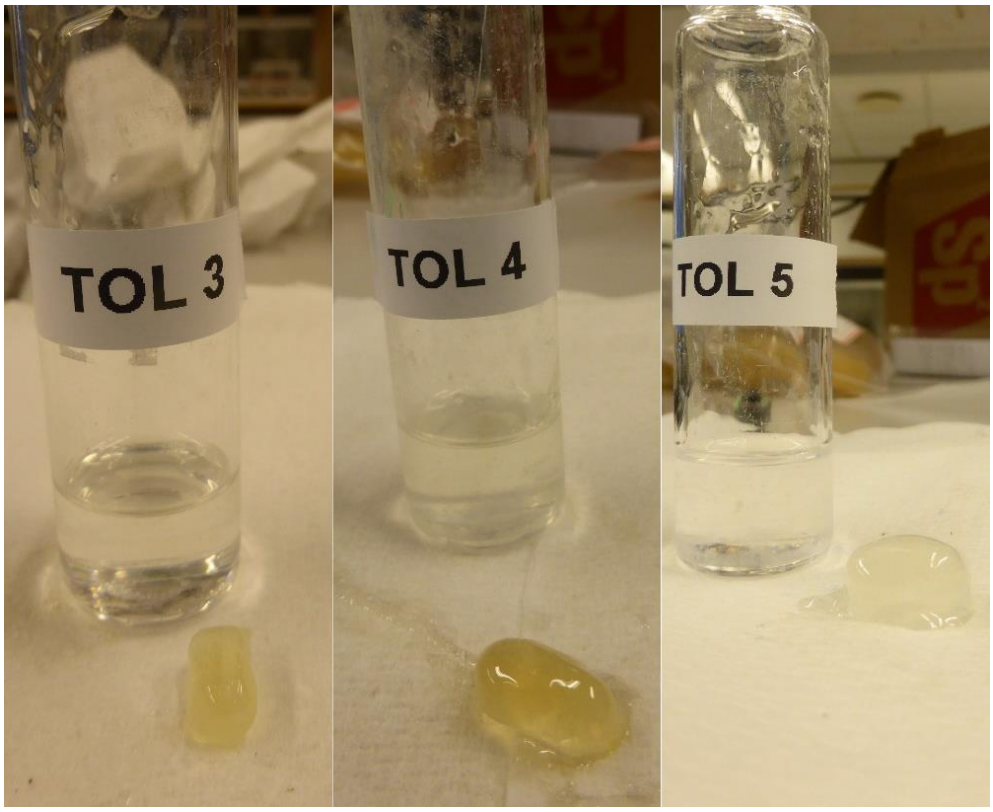

Figure 4-1: Elastomers after immersion in pure Toluene. From left to right, 41ACN, 5STY, 45STY

In the case of Heptane as a primary constituent, the swelling effect was too insignificant for it to be a viable option for further investigation. Heptane NSA behaved the exact same way as pure Heptane solution and yielded no substantial results with bare minimal swelling. This concluded that five elastomers in the presence of pure Heptane and Heptane NSA are not suitable candidates in this thesis work.

The experimental work with Acetone was quite interesting in that all five of the elastomers performed better in pure Acetone solution than Acetone NSA. Since this deviates from the objective of finding a suitable NSA to replace the convention swelling medium, no further investigation was carried out with Acetone either.

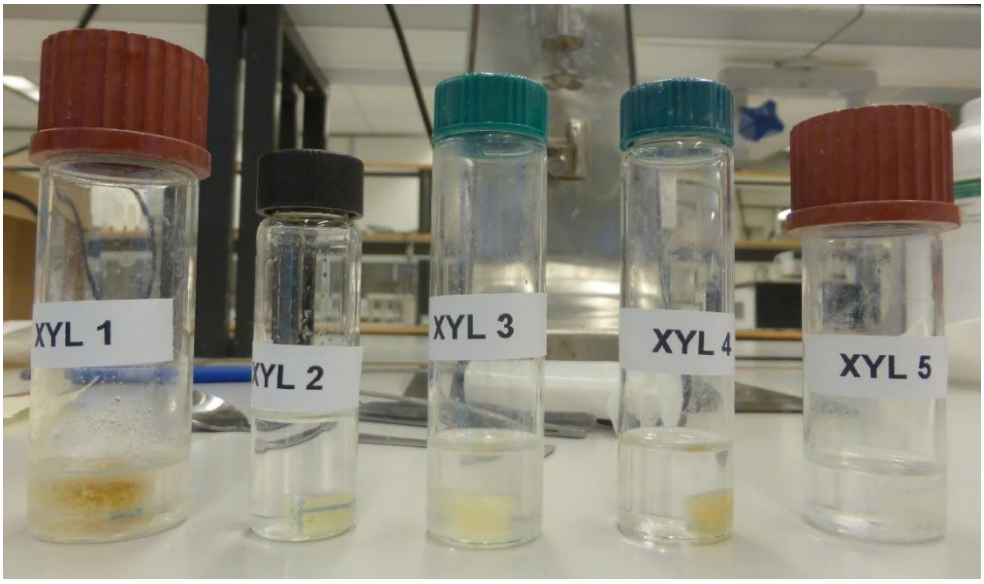

Figure 4-2: Elastomers in pure Xylene solutions

In case of the experiments with Xylene as a primary constituent, most of the elastomers did not yield a positive results in both pure solution as well as Xylene NSA. From Figure 4-3, upon closer inspection after several hours of immersion in Xylene NSA, the elastomers 31ACN, 5STY and 45STY appeared to be losing their structural integrity and became rather sticky. While 21ACN had good structural integrity and swelled considerably well, it was extremely soft to touch and therefore deemed not suitable to proceed with as well.

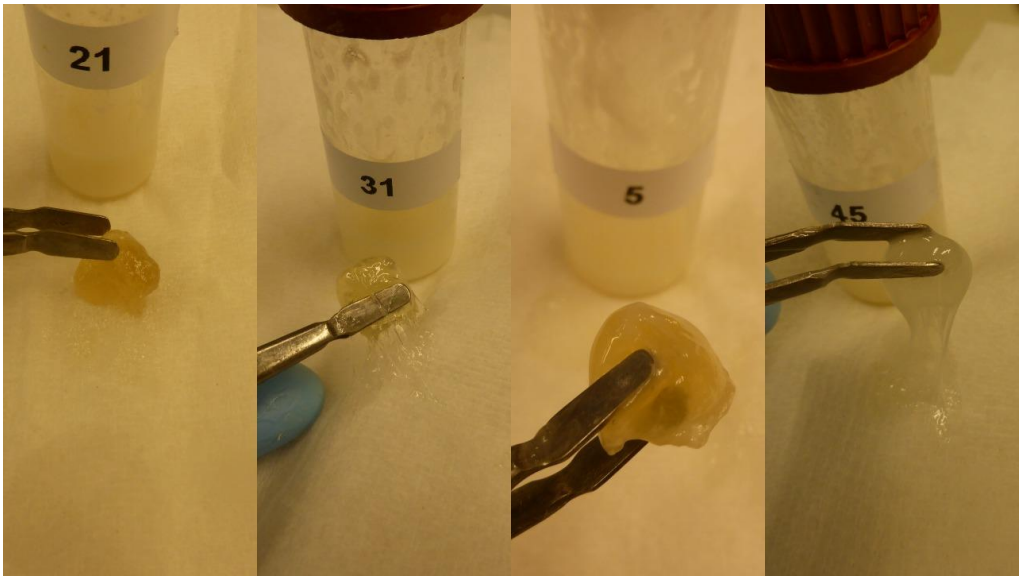

Figure 4-3: Elastomers exposed to Xylene NSA. From left to right: 21ACN, 31ACN, 5STY and 45STY

The only elastomer which could potentially be a contender when exposed to Xylene based solutions was 41ACN. In the presence of only pure Xylene, 41ACN swelled considerable well with 55% volume increase. However it did not endure particularly well past 24 hours and became too unstable structurally. On the other hand, in Xylene NSA, 41ACN was able to swell up to 185% with good form and hence chosen as one of the potential elastomers to move forward in stage 1 to experiment 2.

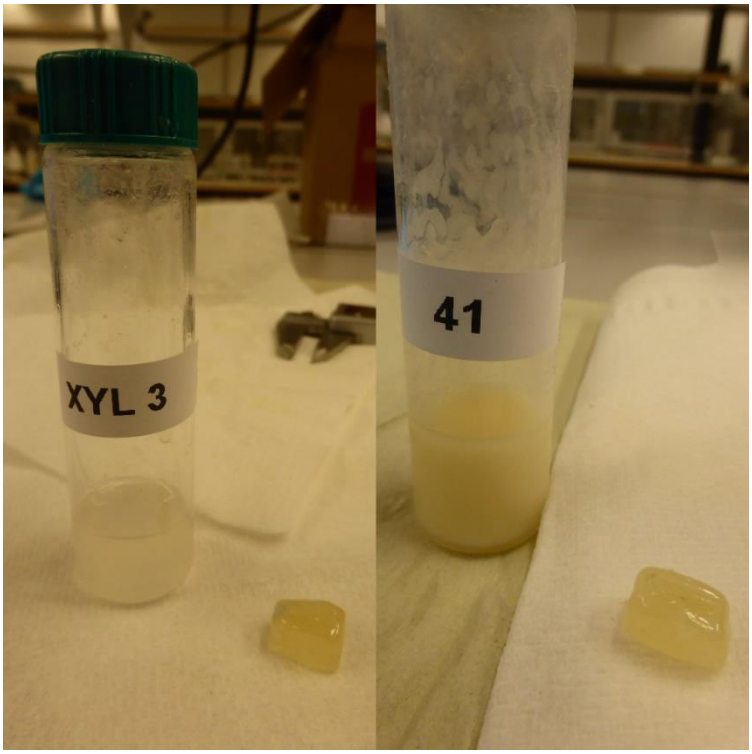

Figure 4-4: 41ACN in pure Xylene (left) and in Xylene NSA (right) after immersion

4.1.2 Stage 1 Experiment 2

As mentioned previously, elastomers in Toluene NSA yielded inconclusive results and hence a review of the default mixture ratios (1 part primary constituent: 1 part nanoparticles) was carried out and a stage 1 experiment 2 was conducted in a bid to optimize the NSAs by varying the mixture ratios and lowering the Toluene part in the NSA. The two primary constituents narrowed down from stage 1 experiment 1 were Toluene and Xylene. In the case for Toluene, all five elastomers were subjected to a mixture ratio varying test in order to narrow down a suitable ratio as well as elastomer. After several rounds of testing, Toluene NSA with 1:5 ratio quickly emerged as the

front-runner with the highest amount of volume increase percentage as well as maintaining a firm structural integrity even after 24 hours of immersion for all 5 of the elastomers.

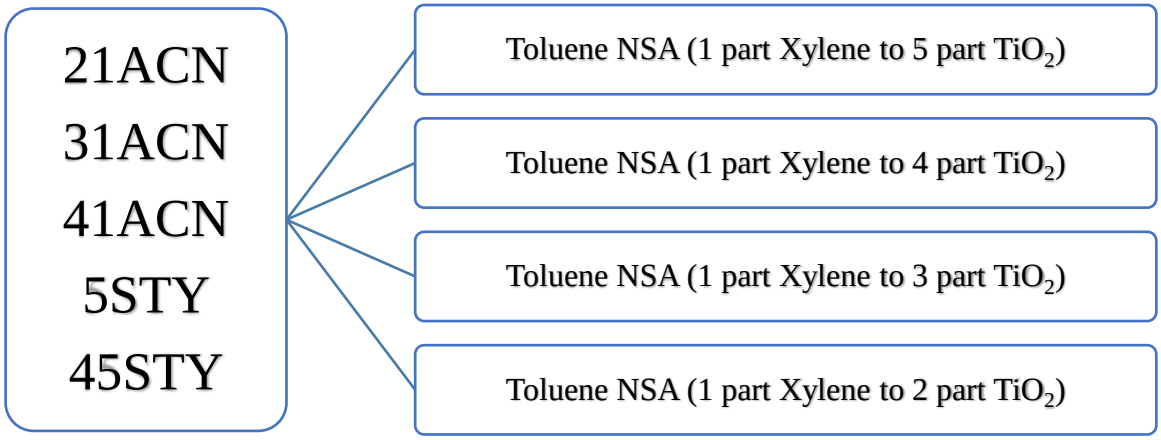

Figure 4-5: Stage 1 experiment 2 for Toluene NSAs

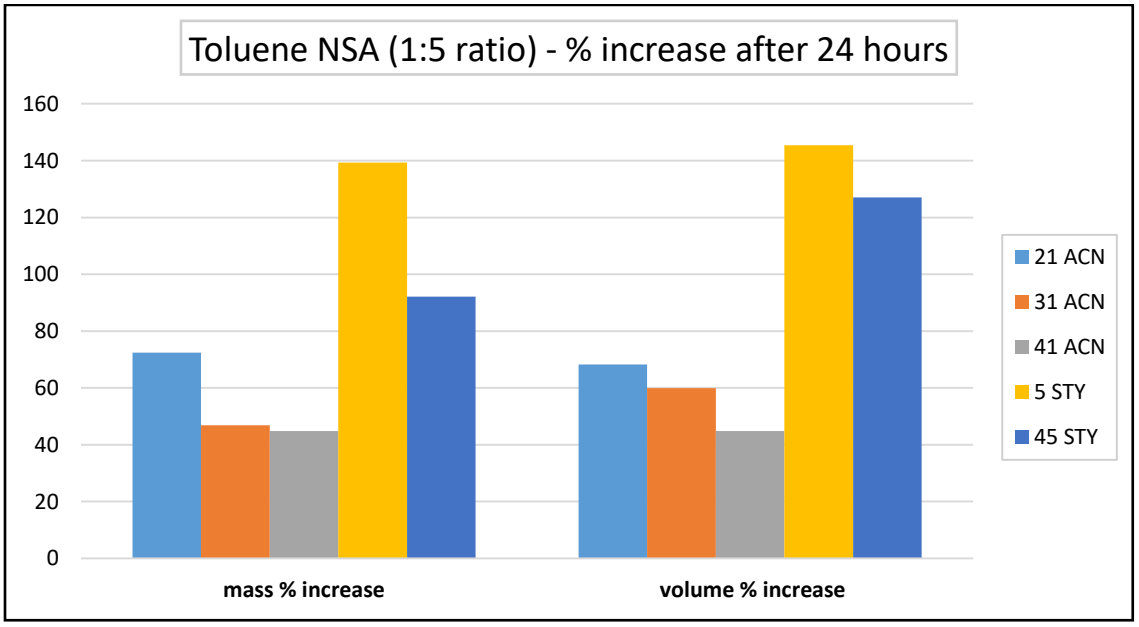

Figure 4-6: Percentage increase of mass and volume for all elastomer specimens in Toluene NSA

Referring to Figure 4-6, the swelling rate of 5STY in Toluene NSA (1:5 ratio) is 145% in just 24hours and this is closely comparable to commercially available oil-based swell packers which can go up to 100%-200% of swelling but with a practical swelling duration of 5 to 100 days [14,

16]. The experiments for Toluene NSA continued on till 72 hours and swelling percentages did not increase any further for all five of the elastomers.

This bonus observation led to the conclusion that specimens reached swelling stability within 24 hours and subsequent experiments were modified to stop after 24 hours of immersion. From Figure 4-7, it became apparent that different elastomers would have different rates of swelling and therefore, should be factored into preceding experiments in order to capture the dynamics of swelling rate with time. The next close contender in Toluene NSA was elastomer 45STY which has gained an impressive 127% volume increase. By lowering the amount of Toluene in the mixture helped produce a stable and effective system.

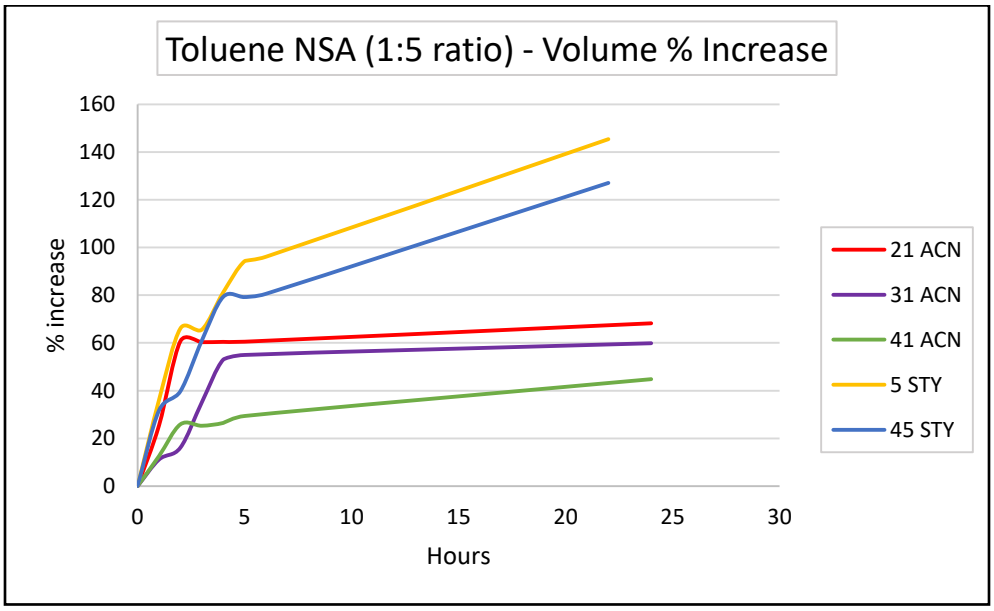

Figure 4-7: Hourly chart for percentage volume increase or swelling percentage for Toluene NSA

Since 41ACN was identified as the only viable elastomer candidate in Xylene NSA, the varying ratio of mixtures were conducted only for 41ACN in order to observe if there are any changes to the results obtained. See Figure 4-8 below.

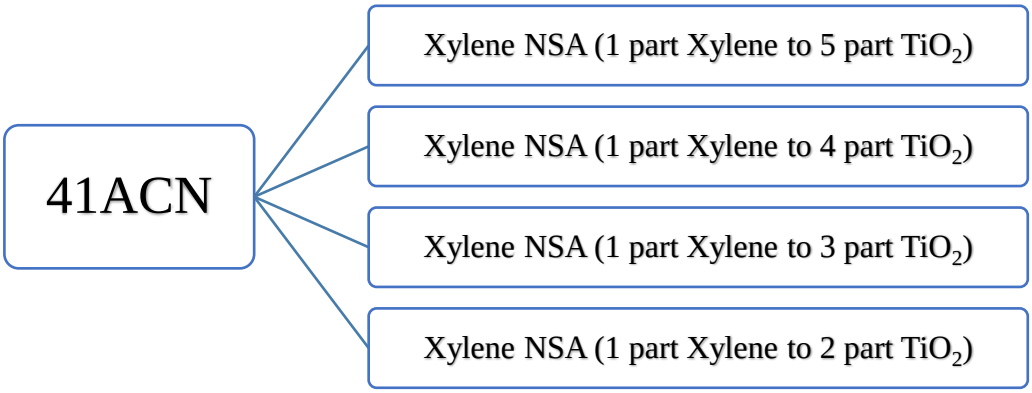

Figure 4-8: Stage 1 experiment 2 for Xylene NSAs

For Xylene NSA systems, the results for decreasing the amount of Xylene in the mixture was not as favorable as it was in the case of Toluene NSA. This action appeared to decrease the percentage of volume as well as mass increase for 41ACN as appeared in Figure 4-9. In 1:1 system, 41ACN had 185% in volume increase whereas in 1:5 system, it only swelled to 69%. This difference between Toluene NSA and Xylene NSA might be due to the fact that Toluene is a stronger primary constituent and hence lesser amount is required for an effective reaction.

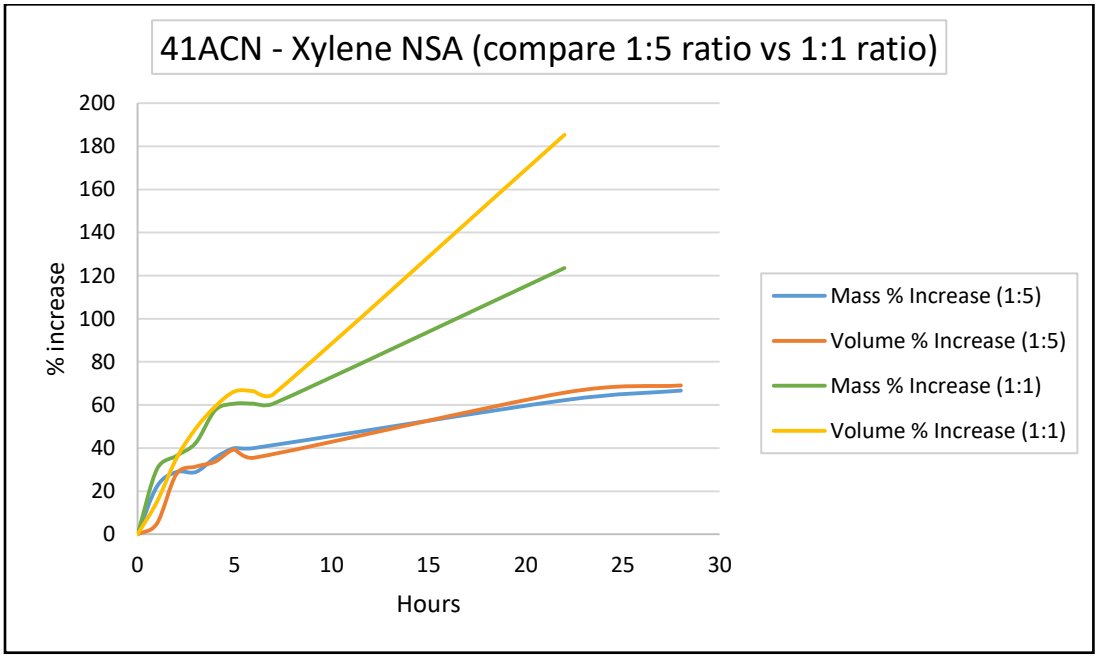

Figure 4-9: Comparing mass and volume percentage increase for Xylene NSA with 41ACN in 1:5 mixture ratio and 1:1 mixture ratio

Figure 4-10 illustrates the volume increase percentages for all three potential NSA systems. It is clear that although 41ACN in Xylene NSA swelled the most at the end of the experiment with 185%, 5STY and 45STY had a higher swelling rate during the first 12 hours. To put things into perspective, take for example it took 4 hours for 5STY to reach 80% volume increase but 9 hours for 41ACN. This phenomenon is noteworthy since available swelling reaction time in an operation could be an important factor in deciding which system would perform best.

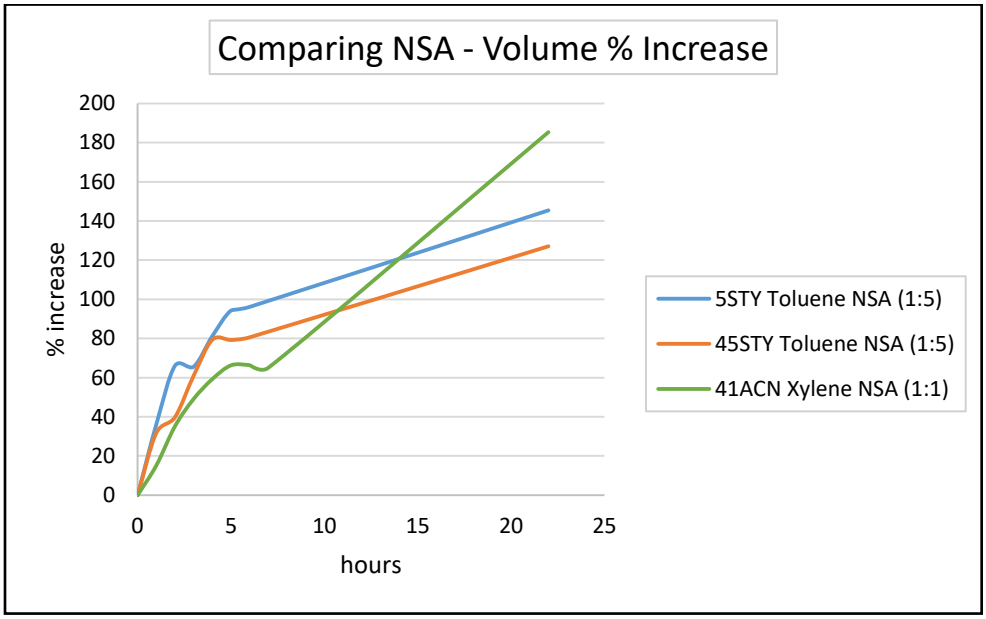

Figure 4-10: Comparing volume increase percentages among all three potential NSA with their respective elastomers

At the end of stage 1 experimentations, three potential systems in NSA have been identified for further experimentation.

	21ACN	**31ACN**	**41ACN**	**5STY**	**45STY**
Toluene with 15wt% TiO_2 (1:5)	Swelled 68%	Swelled 59%	Swelled 44%	Swelled 145%	Swelled 127%
Xylene with 15wt% TiO_2 (1:1)	Swelled 167% but too soft	Swelled 70%	Swelled 185%	Swelled 116%	Swelled 82%

Table 4-2: Successful NSA systems at the end of stage 1. Green boxes indicates potential candidates

4.2 Stage 2 Results and Discussions: Elimination of Possible Swelling Effect from Other Constituents of NSA

As detailed in section 3.3.2 as part of the experiment procedures, three separate experiments were conducted in stage 2 in order to study the effects of the other constituents of NSA. In the first experiment, all five elastomers were immersed in distilled water and showed no signs of any reaction after 24 hours. The pictures as per Figure 4-11 and Figure 4-12 showed the specimens after which were exactly the same as before immersion.

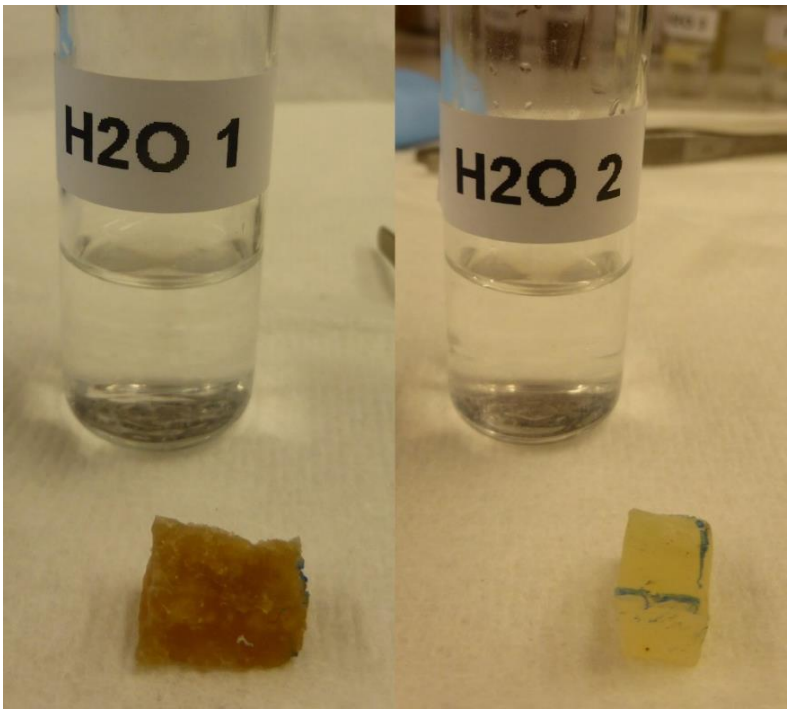

Figure 4-11: Elastomers after 24 hours of immersion in distilled water. 21ACN (left) and 31ACN (right)

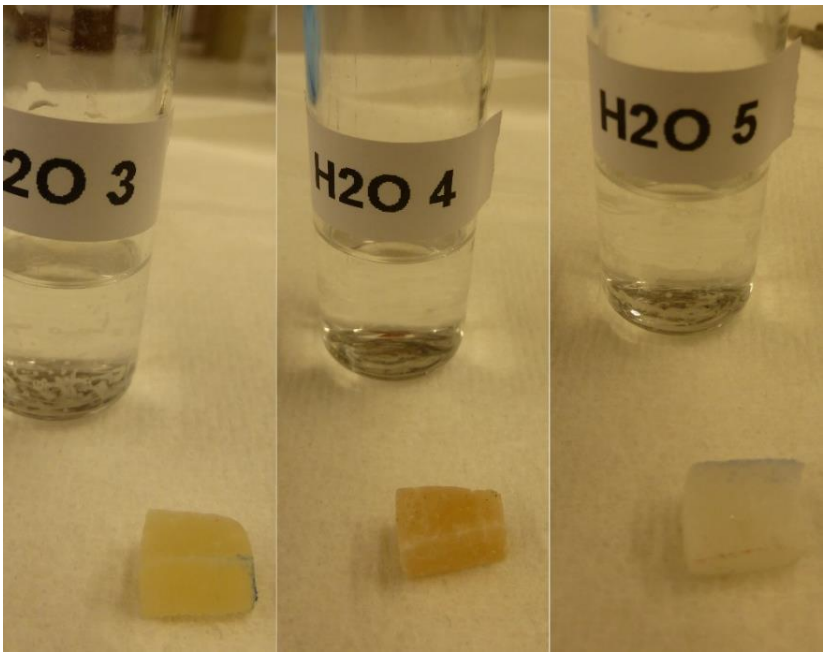

Figure 4-12: Elastomers after 24 hours of immersion in distilled water. From left to right, 41ACN, 5STY and 45STY

Table 4-3 details the measurements taken for all experiments in stage 2. The mass and volume percentage increase for experiment 1 is 4.7% at the highest and can be considered negligible when put side by side with the results from stage 1. It can also be construed as potential measuring equipment parallax error since the percentages were so insignificant. This result is a welcome one as accidental exposure of swell packer elements to water any time during the operations will not generate any form of reactions and unwanted swelling, subsequently causing potential well hang ups.

In experiment 2, the elastomers immersed in pure TiO_2 nanoparticle solutions also did not yield any reaction. Both mass and volume increase percentages were very minor with 4.5% as the highest and this concludes that elastomers will only swell effectively in the presence of both a primary constituent as well as a nano-based catalyst as discussed in stage 1. Without one another, the solution will not bear any desirable results.

For experiment 3 where elastomers were covered with emulsifier, the result indicates that it does not interfere with the swelling process as it generates no effect. Except for a coat of viscous and tacky fluid on the specimens, no other visible alterations were observed. Although the presence of

emulsifier does not seem to affect the NSA, the amount used to assist in ensuring a homogenous mixtures were still kept to a minimal for preceding experiments.

	Pure Water	**TiO_2 Nanoparticles Solution**	**Emulsifier**
21ACN	Mass Increase: 0% Volume Increase: -2%	Mass Increase: 3% Volume Increase: 4.5%	Volume Increase: 2.6%
31ACN	Mass Increase: 0% Volume Increase: 3%	Mass Increase: 1.7% Volume Increase: -4.5%	Volume Increase: 0.4%
41ACN	Mass Increase: -3.8% Volume Increase: 4.7%	Mass Increase: -5% Volume Increase: 0.2%	Volume Increase: -0.8%
5STY	Mass Increase: 0% Volume Increase: 3.6%	Mass Increase: 1.6% Volume Increase: -4.8%	Volume Increase: -3.3%
45STY	Mass Increase: -2.7% Volume Increase: 1.7%	Mass Increase: 4.1% Volume Increase: -0.7%	Volume Increase: -3.3%

Table 4-3: Results of all experiments in stage 2 after 24 hours

This concludes stage 2 experiments where none of the constituents tested have an effect on the elastomers.

4.3 Stage 3 Results and Discussions: Investigating the Effects of Acidic Versus Basic Conditions

The best systems determined from stage 1 (refer to Table 4-2) were subjected to further examinations in stage 3 for the effects of acidic or basic environment. Before proceeding with the results and discussion for this stage, it is worth noting down some of the physical changes of the NSA mixtures after pH alterations. Toluene NSA and Xylene NSA are naturally acidic with a pH of less than 2, it is also a slightly viscous fluid when left standing and undisturbed. With the addition of 5% Sodium Hydroxide (NaOH) to modify the pH into basic for both the solutions, the mixtures appeared visibly less viscous when handled and the coloration were whiter than before. This change of coloration indicates that perhaps chemical interaction has taken place and would make for an interesting potential further research topic.

The change of pH also caused some changes to the dispersion in the mixtures. In Toluene NSA high pH solution, white deposits on the surface of the specimens were a lot more noticeable than the lower pH counterpart. On the contrary for Xylene NSA high pH solution, the mixtures appeared to be even more homogenous than the original acidic solutions.

In Table 4-2, even though 5STY in Toluene NSA was a more superior system in terms of volume increase percentages compared to 45STY in the same system. The decision was made to examine 45STY in Toluene NSA (1:5 ratio) for acidic and basic conditions as well to allow a more comprehensive options to select later. Figure 3-19 shown in section 3.3.3 was two specimens of 5STY in Toluene NSA with 1:5 ratio. Figure 4-13 indicates two samples of 45STY in Toluene NSA, sample 3 on the left is the natural acidic conditions with a pH of 1.3 and sample 4 on the right is of pH 11.1 with the addition of 5% NaOH solution.

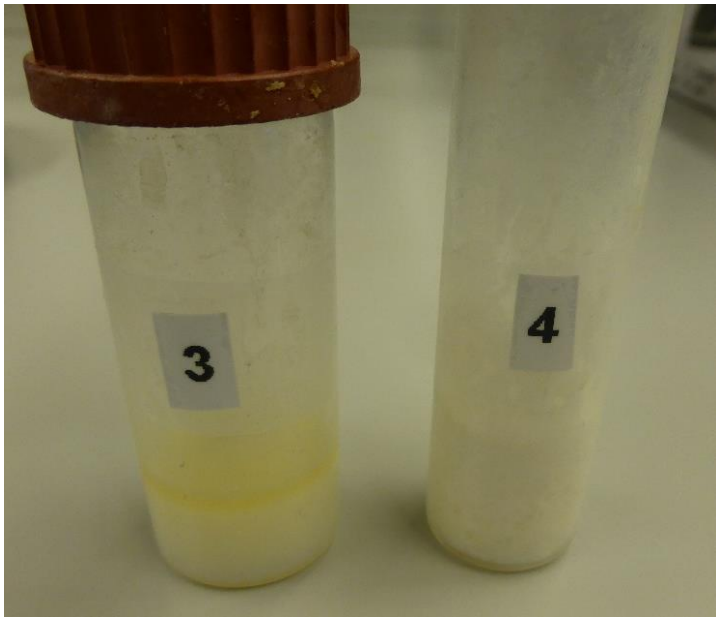

Figure 4-13: 45STY in Toluene NSA, left is acidic while right is basic

Figure 4-14 shows 41ACN elastomers in an acidic Xylene NSA system (sample 5) and a basic system (sample 6), both with 1:1 ratio per results from stage 1. The natural pH of sample 5 Xylene NSA is 1.7 and sample 6 is modified to pH 9.8 with the help of 5% NaOH as well.

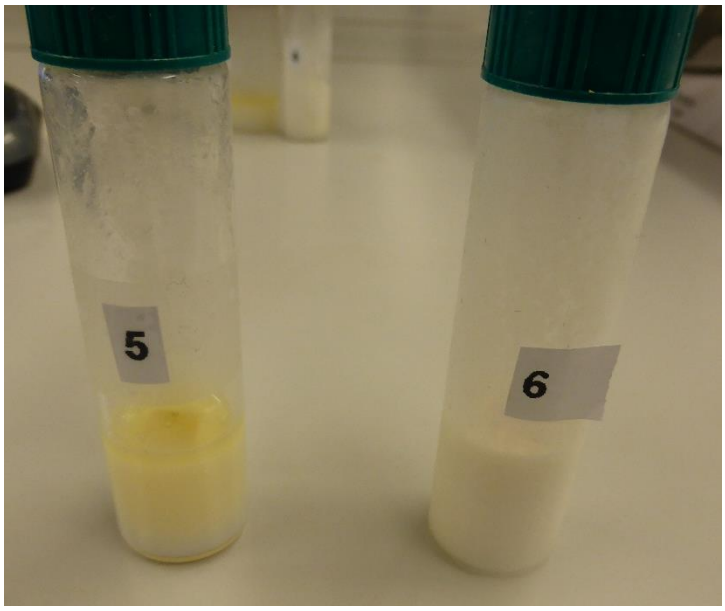

Figure 4-14: 41ACN in Xylene NSA, left sample is acidic while right is basic system

Figure 4-15 shows the comparative results for 5STY elastomer immersed in acidic Toluene NSA versus basic. The favorable outcome from this experiment is clearly evident with the volume

increase percentage gap between acidic conditions and basic to be an astounding 100%. The basic Toluene NSA did not perform well and this could be attributed to the fact that the chemical composition of the solution might have been altered due to the pH change. Care was taken to rinse and wipe off the additional precipitation of deposits on the surface of the specimens before measurements were taken.

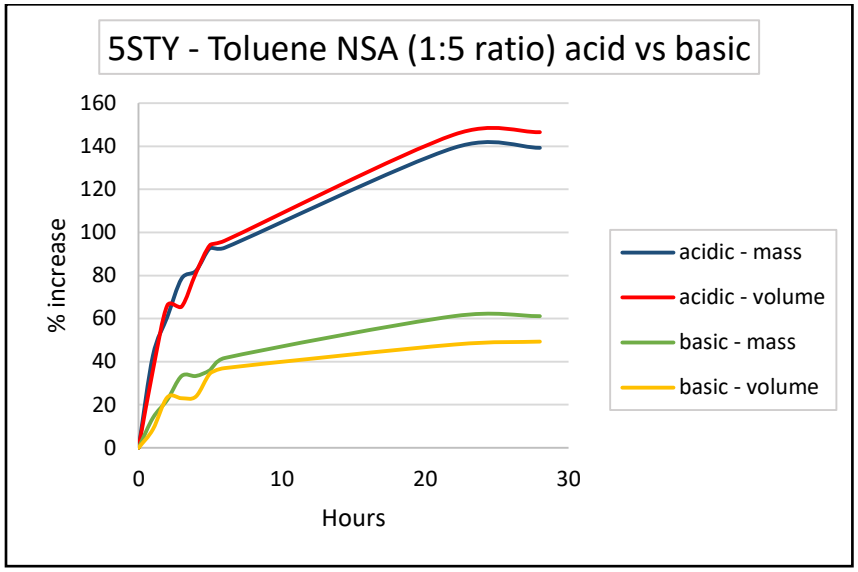

Figure 4-15: 5STY in Toluene NSA acid and basic solutions

The 45STY elastomer in this experiment behaved similarly to the 5STY above with acidic system volume increase percentages surpasses the basic. The difference between the two however was lower with 35% for volume increase and less than 20% for mass as per Figure 4-16.

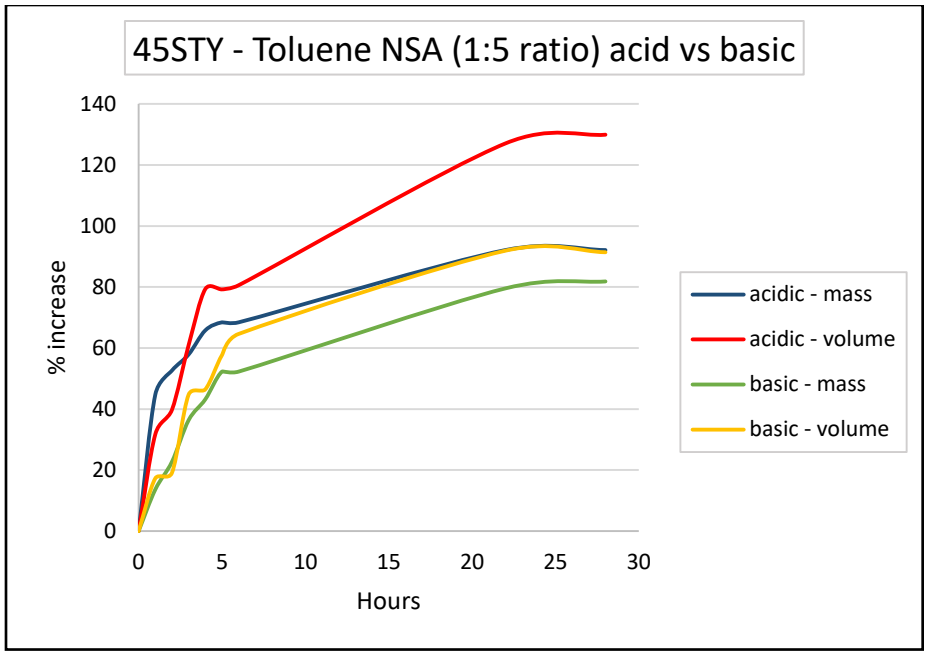

Figure 4-16: 45STY in Toluene NSA acid and basic systems

The results from Xylene NSA systems were the most interesting and surprising as both the acidic system and basic performed on par with each other and the difference between the two in volume increase percentages was negligible. This outstanding performance by both systems could be explained by the solution homogeneity as described earlier.

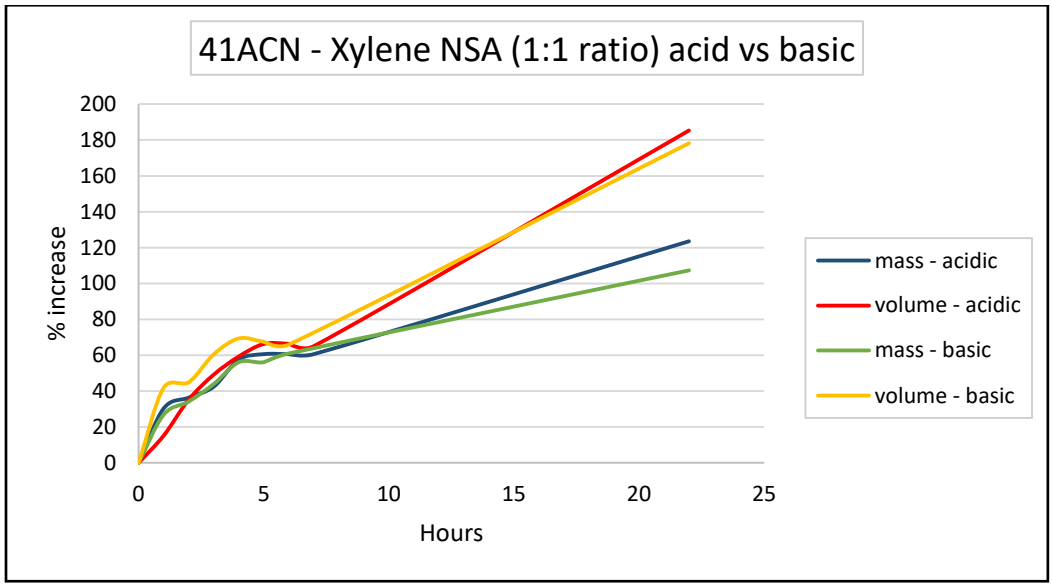

Figure 4-17: 41ACN in Xylene NSA acid and basic solutions

Stage 3 experiments successfully distinguish the effects of low versus high pH for the potential NSAs. The goal of this stage is only to establish what the effects of acid or basic conditions are for the elastomers and hence the individual pH numbers were not taken into account. Figure 4-18 summarizes conclusively that 5STY in Toluene NSA is better than 45STY for lower pH conditions, however the reverse is true for higher pH and when it comes to 41ACN there is no difference in performance for any pH range.

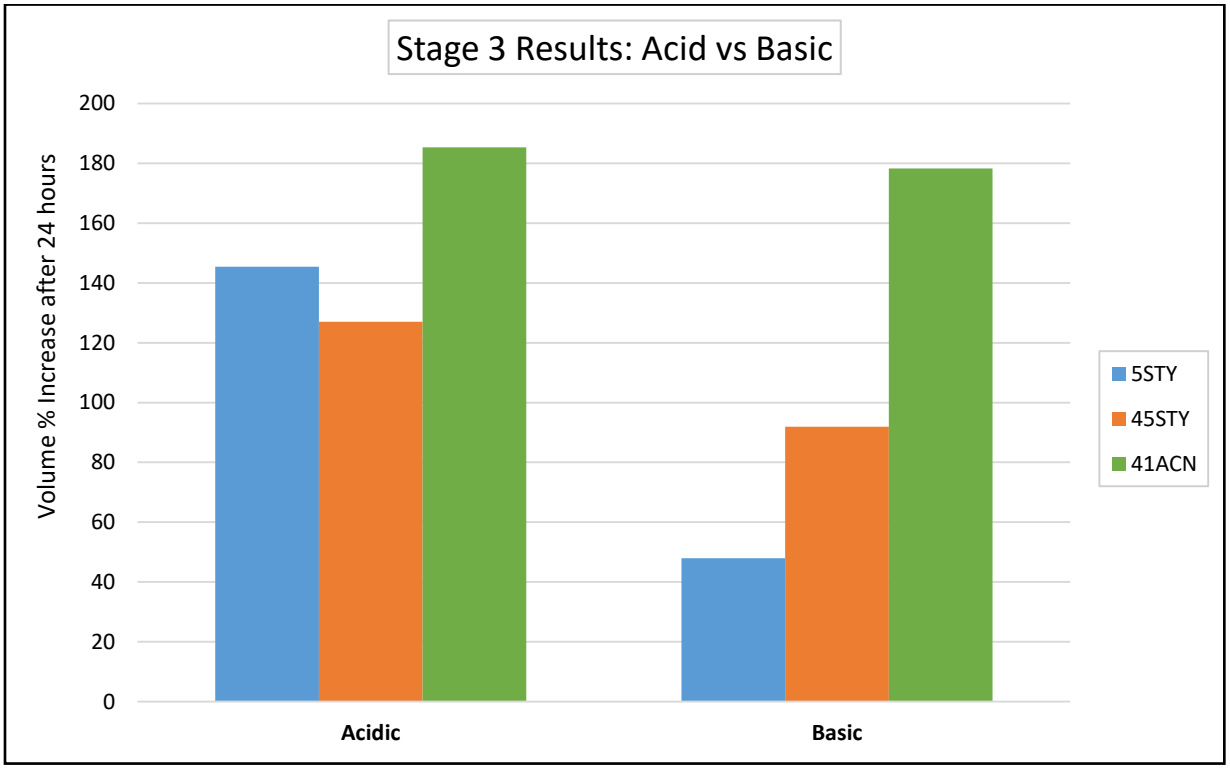

Figure 4-18: Comparative chart for stage 3 results

Choosing the systems with the highest swelling performances, the following systems have been narrowed down to proceed for further investigation in stage 4.

a. 5STY in Toluene NSA (1:5 ratio) acidic
b. 41ACN in Xylene NSA (1:1 ratio) acidic
c. 41ACN in Xylene NSA (1:1 ratio) basic

4.4 Stage 4 Results and Discussions: Studying the Effects of Varying Concentration of Nano-Particle Solutions

As detailed in section 3.3.4, the possibility of lowering the TiO_2 nanoparticle solution concentration while yielding higher volume increase percentages is desirable. This is because a 1wt% TiO_2 nanoparticles solution would be 93% cheaper in cost for an equivalent volume of 15wt% TiO_2 nanoparticle solution. This amount is calculated based on original purchase price of 15wt% TiO_2 nanoparticle solution. The potential huge cost savings would allow for the marketing of NSA swell packers to be even more competitive and enticing when pitted against existing swell packers. This section will look at the results from stage 4 and their cost implications.

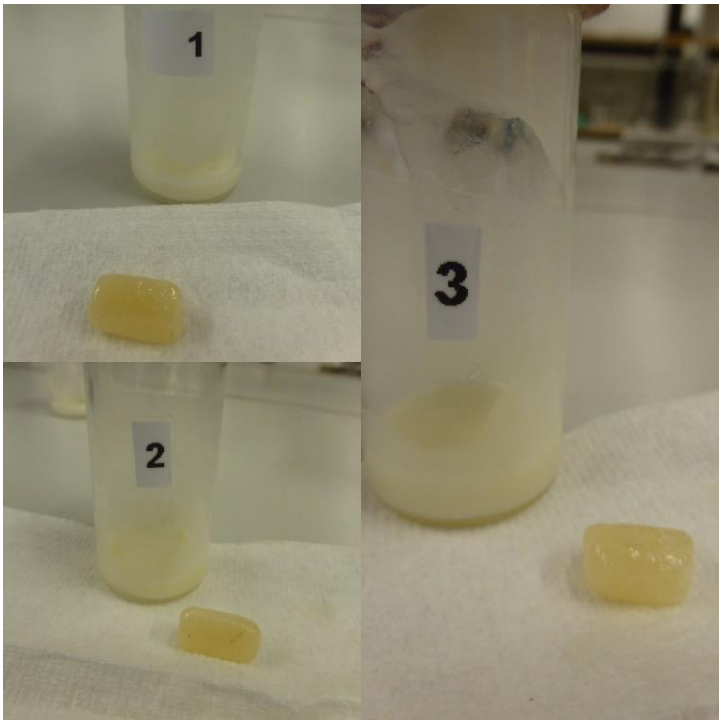

Figure 4-19: 5STY in acidic Toluene NSA with different concentration of TiO_2 after 24 hours

The first experiment in discussion is 5STY in acidic Toluene NSA with 1:5 ratio (Figure 4-20). The 5STY specimens in 1wt%, 5wt% and 10wt% mixtures after 24 hours did not differ much from each other in terms of handling. 10wt% TiO_2 nanoparticles solution in the NSA mixtures outperformed all other combinations in this experiment by quite a good margin. 1wt% and 5wt% mixtures concentrations yielded rather similar results and both have lower volume increase

percentages after 24 hours with only 120%. Not only did 10wt% Toluene NSA generate a higher volume percentage increase with 165%, it also had a higher swelling rate compared to 15wt% Toluene NSA. For instance, after only 2 hours of swelling time, the 5STY specimen in 10wt% Toluene NSA had already reached 111% while in 15wt% it was only at 66% volume increase. Therefore, 10wt% acidic Toluene NSA was chosen for the next stages for specimen 5STY.

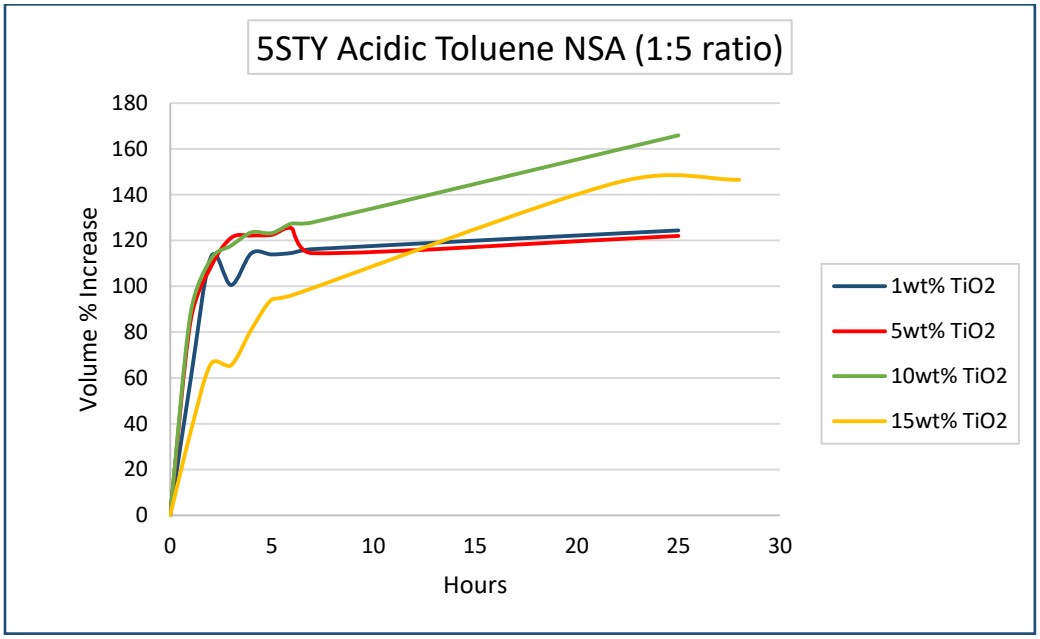

Figure 4-20: Elastomer 5STY in different concentration of TiO_2 for acidic Toluene NSA

The next experiments involved 41ACN in acidic Xylene NSA with a 1:1 ratio for different TiO_2 nanoparticles solution concentration (Figure 4-21). 41ACN in 15wt% Xylene NSA remained the front-runner with the highest amount of 185% in volume increase. Though the swelling rate of the others were slightly higher at the beginning of the experiment, the specimen in 15wt% Xylene NSA quickly caught up 5 hours in and the gap between the swelling rates is not high enough to be of an interest.

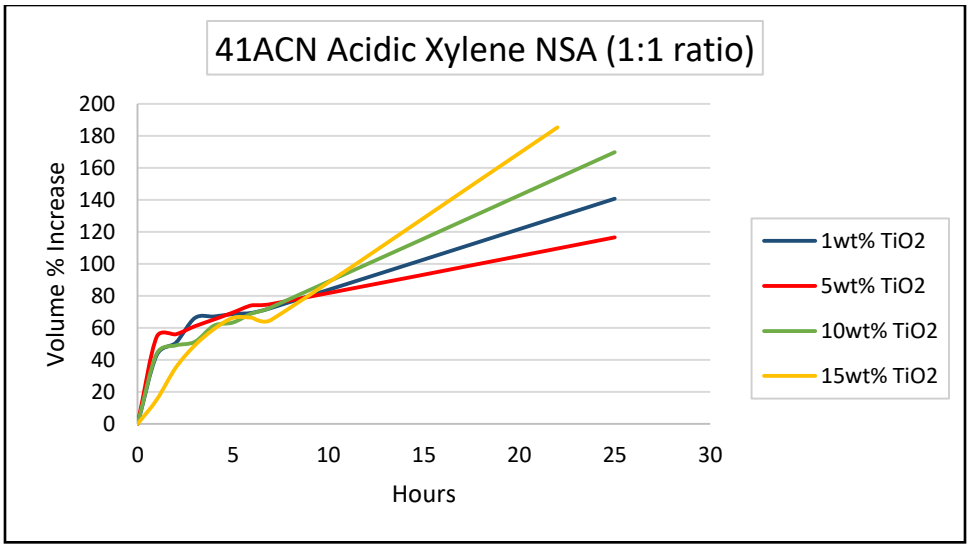

Figure 4-21: Elastomer 41ACN in an array of acidic Xylene NSA solutions with different concentrations of TiO_2

Figure 4-22 shows the results for 41ACN in basic Xylene NSA solutions while varying the TiO_2 nanoparticles concentrations. The results obtained from testing four different concentrations were rather similar though 5wt% and 15wt% systems were just slightly better. 41ACN specimens in 15wt% Xylene NSA still performed the best with 178% in volume increase but 5wt% comes closely behind with 170% at the same amount of hours.

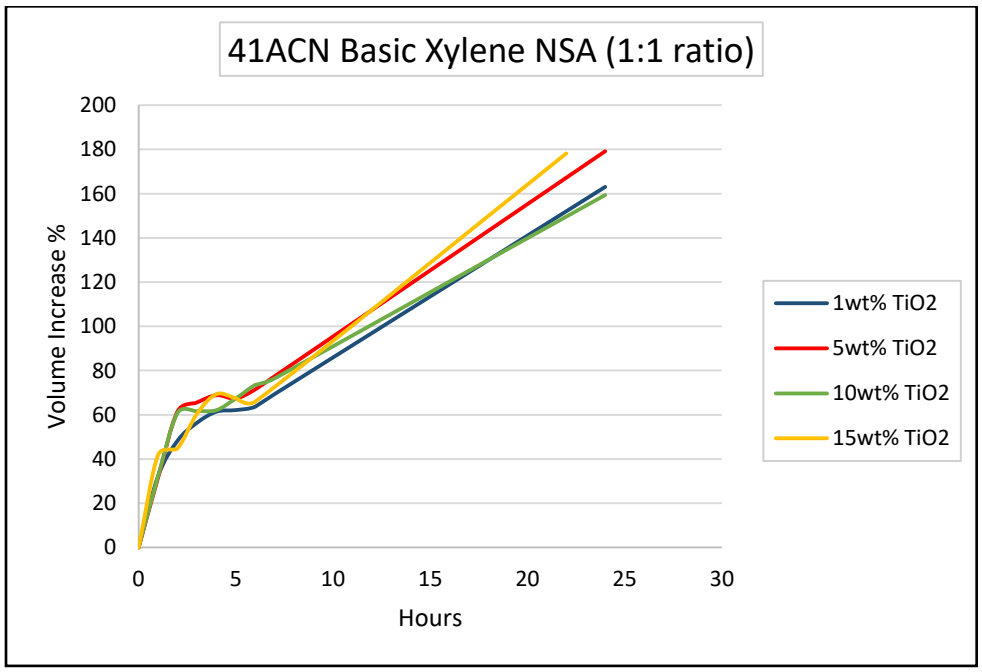

Figure 4-22: Elastomer 41ACN with different concentrations of TiO_2 in basic Xylene NSA

A closer look in Figure 4-23 indicates that the swelling rate between the two also looked to be comparable. Therefore, even though 15wt% Xylene NSA is still technically the best performed system, 5wt% mixture is definitely a close contender considering the potential cost savings. With the same method of quantifying cost as explained earlier in this section, if a 1000ml 15wt% TiO_2 nanoparticles solution cost USD 100, the same volume 5wt% TiO_2 nanoparticles solution would only be USD 33.

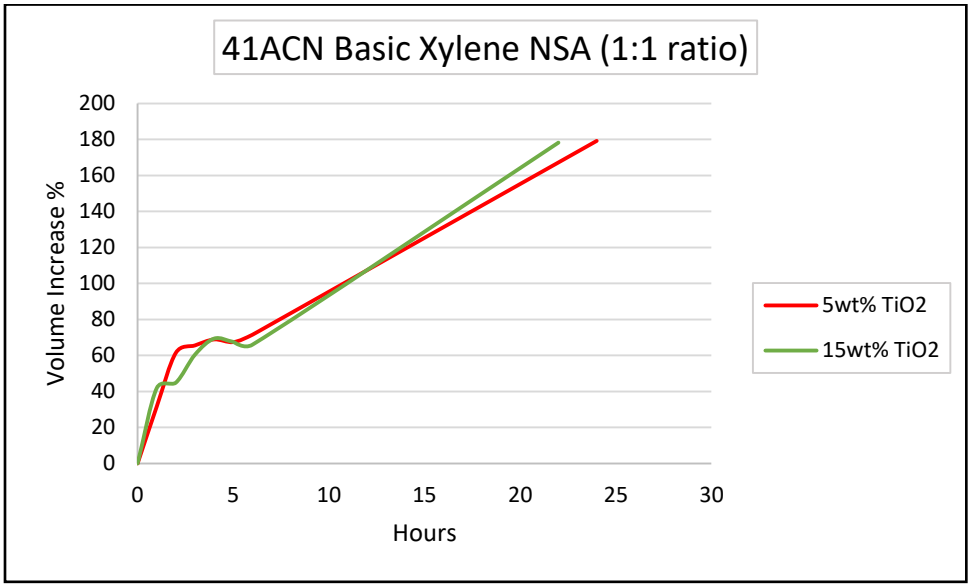

Figure 4-23: Closer look at 41ACN in basic Xylene NSA for 5wt% and 15wt%

In Figure 4-24 all four of the best systems were compared. Interestingly, regardless of the TiO_2 nanoparticle solution concentration used in Xylene NSA, the outcome of the volume increase are very similar.

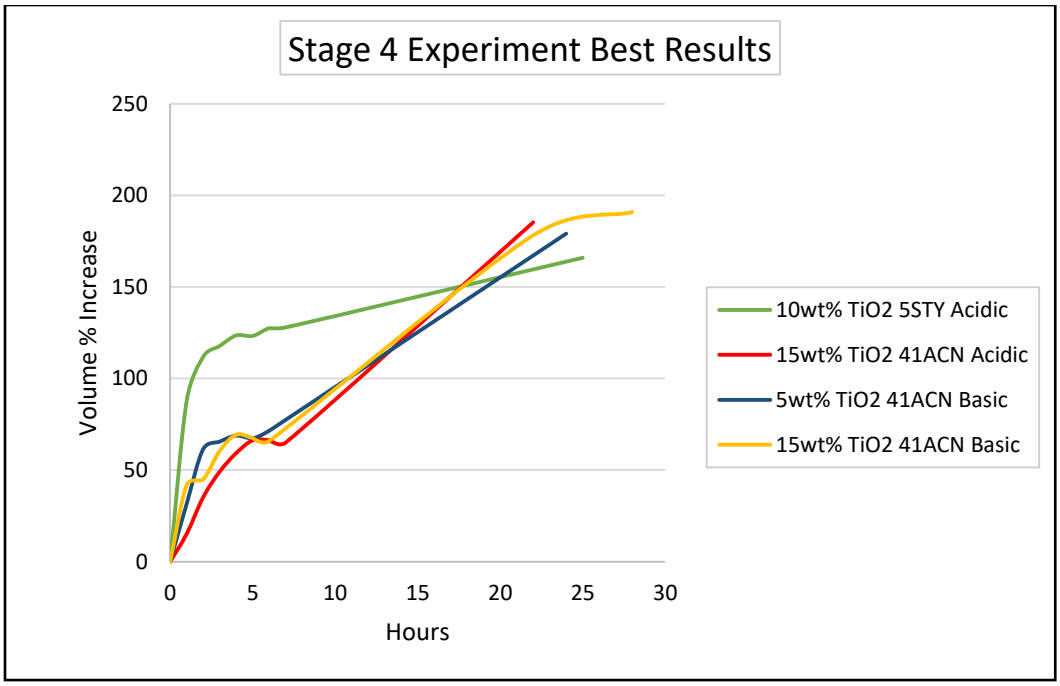

Figure 4-24: Stage 4 best systems

Figure 4-25 further narrows it down to only best performing systems in acidic conditions. Elastomer 5STY in 10wt% Toluene NSA had a much faster swelling rate than 41ACN in 15wt% Xylene NSA. In just 5 hours into the experiment, it has grown 123% in volume while 41ACN only experienced 66% in volume increase. With the cost of 10wt% TiO_2 nanoparticles solution only 67% of 15wt% TiO_2, it might be tempting to rule out 41ACN in 15wt% Xylene NSA immediately. However, the latter eventually redeemed itself and had a higher end volume increase with 185% while 5STY tapered down to 165%.

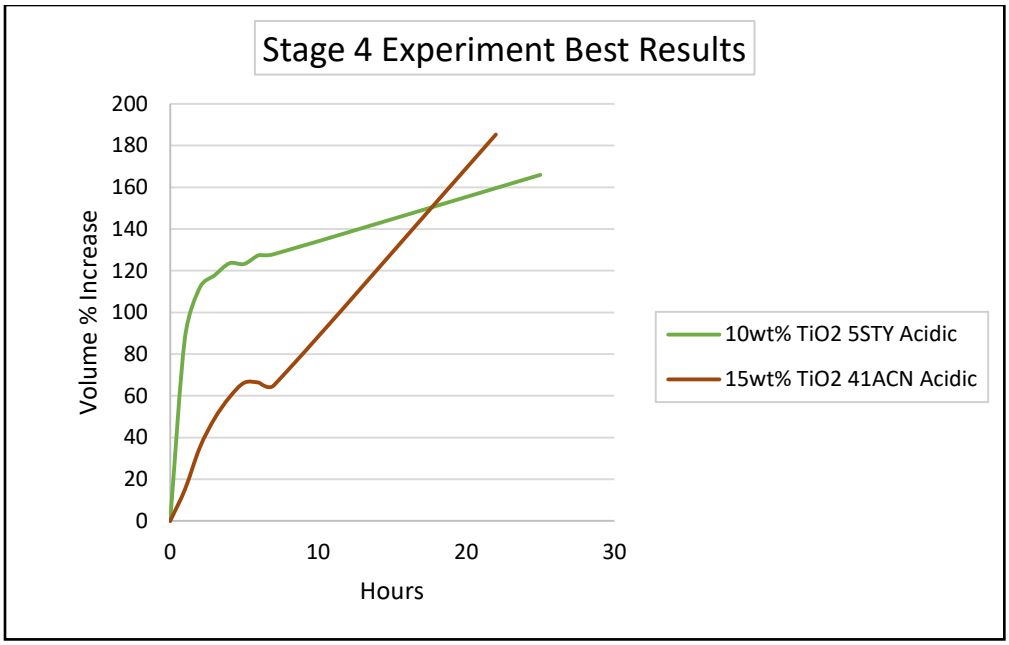

Figure 4-25: Stage 4 best systems in acidic conditions

The cost implication also need to factored in the ratio of liquid used since Toluene NSA is a 1:5 ratio while Xylene NSA is 1:1 and will be further discussed in section 5.3 as part of the NSA selection chart building process. All four of the best systems will move on to the next stage as each elastomer NSA combination has its pros and cons in terms of operation time needed, swelling rate, potential cost savings and wellbore conditions.

4.5 Stage 5 Results and Discussions: Temperature Effects on NSA

As detailed in section 3.3.5, the purpose of this stage is to examine the effects higher temperatures have on the elastomeric NSA systems and to document the observations rather than to functionally qualify the suitability of these systems in a higher temperature range. The varying temperatures 40°C/104°F, 60°C/140°F and 80°C/176°F chosen for this experiment is both for simulation and practical purposes. Since the experiments run through the night for a period of 24 hours, the temperature chosen was at a level where the laboratory engineers were comfortable with its safe handling.

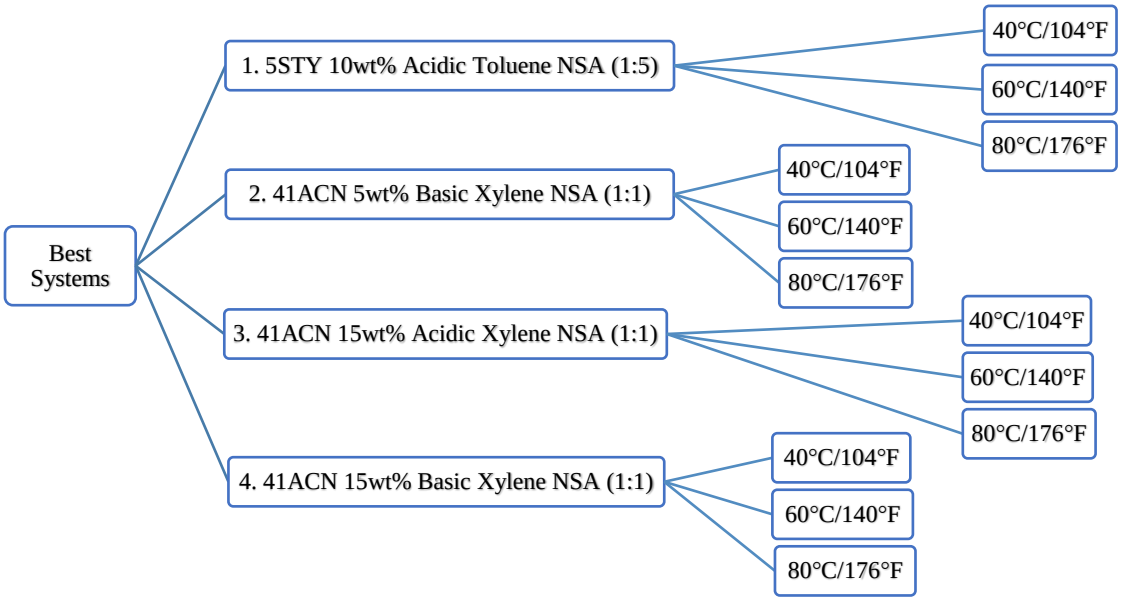

Figure 4-26: Stage 5 experiments setup

For ease of illustrations and comparisons, the charts in this stage will be presented as per Figure 4-27 and Figure 4-28. In the previous stage, four working elastomer NSA systems were narrowed down (refer to Figure 4-26) among which 5STY in 10% acidic Toluene NSA (1:5 ratio) was determined to have a higher swelling rate than the rest. While the three 41ACN systems lack behind in swelling rate, the ultimate volume increase percentages for these three systems were higher than of 5STY.

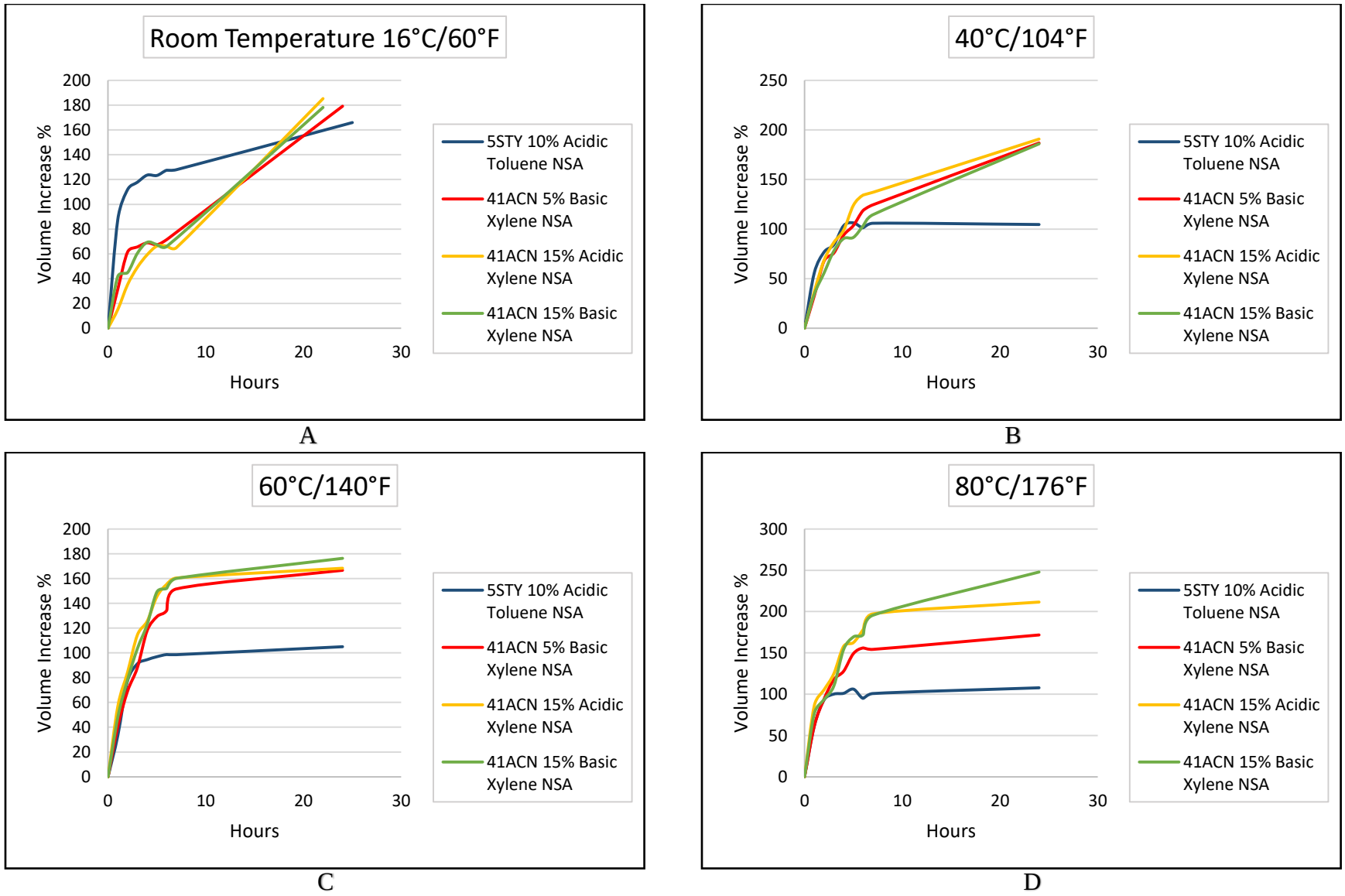

Figure 4-27: Volume Increase percentages for various temperature

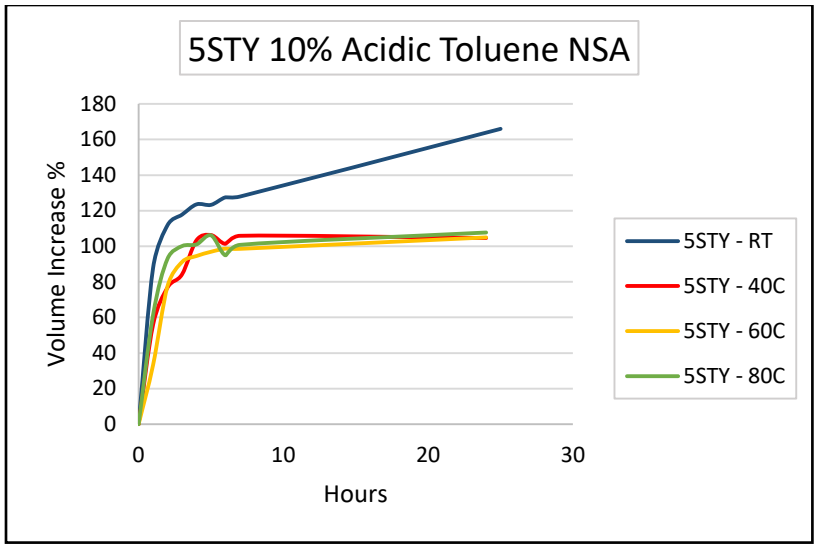

A

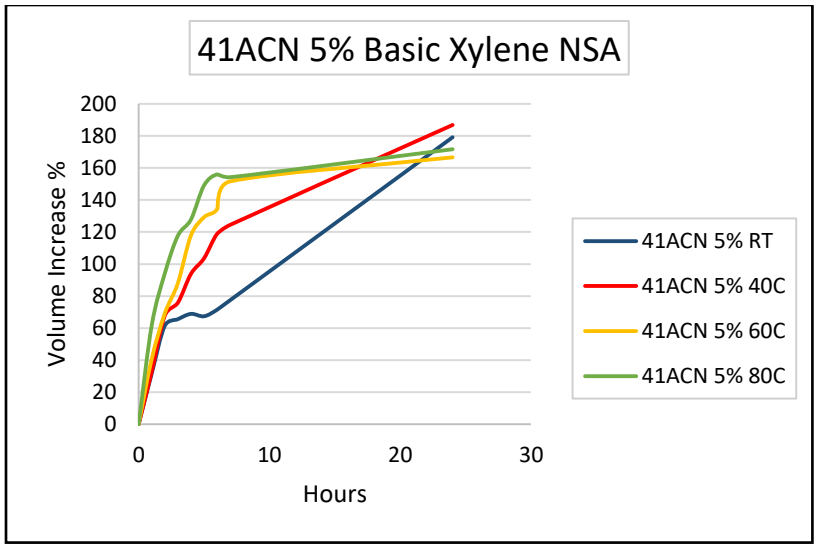

B

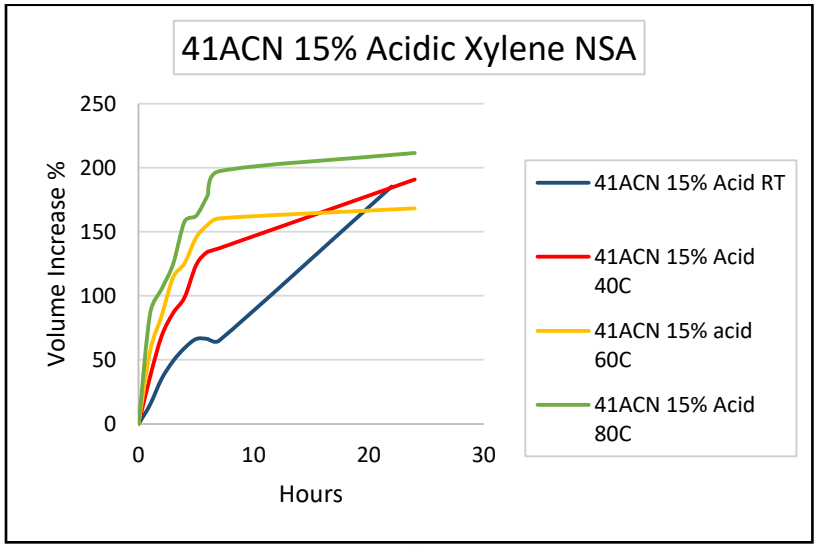

C

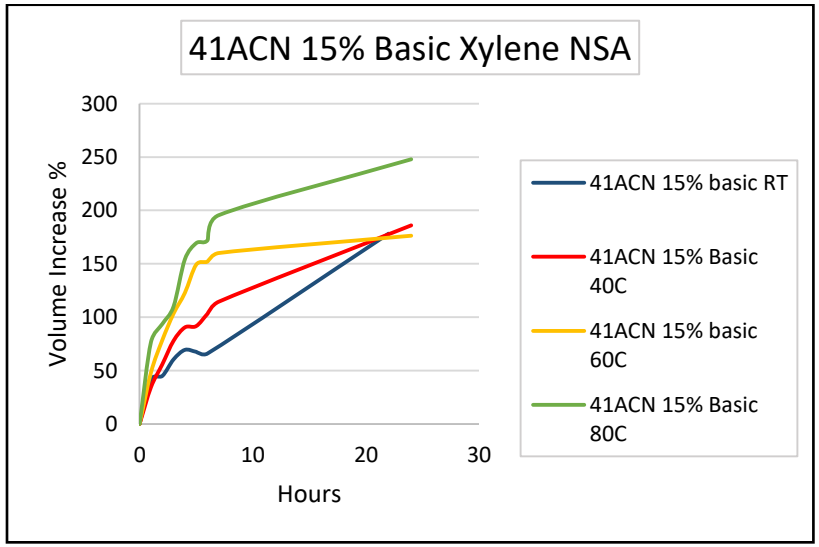

D

Figure 4-28: Comparative chart for different elastomeric NSA systems in different temperature

For experiment in 40°C/104°F as shown in Figure 4-27 (B), the higher temperature seemed to have reduced the rate of swelling for 5STY in 10% Toluene NSA as well as its volume increase percentage after 24 hours to 104%. The 41ACN systems in 5% basic, 15% acidic and basic Xylene NSA however were affected by this elevated temperature. The volume increase hovers about 185% for all three systems which is comparable to the results obtained in controlled room temperature. Though the final volume increase amounts to the same as controlled temperature, the swelling rate appeared to be higher. After just 5 hours into the experiment, the 41ACNs had swelled up to 100% while in controlled temperature it was only about 60%.

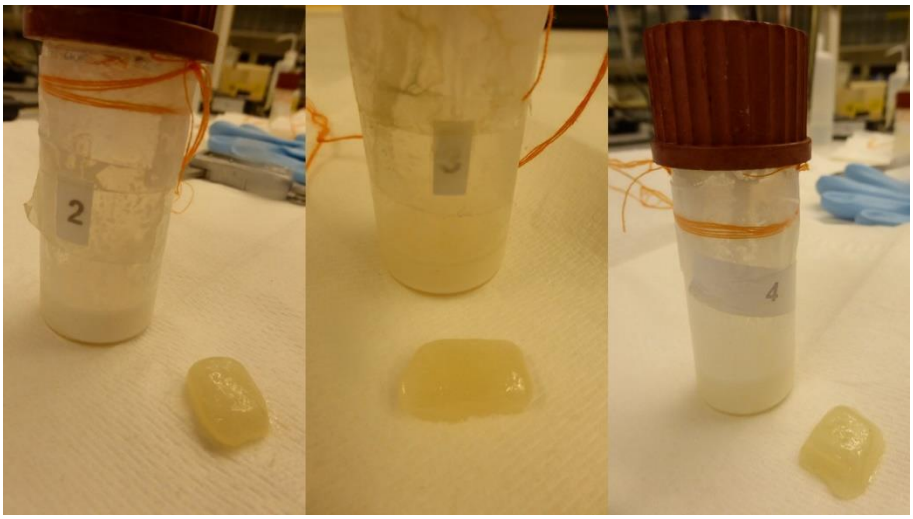

Figure 4-29: 41ACN elastomers in different systems after 24 hours in 40°C/104°F experiment

In the experiment for 60°C/140°F as shown in Figure 4-27 (C), the results obtained were very similar to the experiment in 40°C/104°F. 5STY in 10% acidic Toluene NSA achieved the same volume at 104% before stabilizing and 41ACNs in the other 3 systems swelled to a little lesser at 170%. The swelling rate however seemed to be even better in this experiment than the previous for the 41ACNs as it reached 120% with just 5 hours. Compared to 40°C/104°F, that is a 20% increase in volume expansion.

In the experiment for 80°C/176°F, things got little bit more interesting as the three 41ACN systems have different swelling reactions. 41ACN 15% Xylene NSA had similar reactions for both acidic and basic environment up to hour 7, then it separates with 41ACN 15% basic system ultimately having a higher volume increase with 247% while 41ACN 15% acidic system tapered off to 211%.

5STY in 10% acidic Toluene seemed to be behaving the same way as previous experiments as well.

To compare how all the systems have performed overall in different temperature, Figure 4-28 serves as a better indicator. As discussed previously, 5STY in 10% acidic Toluene NSA seemed to be performing rather consistently regardless of the higher temperature administered. Figure 4-28 (A) shows that the highest volume increase for 5STY system happened in controlled room temperature, while the elevated temperature did reduce the volume expansion, the specimen remained stable physically as per Figure 4-30.

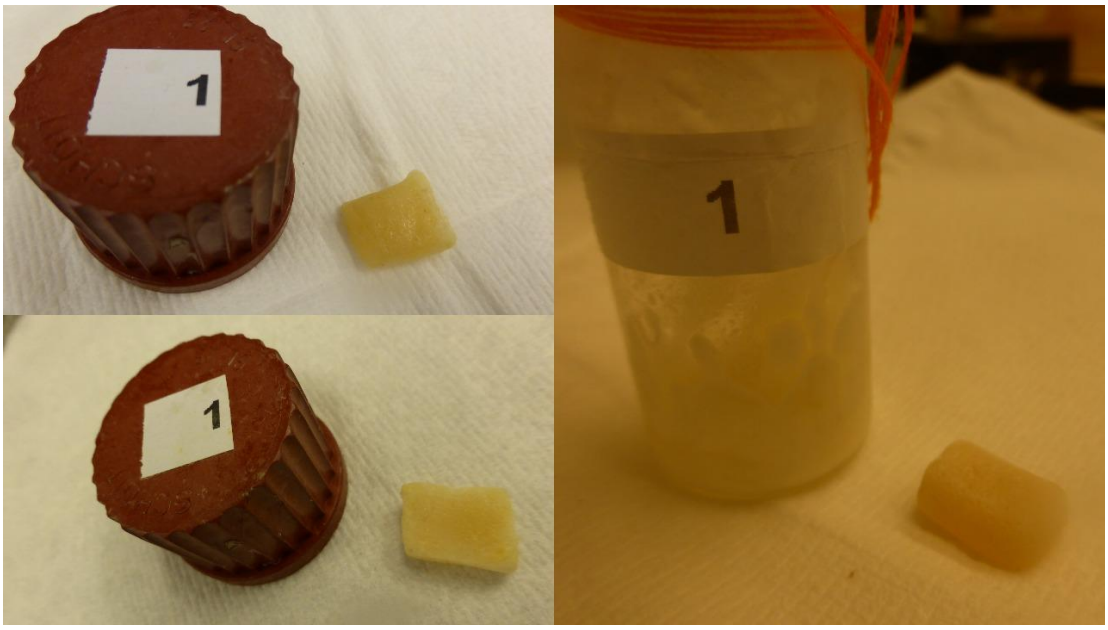

Figure 4-30: 5STY specimens after 24 hours in experiments with temperature 40°C, 60°C and 80°C

Figure 4-28 (B) (C) (D) made it clear that with increasing temperature, the swelling rate also increases for 41ACN specimens in all three systems. 41ACN in acidic and basic 15% Xylene NSA had the highest volume expansion in 80°C/176°F while 41ACN in 5% basic Xylene NSA was an anomaly with the highest volume increase percentages for 40°C/104°F though the outcome from 60°C/140°F and 80°C/176°F trail closely behind. This stage's results gave some important information and insights on volume expansion modeling for potential elastomeric NSA systems as temperature may or may not positively affect the final outcome and it is important to have an accurate model when choosing the suitable swell packer for operational use.

In summary, 5STY in 10% acidic Toluene NSA performed best at lower temperatures while 41ACN in 5% basic Xylene NSA did not differ much for any of the temperature. At higher temperatures, 41ACN in 15% Toluene NSA acidic or basic systems were the best performing systems.

4.6 Stage 6 Results and Discussions: Water-based Mud vs Oil-based Mud

In this last stage, the two front runner elastomers 5STY and 41ACN were put to tests in WBM and OBM in order to help create a better selection chart which will be discussed further in section 5.2. The most commonly available 80/20 oil water ratio OBM and 5% bentonite WBM were used in this experiment to simulate the likely contaminant accessible on rig sites using the essential components typically found in the fluid mixtures. The default 15wt% TiO_2 nanoparticles solution was also added to the muds for additional testing.

Figure 4-31: 5STY after 24 hours testing in OBM and OBM with TiO_2 nanoparticles solution

Figure 4-31 shows the results for 5STY elastomer after a 24 hours immersion in OBM as well as OBM with TiO_2 nanoparticles solution. Physically the specimen in pure OBM was coated with a layer of mud and had to be rinsed and cleaned multiple times before an accurate measurement could be taken. The coloration of the specimen also changed after 24hours and no longer resembled its original state. 5STY had a volume expansion of 87% in pure OBM and would therefore have an impact on the NSA selection chart as it might not be suitable in operations employing OBM

systems. The physical changes were not as obvious in OBM with TiO_2 nanoparticles solution as there is no evidence of coloration and physical changes of the specimen. Dimensional measurements revealed that the specimen gained about 54% in volume after a period of 24 hours. While this is a noteworthy observation, the amount of swelling is far lesser than any of the NSA systems we have explored in previous stages and hence deemed to not worthwhile to be pursued as an area of interest.

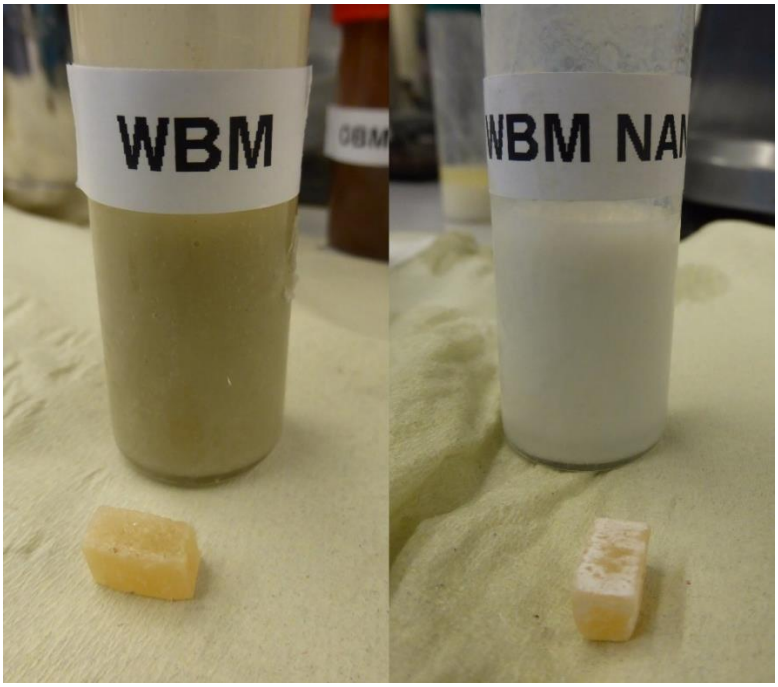

Figure 4-32: 5STY after 24 hours testing in WBM and WBM with TiO_2 nanoparticles solution

The 5STY specimens immersed in WBM and WBM with TiO_2 nanoparticle solutions as illustrated in Figure 4-32 had no visible physical changes after 24 hours of testing. The mass and volume changes measurements reflects this with 0% and 0.9%. This means that 5STY elastomeric NSA systems will be safe in the operational use with WBM fluids presence. 41ACN specimens were also exposed to OBM and OBM with TiO_2 nanoparticles for testing and they lacked any reaction in pure OBM as per Figure 4-33. The dimensional measurements concurred with this finding with -3% as expansion which could be attributed to measurement inaccuracies. 41ACN in OBM with TiO_2 nanoparticles solution yielded some swelling at 14%, however this amount is again too insignificant to warrant an in-depth study of this combination.

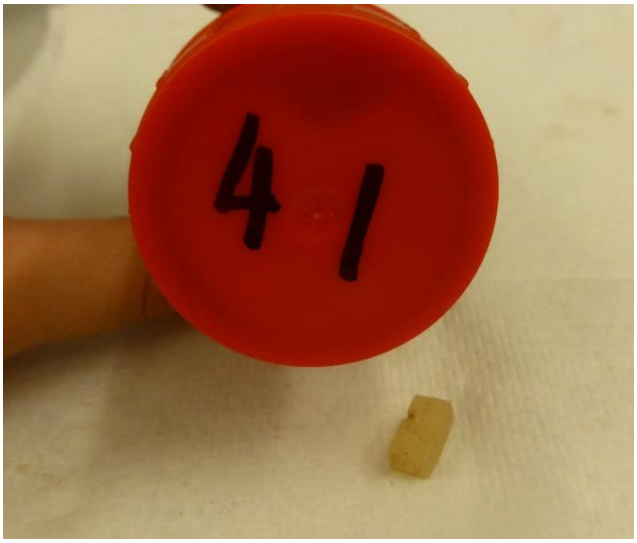

Figure 4-33: 41ACN in pure OBM after 24 hours

This outcome means that the 41ACN systems are good candidates for operational use if OBM is part of the job without the risks of premature swelling or accidental well hang ups. In the last experiment, 41ACN specimens were left exposed to WBM and WBM with TiO_2 nanoparticles solution for a period of 24 hours like the others. From Figure 4-34, the results are strikingly clear that no reaction or swelling has taken place as the specimens looked exactly the same as before fluid immersion.

Figure 4-34: 41ACN after 24 hours testing in WBM and WBM with TiO_2 nanoparticles solution

Table 4-4 below summarized the results for stage 6. Overall, 41ACN and 5STY NSA systems would be safe in a WBM operation while only 41ACN is recommended in the presence of OBM to avoid any unnecessary problems and cost.

	5STY	**41ACN**
OBM	Mass Increase: 80% Volume Increase: 87%	Mass Increase: 0% Volume Increase: -3%
OBM with TiO_2	Mass Increase: 42% Volume Increase: 54%	Mass Increase: 2.4% Volume Increase: 14%
WBM	Mass Increase: 0% Volume Increase: 0.9%	Mass Increase: 0% Volume Increase: -1.5%
WBM with TiO_2	Mass Increase: 0% Volume Increase: 1.2%	Mass Increase: 0% Volume Increase: -1.3%

Table 4-4: Stage 6 results summary

5 Summary: Analyses and Further Discussions

5.1 Narrowing Down to the Optimized Swelling Systems

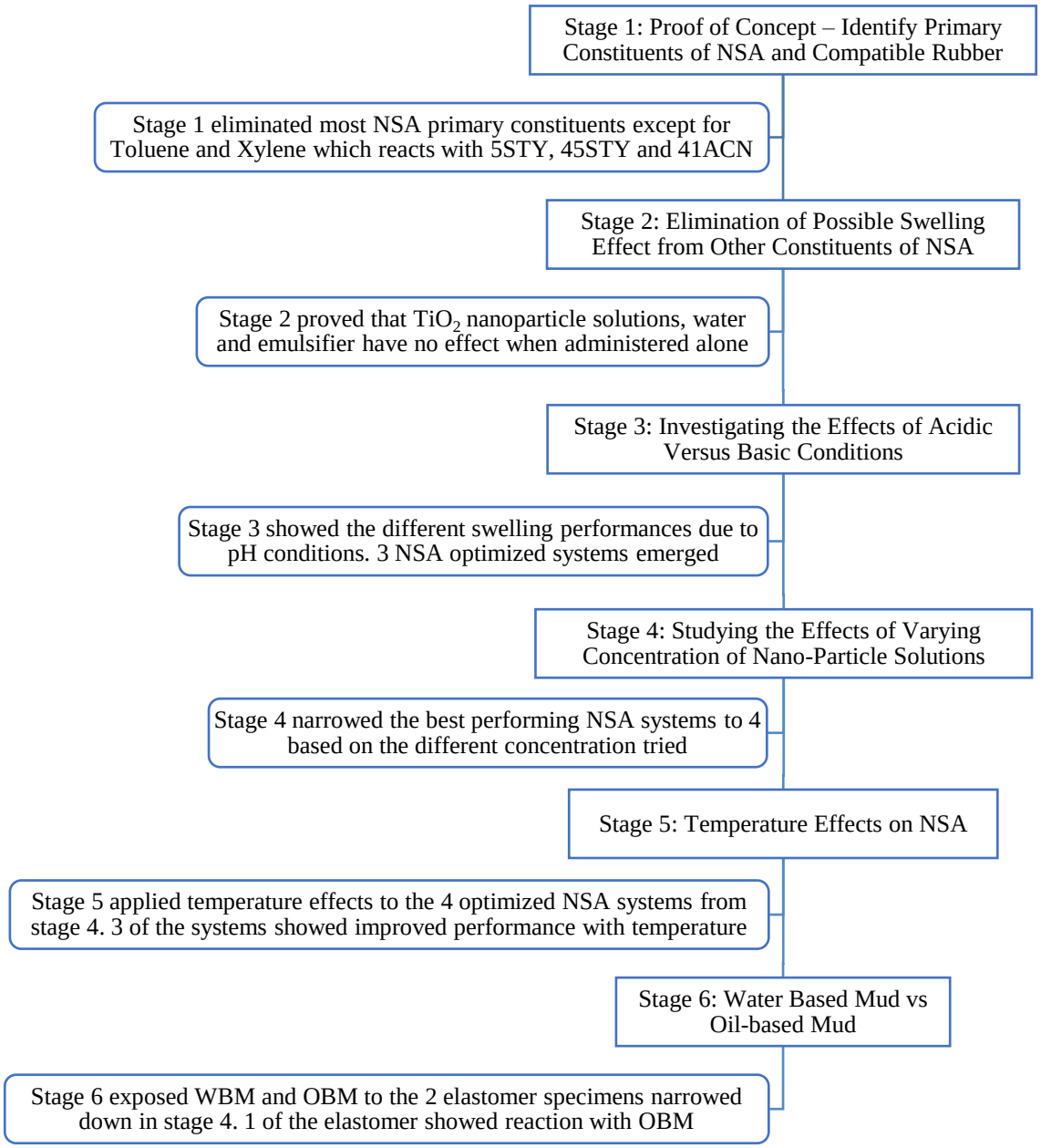

Figure 5-1: Summary of experimental work from Stage 1 to Stage 6

Figure 5-1 shows a summary of the overall process of systematically narrowing down from the initial candidates consisting of 5 elastomer specimens and 4 primary NSA constituents (identified at the start of stage 1), to the final 4 best performing systems (at the end of stage 6).

The main goal in Stage 1 was to identify suitable combinations of primary constituents and TiO_2 nanoparticle solutions with elastomer specimens which demonstrated promising swelling behavior. 3 potential systems were pinpointed after a series of 24-hour experiments. 5STY and 45STY with Toluene based NSA as well as 41ACN with Xylene based NSA showed good swelling performance.

The sole purpose of Stage 2 was to examine if the individual NSA constituents, specifically - TiO_2 nanoparticle solution, water and the emulsifier - might have had any swelling effects on the elastomer specimens. The experiments at this stage demonstrated that none of the examined constituents caused elastomer swelling when administered alone.

Stage 3 investigated the role acidic and basic conditions played on the 3 potential systems narrowed down in Stage 1. 5STY and 45STY in Toluene NSA performed better in acidic environment while 41ACN in Xylene NSA performed equally well in both acidic and basic conditions. Since 5STY performed better than 45STY, the 3 best systems moving forward were: 5STY in Toluene NSA (1:5 ratio) acidic, 41ACN in Xylene NSA (1:1 ratio) acidic and 41ACN in Xylene NSA (1:1 ratio) basic.

These 3 systems were subjected to further experiments by varying the concentration of nanoparticle solutions in Stage 4. At the end of Stage 4, there were 4 elastomer-NSA systems remaining with notable swelling behaviors. Table 5-1 below lists the optimized systems at the end of stage 4.

System Number	Elastomer Specimen	Nano-based Swelling Agent (NSA)
System 1	5STY	10% Acidic Toluene NSA
System 2	41ACN	5% Basic Xylene NSA
System 3	41ACN	15% Acidic Xylene NSA
System 4	41ACN	15% Basic Xylene NSA

Table 5-1: The four optimized NSA systems

Stage 5 was carried out to investigate the effects varying temperatures on the 4 optimized systems identified in the previous stage. In general the temperature increased the swelling performance on all the 41ACN elastomer systems, i.e., Systems 2 - 4. However, in 5STY elastomer (System 1) the swelling performance reduced with increase in temperature.

Stage 6 was a study on the possible effect of the type of wellbore fluids used, namely, OBM and WBM on the swelling behavior of the elastomers - 5STY and 41ACN. Other than the fact that OBM caused some swelling in 5STY, OBM and WBM did not have major effects.

5.2 NSA Selection Chart

Four systems with promising swelling performances have been narrowed down based on the gradual stage-wise experimental investigations. The four most favorable systems as listed in Table 5-1 each have their advantages and disadvantages in terms of the operating conditions, cost involved, rate of change as well as final swell volume. In this section, an NSA systems selection charts will be presented in order to provide assistance in deciding which NSA system would be ideal a specific swell packer application.

In stages 3 and 6, common operation environment consideration such as the pH conditions and wellbore/drilling fluid systems were experimentally examined. In stage 3, the purpose of these tests were to determine if the elastomeric NSA systems would react differently when exposed to low pH or high pH well conditions. There are a multitude of reasons why operators may choose a high or low pH system depending on their current operation needs, some wells' pH conditions may even subject to changes in a single life cycle. It is therefore important for the NSA systems to be chosen based on the most likely pH environment the well will see at the initial installation as well as the likely immediate operation processes. As for drilling fluid systems experiments in stage 6, it is imperative that the elastomer chosen would be able to handle possible cross contamination on the rig during preparations as well as down in the wellbore. This reduces the risk of unintended premature swelling of elastomer which could lead to well hang up situation, resulting in non-productive time and expenses.

Seeing how important these two wellbore operating conditions are in the selection of NSA systems, Figure 5-2 below presents a clear and concise flow chart to aid the decision process. The first line of filter is the type of mud chosen for the system, if it is an OBM, then systems 2,3,4 are recommended for proceeding. If the drilling fluid system is not OBM, the only other option in this scenario would be WBM and hence four of the systems are still allowed. The next line of filter would be the pH conditions, in this flow chart above pH 7 is considered basic while below pH 7, an acidic system is endorsed instead.

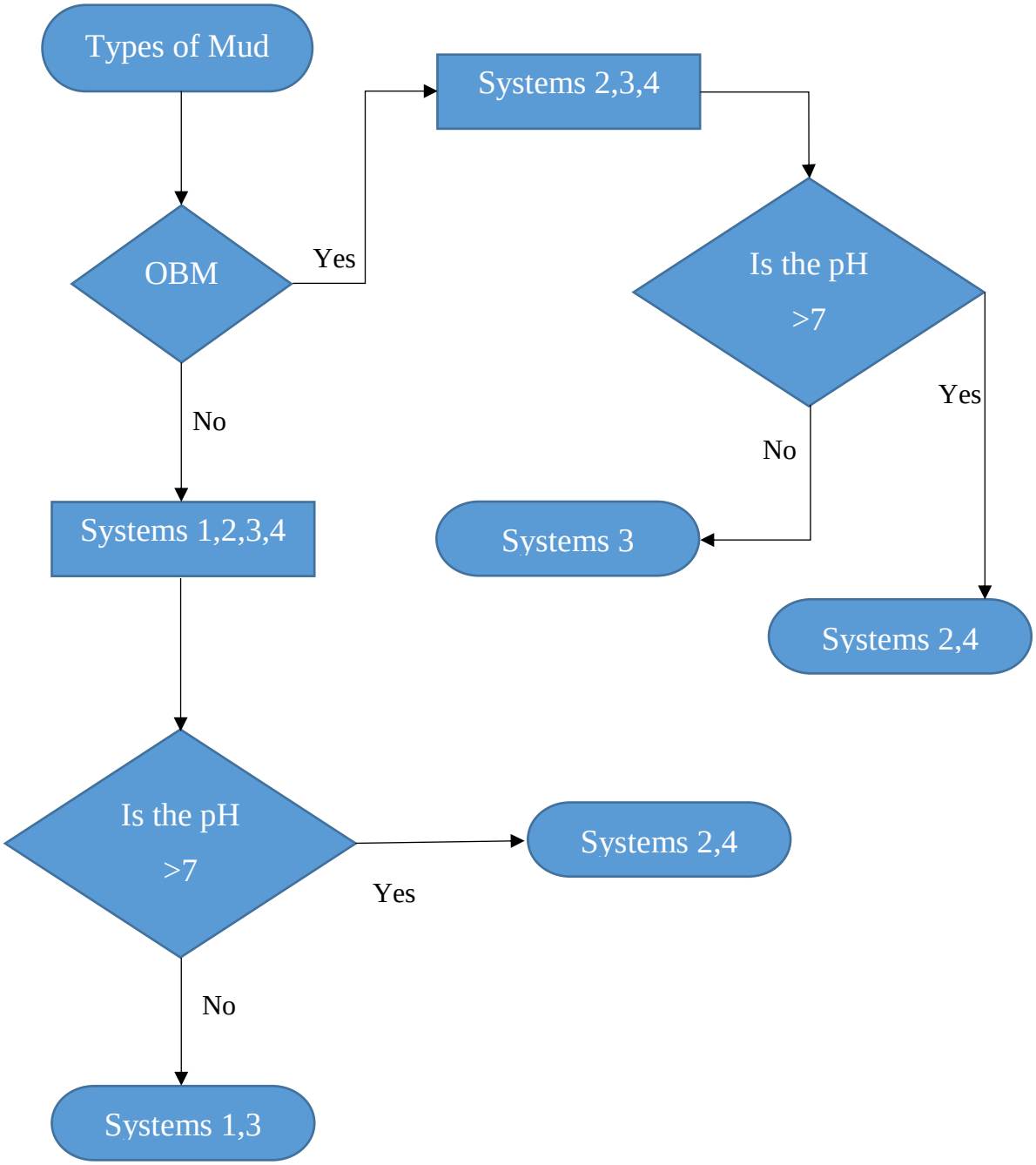

Figure 5-2: Flow chart on NSA systems selection for different pHs and drilling fluids

5.3 Cost-Benefit Evaluation Chart

While Figure 5-2 is important in helping to select the best system based given operating conditions, these conditions such as pH and drilling fluids are often fixed variables which are difficult to change once the drilling location and completion program have been planned. Figure 5-3 below addresses the other important selection factors which are user driven and play an equally important role in the NSA system selection process. These selection factors include:

- Cost involved
- Required rate of change: Rate of change of elastomer swelling, $\frac{d\Delta V}{dt}$, where ΔV refers to the % increase in elastomer specimen volume relative to its initial volume. Rate of change in this chart refers to the highest, $\frac{d\Delta V}{dt}$ value for a single system which is an indicator of how fast the elastomers swell upon exposure to the NSA.
- Final steady state increase in volume, ΔV_{SS}: This is the total increase in volume measured at steady state after the system has stabilized.

In order to quantify the cost involved for all four of the systems, the consideration must go back to as early as stage 1 experiment 2 where the varying mixture ratio experiment was conducted. As a result of the stage 1 experiments, Toluene NSA with a 1:5 ratio and Xylene NSA with a 1:1 ratio were discovered to be the best options for moving forward. This difference in ratio of mixtures inadvertently caused quite an impact in costs estimation. For every 1 part of Toluene in Toluene NSA, 5 part of TiO_2 nanoparticles solution has to be added in order to form the mixtures. On the other hand, for every 1 part of Xylene in the Xylene NSA, only 1 part of TiO_2 nanoparticles solution is required to form the concoction. Since Toluene and Xylene solutions are readily available at a relatively cheap rate, only the cost of TiO_2 nanoparticles solutions will be taken into account for this cost estimate exercise.

In addition to the difference in mixture ratios for the NSA systems, the varying concentration of TiO_2 nanoparticle solutions which was studied in details at stage 4 also plays an important role in quantifying the cost for these NSA systems. The four systems as listed in Table 5-1 have three different TiO_2 nanoparticle solution concentrations, namely 5%, 10% and 15%. Using the cost of the default 15% solution, the price for the diluted solutions of 5% and 10% can then be computed.

As cost of operation and equipment is generally a great concern for the oil and gas industry especially with the low oil prices, it will henceforth be used as a benchmark for ratio comparison for the following Figure 5-3.

In reality, the order of priority for rate of change, cost and ΔV are often shuffled around depending on the specific user and operation needs. As an example, if operation time is in a crunch but the annulus volume to seal is not of a big concern, then a user might wish to select a system with high rate of change instead of high ΔV to ensure a quick reaction instead.

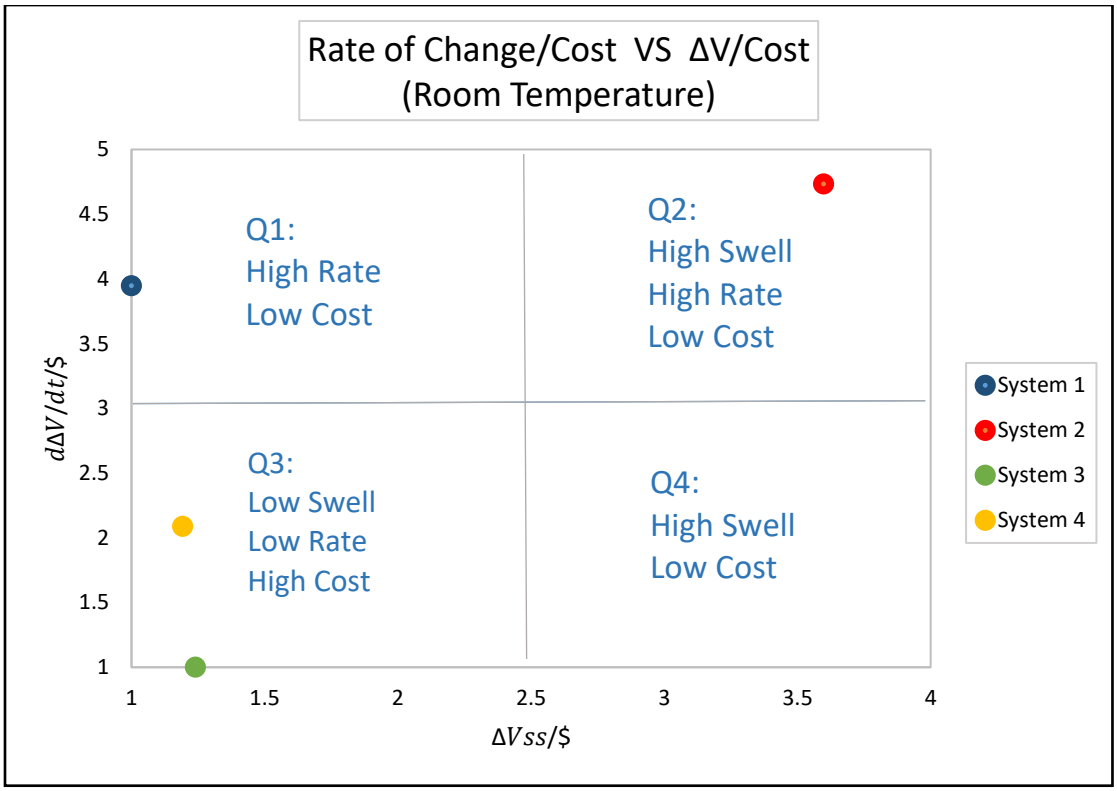

Figure 5-3: NSA systems cost-benefit evaluation chart

In Figure 5-3 above, the axes are defined as below:

- X axis – Ratio of increase in volume to the cost of the NSA ➔ $\Delta V_{ss}/\$$
- Y axis - Ratio of rate of increase in volume to the cost of the NSA ➔ $\frac{d\Delta V}{dt}/\$$

The purpose of defining the axis value as ratios is to allow the simultaneous consideration of 3 user preference factors in the selection process: Increase in volume (ΔV_{ss}), Rate of increase in volume ($\frac{d\Delta V}{dt}$) and cost of NSA ($).

The chart axes values in this case have been normalized against the lowest value in order to obtain a relative graph for ease of interpretation. Along the X axis, the higher the value in which a system lands, the better it is as it means that the system has a very high ΔV with a relatively low cost. The same can be said for along Y axis as well, the higher the value, the faster the rate of change with a lower cost of operation.

To gain an even deeper understanding on how Figure 5-3 can aid the selection process, four quadrants have been marked on the chart area. Quadrant 2 is the most ideal quadrant as it represents high ΔV and high rate of change with the lowest cost relatively while quadrant 3 represents the direct opposite. Quadrant 4 is good as well as it represents high ΔV with low cost and the same can be said for quadrant 1, which has high rate of change/cost ratio. Therefore, depending on the operational needs, users may first utilize Figure 5-2 to narrow down the options based on pH and drilling fluid system and then proceed with Figure 5-3 to aid the elastomeric NSA selection process factoring the other concerns.

As observed in the above chart, the four systems have been quantified and sorted into their respective quadrant based on their experimental results at room temperature. In terms of relativity, system 2 is in the best quadrant possible since quadrant 2 represents the best in $\Delta V_{ss}/\$$ as well as $\frac{d\Delta V}{dt}/\$$. Should the operational conditions fit, users should definitely choose system 2. Looking at axis $\Delta V_{ss}/\$$ only, the next best systems would be system 3, system 4 and followed by system 1. However, if the user's preference is $\frac{d\Delta V}{dt}/\$$, then the next best systems would be system 1, system 4 and system 3.

Other similar selection charts have been generated for NSA systems in temperatures 40°C, 60°C and 80°C and can be found in Appendix I for further references.

5.4 Simulations: Developing a Predictive Model

5.4.1 Approach

In stage 5, all four of the optimal NSA systems were tested at different temperatures to obtain a characteristic curve for each of the systems. In this section, regression curve fitting techniques were used to model the swelling behavior of different NSA systems as functions of time and temperature. The models developed are aimed at accurately predicting the performance of different NSA-elastomer systems.

The discussion below will focus on System 4, which is 41ACN elastomer in 15% TiO_2 nanoparticle solutions with basic conditioned Xylene NSA. Similar predictive models have been developed for Systems 1, 2 and 3 and are attached as part of the appendix for the in-depth audience.

The goal was to model the volumetric expansion of the abovementioned System 4 as functions of temperature and time:

$\Delta V = f(t, T)$

Where,

ΔV = Percentage (%) increase in volume of the rubber relative to initial volume

t = Cumulative exposure time of elastomer to Nano-swelling agent (NSA) in hours

T = Temperature in °C

In order to fit the experimental data onto an equation to determine the coefficients, the first step was to determine the form of the equation that the data was to be fitted to. Since the aim was to model the simultaneous dependence of volume increase (ΔV) on 2 independent variables (t & T), the approach taken was to first break down the problem into 3 steps:

Step 1 – The nature of the equation characterizing the dependence of V on time (t) at constant temperature was determined:

➔ $\Delta V = f(t)$ @ constant T

Step 2 - The nature of the equation to model the dependence of V on Temperature (T) at the fixed duration was determined:

➔ $\Delta V = f(T)$ @ constant t

Step 3 – The results from Steps 1 & 2 were used to make a hypothesis on the nature of the equation modelling the simultaneous dependence of volume increase on both time and temperature:

➔ $\Delta V = f(t, T)$

The curvefitting toolbox in Matlab was then used to determine the coefficients of this equation and the coefficient of determination (R-squared) was used to verify the validity of this predictive model.

5.4.2 Definitions of relevant regression terms and methods

a. Power Law Model:

The power model typically has a function with the form of equation $y = qx^n$, where the terms y and x are variables of interest, n is the power law exponent and q is the constant term. There are many variations of power model such as direct variation power model, inverse variation power model as well as quadratic power law, the one which resembles closest to Figure 5-5 below is a radical or fractional power model which means the q term in the equation is a fraction greater than zero [43].

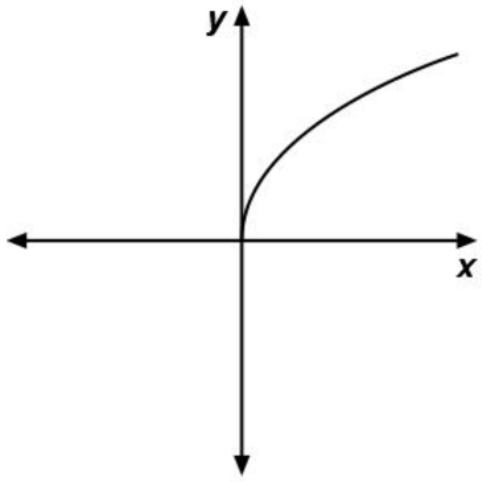

Figure 5-4: Typical radical or fractional power model

b. R-squared:

Coefficient of determination, or better known as R-squared is the statistical method in measuring how close the data is to the fitted curve. This statistic measures how successful the fit is in explaining the variation of the data. Put another way, R-square is the square of the correlation between the response values and the predicted response values [44].

R-squared values are typically between 0 and 1, where 0 indicates the poorest fit possible for the model generated and 1 being that the model is able to represent all the data accurately. Overall, a model which has a high R-squared value is much sought after since it means a good fit of data. For

example, an R-square value of 0.8234 means that the fit explains 82.34% of the total variation in the data about the average [44].

5.4.3 Implementation

Step 1: $\Delta V = f(t)$ @ constant T

In Figure 5-5 below, the percent volume increase (ΔV) is plotted versus time for a constant temperature for System 4 – 41ACN in 15% Xylene based NSA in basic condition. The trendline that best represented the experimental data was found (using Microsoft Excel) to be of the power law form with an R-squared value of 0.97 indicating excellent correlation between the modelled equation and the experimental data. The relationship between ΔV and time was given by:

$\Delta V = 32.427 * t^{0.5247}$ at a constant temperature of 40 °C

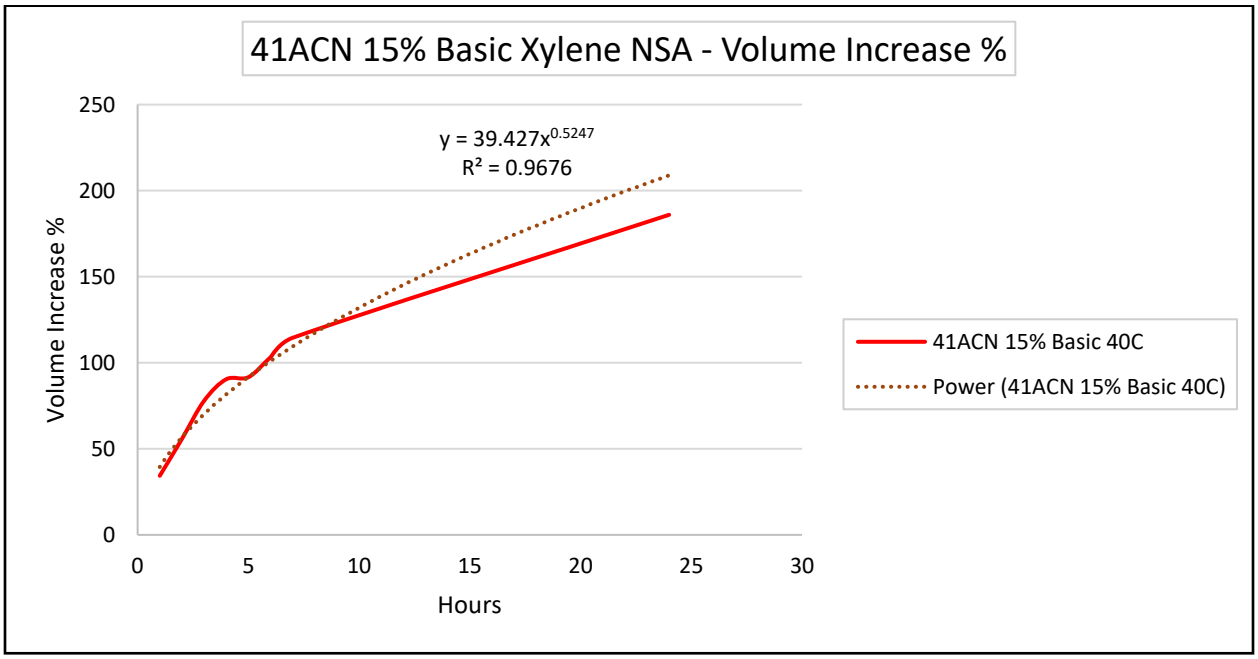

Figure 5-5: Characteristic curve for system 4 NSA systems at temperature of 40°C/104°F

Step 2: $\Delta V = f(T)$ @ constant t

In Figure 5-6 below, the percentage volume increase (ΔV) is plotted versus temperature after a fixed duration for the same system. The trendline (using Microsoft Excel) that best represented the experimental data was found to be of the power law form again with an R-squared value of 0.95 indicating excellent correlation between the modelled equation and the experimental data. The relationship between ΔV and temperature was given by:

$\Delta V = 14.132 * t^{0.5782}$ after a fixed duration of 6 hours

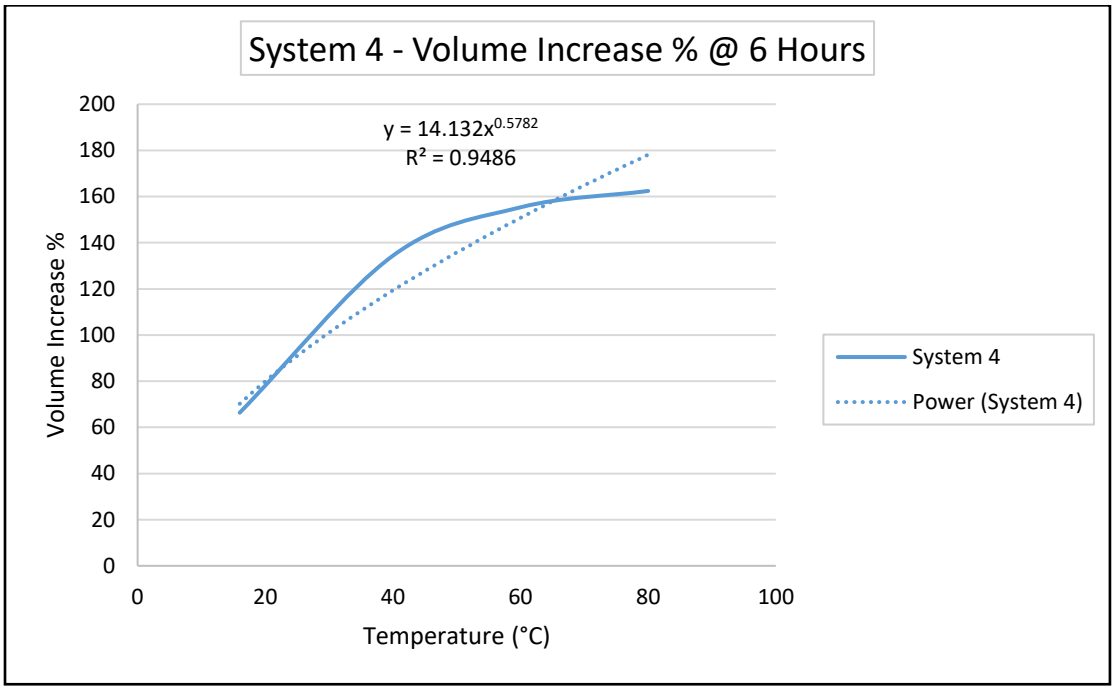

Figure 5-6: System 4 volume increase percentages after 6 hours for different temperatures

Step 3: $\Delta V = f(t,T)$

From steps 2 & 3, it was observed that the % increase in volume (ΔV) varied with both temperature (T) and time (t) in the form of a power law. Consequently, it was hypothesized that the equation representing the simultaneous variation of ΔV on the 2 independent variables would be of the following form:

ΔV(t, T) = a*t^b + c*T^d + e ---------- Equation 1

Where a, b, c, d & e are coefficients that are constant for a given system of elastomer & NSA.

Matlab's Curve Fitting toolbox was used to determine the above coefficients using an iterative non-linear regression analysis. The coefficients are determined so as to provide the best fit of the equation with the experimental data. The corresponding R-squared values were also determined to validate the proximity between the model and the experimental data.

Figure 5-7, shows the 3D-curve fitting results for System 4 – 41ACN in 15% Xylene NSA in basic condition. The 3D surface generated by the curve-fitted equation is shown along with the experimental data points (shown as black points). The colour gradient in Figure 5-7 is representative of the volume increase percentages with blue being the lowest and yellow the highest.

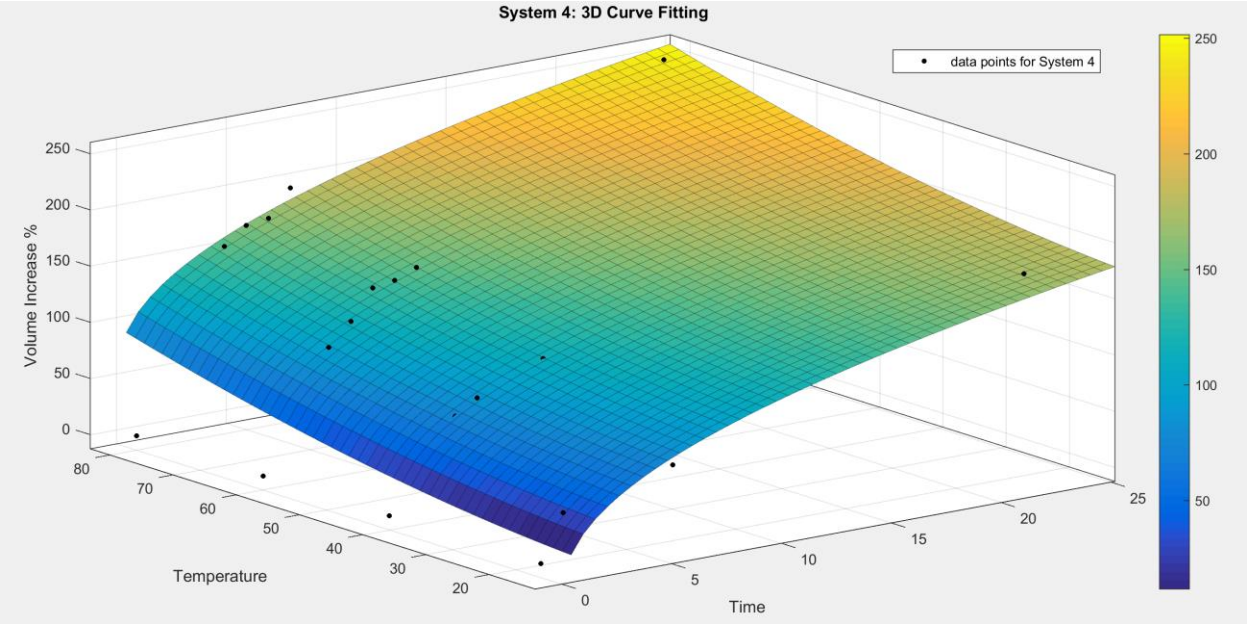

Figure 5-7: System 4 curve fitting with multi-variable regression method

a	63.5
b	0.3762
c	0.0273
d	1.793
e	-37.89

Table 5-2: Coefficients for system 4's general model

The values of the constant coefficients (a-e) for System 4 are tabulated above. The R-squared value of the above was found to 0.9187 which shows excellent correlation between the equation and the experimental data.

Thus, Equation 1 in conjunction with Table 5-2 is a characteristic model of the swelling behavior of system 4. This predictive model can be used to determine the expected swelling performance for this system at desired temperatures and durations. Such predictive models will be of paramount importance in planning well operations and selecting the correct NSA depending on downhole temperature conditions and time constraints.

These characteristic equations were developed for the other 3 systems (Systems 1 – 3) as well and can be found in the Appendix II. It was found that a variation of the power law was the best form to represent the swelling performance of all the systems.

While it is not within the scope of this thesis to delve deep into the mathematics behind the curve fitting methods used by Matlab, the code used to generate this curve has been attached to Appendix III.

6 Conclusions and Recommendations

6.1 Conclusions

One of the main goals for this thesis work was to create an elastomer swelling system with a dedicated nanomaterial based trigger which can help to achieve precise control for the setting of a swell packer. The desired operational requirement is for the swell packer to be run downhole without the risk of unintended premature swell activation. A swell packer which inadvertently reacts due to wellbore or rig site contamination has dire consequences as it will result in non-productive time and drive up the operation cost in the effort to unseat and re-run the packer. Another important factor is being able to precisely determine the time taken for a swell packer to activate and seal off the annulus at the required depth and time.

A new idea which was based on creating a nanoparticles-based swelling agent that allows for controlled and targeted activation of a swell packer was investigated in this thesis. The following conclusions can be drawn with each stages of experimentation:

- 15wt% TiO_2 nanoparticle solution along with the primary constituents (Toluene and Xylene) and emulsifier form the nano-based swelling agent (NSA). These NSAs were capable of swelling elastomer specimens such as 5STY (volume increase of 145%), 45STY (volume increase of 127%) and 41ACN (volume increase of 185%) successfully with good rubber integrity and high volume increase percentages after only a period of 24 hours.
- Pure TiO_2 nanoparticle solutions, water as well as emulsifier proved to have no effect at all on the elastomer specimens when administered individually.
- The pH of NSAs was found to have an effect on the final volume increase percentages. 5STY and 45STY in acidic Toluene NSA reacted with a better outcome than 5STY and 45STY in basic Toluene NSA with 97% difference for 5STY and 35% for 45STY. On the other hand, 41ACN gave an equal reaction in acidic and basic Xylene NSA with a bare 7% difference.
- The concentration of TiO_2 nanoparticles solution has an effect on the performance of the NSAs. The NSA with 10wt% TiO_2 as a constituent for 5STY Toluene based acidic system performed much better than the others with volume increase of 165% while 15wt% TiO_2

remained the front runner for 41ACN Xylene acidic system with 185% increase of volume. The outcomes from both 5wt% TiO_2 and 15wt% TiO_2 in 41ACN Xylene basic systems were on par with 170% and 178% respectively. With the different concentrations, certain systems such as 10wt% TiO_2 5STY Toluene NSA have a higher rate of change than others.

- An increase in temperature improved the rate of swelling for systems 2 to 4 - 41ACN 5% basic Xylene NSA, 41ACN 15% acidic Xylene NSA and 41ACN 15% basic Xylene NSA. The exception was in the case of System 1 - 5STY 10% acidic Toluene NSA, where the opposite effect was true as room temperature results were better than those at elevated temperatures.
- The presence of oil-based mud and water-based mud in operations are common and their reaction with the elastomer specimens 5STY and 41ACN were investigated. While 41ACN does not have any reaction with OBM or WBM, 5STY experienced swelling with OBM but not WBM.
- The data gathered from all the experiments are then used to generate a predictive model to determine the performance for different NSA-rubber systems as a function of the operating temperature and exposure time.
- The equations for the different systems generated were a variation of power law form with an R-squared value of more than 0.9 indicating a good correlation between prediction and actual data.
- With so many different parameters for considerations and possible NSA options to choose from, an NSA selection chart was created to aid users to select the most suitable systems for their operational needs based on cost, wellbore pH, drilling fluids present, rate of change, final volume increase and available time.

6.2 Recommendations for Future Work

Since nano-based swelling agents for targeted activation of swell packer is an unexplored arena, there are many areas with abundant potential for future exploration. As a logical follow-up to the work done in this thesis, the pressure sealing capabilities of the identified elastomers post-swelling could be investigated. This would allow for a step further in helping to create a more elaborate system selection chart based on the elastomer pressure rating in addition to the other operational requirements previously discussed.

A small scale prototype design of a swell packer can be made comprised of the elastomers - 41ACN and 5STY and these can be swollen to set inside a test casing. Characterizing the swelling behavior as well as pressure sealing capabilities of this prototype inside a test casing would be very valuable since it closely mimics the true operational use of the packer. In addition to this, a comparative study may be done by repeating the tests on commercially available swell packers from service providers.

Furthermore, it is well known that the pressure sealing capabilities of elastomers are heavily temperature dependent. Thus, test procedures and fixtures can be developed based on industry standards like ISO to map out the pressure sealing capabilities of the NSA-triggered swell packers at different temperatures.

In an effort to get a glimpse into the complex workings and the chemical interactions of the NSA systems, a material elemental analysis with the help of scanning electron microscope (SEM) could also be a potential future work. The SEM could help to shed a light on why certain NSA systems behave the way they did. A more defined and safe experimental setup according to the recommended practices from ASTM D471 is available for reference. This more complex and expensive experimental setup would be worth the exploration for an in-depth investigation of the higher temperature functionality qualification in order to examine temperature ranges which resemble the well conditions.

Besides the above immediate recommendations for expanding current work done, exploring other potential elastomers from the same polymer group as well as identifying additional types of nanoparticles with similar properties could also be an interesting route for further development.

Bibliography

1. Bardsen, J., et al. *Improved Zonal Isolation in Open Hole Applications*. in *SPE Bergen One Day Seminar*. 2014. Society of Petroleum Engineers.

2. Rogers, H.E., D. Allison, and E.D. Webb. *New equipment designs enable swellable technology in cementless completions*. in *IADC/SPE Drilling Conference*. 2008. Society of Petroleum Engineers.

3. Kennedy, G.P., et al. *The Use of Swell Packer's as a Replacement and Alternative to Cementing*. in *SPE Annual Technical Conference and Exhibition*. 2005. Society of Petroleum Engineers.

4. Laws, M.S., et al. *PDOB's Proactive Approach to Solving a Zonal Isolation Challenge in Harweel HP Wells Using Swell Packers*. in *IADC/SPE Asia Pacific Drilling Technology Conference and Exhibition*. 2006. Society of Petroleum Engineers.

5. Vinches, L., et al., *Swelling of Protective Gloves in Commercial TiO2 Nanoparticles Colloidal Solutions.* Journal ISSN, 2012. **1929**: p. 1248.

6. Krishnamoorti, R., *Extracting the benefits of nanotechnology for the oil industry.* Journal of petroleum technology, 2006. **58**(11): p. 24-26.

7. Yakeley, S., T. Foster, and W.J. Laflin. *Swellable packers for well fracturing and stimulation*. in *SPE Annual Technical Conference and Exhibition*. 2007. Society of Petroleum Engineers.

8. Merritt, J.W. *Premixed Cement Slurry Solves Problems Associated With Conventional Oilwell Cementing*. in *SPE Production Operations Symposium*. 2005. Society of Petroleum Engineers.

9. Antonio, L., O.D. Barrios, and G.A. Martinez Rodriguez. *Swelling packer technology eliminates problems in difficult zonal isolation in tight-gas reservoir completion*. in *Latin American & Caribbean Petroleum Engineering Conference*. 2007. Society of Petroleum Engineers.

10. Halliburton. *Swell Technology*. [cited 2017 June 4]; Available from: http://www.halliburton.com/public/cps/contents/Books_and_Catalogs/web/CPSCatalog/04_Swell_Technology.pdf.

11. Halliburton. *Unconventional Completions Brochure*. [cited 2017 June 4]; Available from: http://www.halliburton.com/public/cps/contents/Brochures/web/Unconventional_Completions_Brochure.pdf.

12. Halliburton. *Swell Packer Slip On*. [cited 2017 June 4]; Available from: http://www.halliburton.com/en-US/ps/completions/well-completions/swell-technology/Swellpacker-Slip-on.page.

13. Sabins, F.L., *Problems in cementing horizontal wells.* Journal of Petroleum Technology, 1990. **42**(04): p. 398-400.

14. Freyer, R. and A. Huse. *Swelling packer for zonal isolation in open hole screen completions*. in *European Petroleum Conference*. 2002. Society of Petroleum Engineers.

15. Hertfelder, G.P., et al. *Are Swelling Elastomer Technology, Pre-perforated Liner and Intelligent Well Technology Suitable Alternatives to Conventional Completion Architecture?* in *SPE/IADC Drilling Conference*. 2007. Society of Petroleum Engineers.

16. Al-Yami, A.S., et al. *Swelling Packers; Lab Testing and Field Application*. in *International Petroleum Technology Conference*. 2008. International Petroleum Technology Conference.

17. Bellarby, J., *Well completion design*. Vol. 56. 2009: Elsevier.

18. Haseeb, A., et al., *Degradation of physical properties of different elastomers upon exposure to palm biodiesel.* Energy, 2011. **36**(3): p. 1814-1819.

19. Delor-Jestin, F., et al., *Thermal ageing of acrylonitrile-butadiene copolymer.* Polymer degradation and stability, 2000. **70**(1): p. 1-4.

20. Yasin, T., et al., *Effect of acrylonitrile content on physical properties of electron beam irradiated acrylonitrile–butadiene rubber.* Reactive and Functional Polymers, 2003. **57**(2): p. 113-118.

21. Ciesielski, A., *An introduction to rubber technology*. 1999: iSmithers Rapra Publishing.

22. Graham, J.L., et al., *Swelling of nitrile rubber by selected aromatics blended in a synthetic jet fuel.* Energy & fuels, 2006. **20**(2): p. 759-765.

23. Stephens, H.L. and A.K. Bhowmick, *Handbook of Elastomers*. 2001: Dekker.

24. Ltd, F.I.C. *NBR/Nitrile Rubber Sheets*. [cited 2017 June 4]; Available from: http://www.rollsheetrubber.com/html.aspx?id=223.

25. Kreyling, W.G., M. Semmler-Behnke, and Q. Chaudhry, *A complementary definition of nanomaterial.* Nano Today, 2010. **5**(3): p. 165-168.

26. Bell, A.T., *The impact of nanoscience on heterogeneous catalysis.* Science, 2003. **299**(5613): p. 1688-1691.

27. Kong, X. and M. Ohadi. *Applications of micro and nano technologies in the oil and gas industry-overview of the recent progress*. in *Abu Dhabi international petroleum exhibition and conference*. 2010. Society of Petroleum Engineers.

28. *Nanotechnology Website*. [cited 2017 June 1]; Available from: http://www.nanocat.co.in/.

29. Rajendran, R.V.a.K.V. *Effect of K+ Doping on the Phase Transformation of TiO2 Nanoparticles*. Available from: http://www.azom.com/article.aspx?ArticleID=5513.

30. Khalil, M., et al., *Advanced nanomaterials in oil and gas industry: Design, application and challenges.* Applied Energy, 2017. **191**: p. 287-310.

31. Mout, R., et al., *Surface functionalization of nanoparticles for nanomedicine.* Chemical Society Reviews, 2012. **41**(7): p. 2539-2544.

32. Xu, S., et al., *Magnetic nanoparticle-based solder composites for electronic packaging applications.* Progress in Materials Science, 2015. **67**: p. 95-160.

33. Wang, X., et al., *Nanoscale metals in Earthgas and mobile forms of metals in overburden in wide-spaced regional exploration for giant deposits in overburden terrains.* Journal of Geochemical Exploration, 1997. **58**(1): p. 63-72.

34. Ryoo, S., et al., *Theoretical and experimental investigation of the motion of multiphase fluids containing paramagnetic nanoparticles in porous media.* Journal of Petroleum Science and Engineering, 2012. **81**: p. 129-144.

35. Ragab, A.S. and A. Noah, *Reduction of formation damage and fluid loss using nano-sized silica drilling fluids.* Petroleum Technology Development Journal, 2014. **2**: p. 75-88.

36. William, J.K.M., et al., *Effect of CuO and ZnO nanofluids in xanthan gum on thermal, electrical and high pressure rheology of water-based drilling fluids.* Journal of Petroleum Science and Engineering, 2014. **117**: p. 15-27.

37. Wang, Z., *Impact Toughness, Dry Shrinkage and Permeability Resistance Properties of Multi-Walled Carbon Nanotubes Reinforced Cement Composites.* Journal of Advanced Microscopy Research, 2015. **10**(1): p. 73-77.

38. Mokhatab, S., M.A. Fresky, and M.R. Islam, *Applications of nanotechnology in oil and gas E&P*. Journal of petroleum technology, 2006. **58**(04): p. 48-51.

39. Yu, J., et al., *Effect of particle hydrophobicity on CO 2 foam generation and foam flow behavior in porous media.* Fuel, 2014. **126**: p. 104-108.

40. Khalil, M., R.L. Lee, and N. Liu, *Hematite nanoparticles in aquathermolysis: A desulfurization study of thiophene.* Fuel, 2015. **145**: p. 214-220.

41. Wei, L., J.-H. Zhu, and J.-H. Qi, *Application of nano-nickel catalyst in the viscosity reduction of Liaohe extra-heavy oil by aqua-thermolysis.* Journal of Fuel Chemistry and Technology, 2007. **35**(2): p. 176-180.

42. Mohammed, M.I., A.A.A. Razak, and M.A. Shehab, *Synthesis of Nanocatalyst for Hydrodesulfurization of Gasoil Using Laboratory Hydrothermal Rig.* Arabian Journal for Science and Engineering, 2016: p. 1-7.

43. Newman, M.E., *Power laws, Pareto distributions and Zipf's law.* Contemporary physics, 2005. **46**(5): p. 323-351.

44. *Coefficient of Determination (R-Squared).* [cited 2017 June 4]; Available from: https://se.mathworks.com/help/stats/coefficient-of-determination-r-squared.html?requestedDomain=se.mathworks.com&requestedDomain=se.mathworks.com.

Appendix I

NSA Selection Chart for 40°C

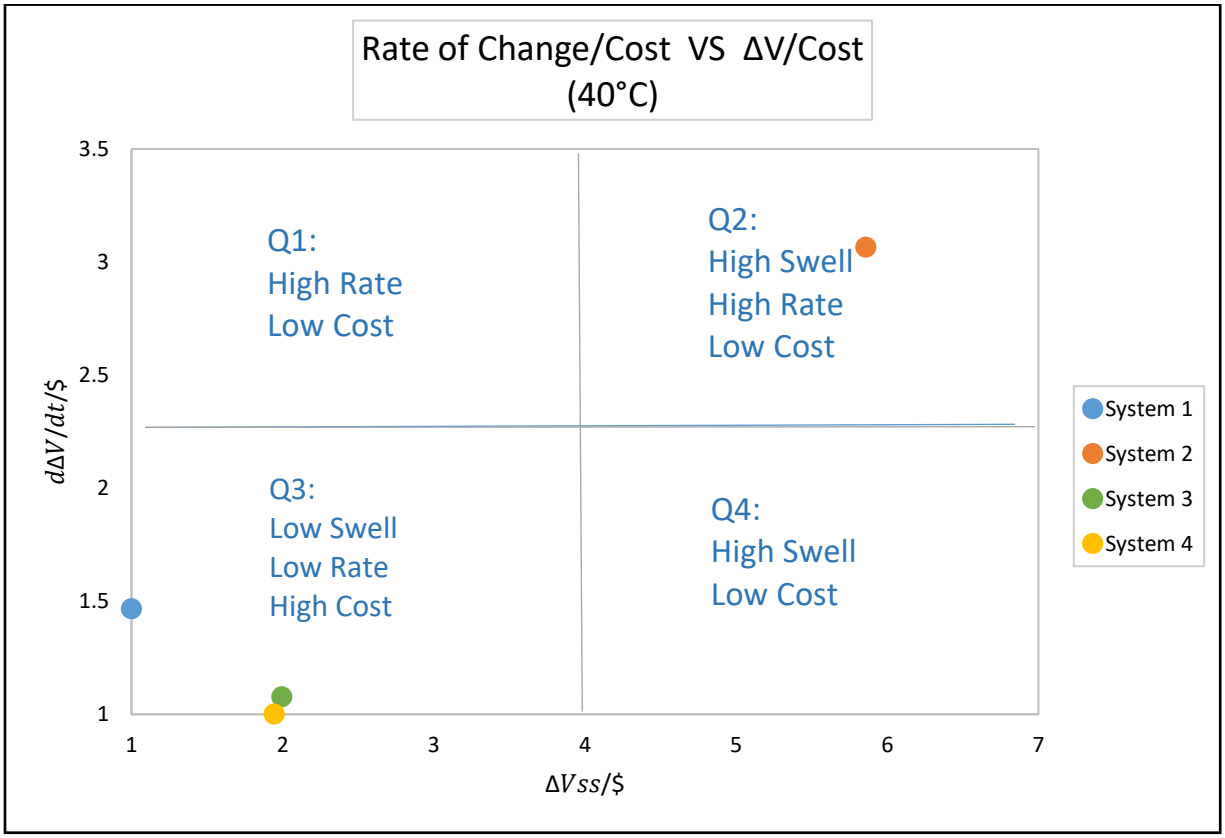

NSA Selection Chart for 60°C

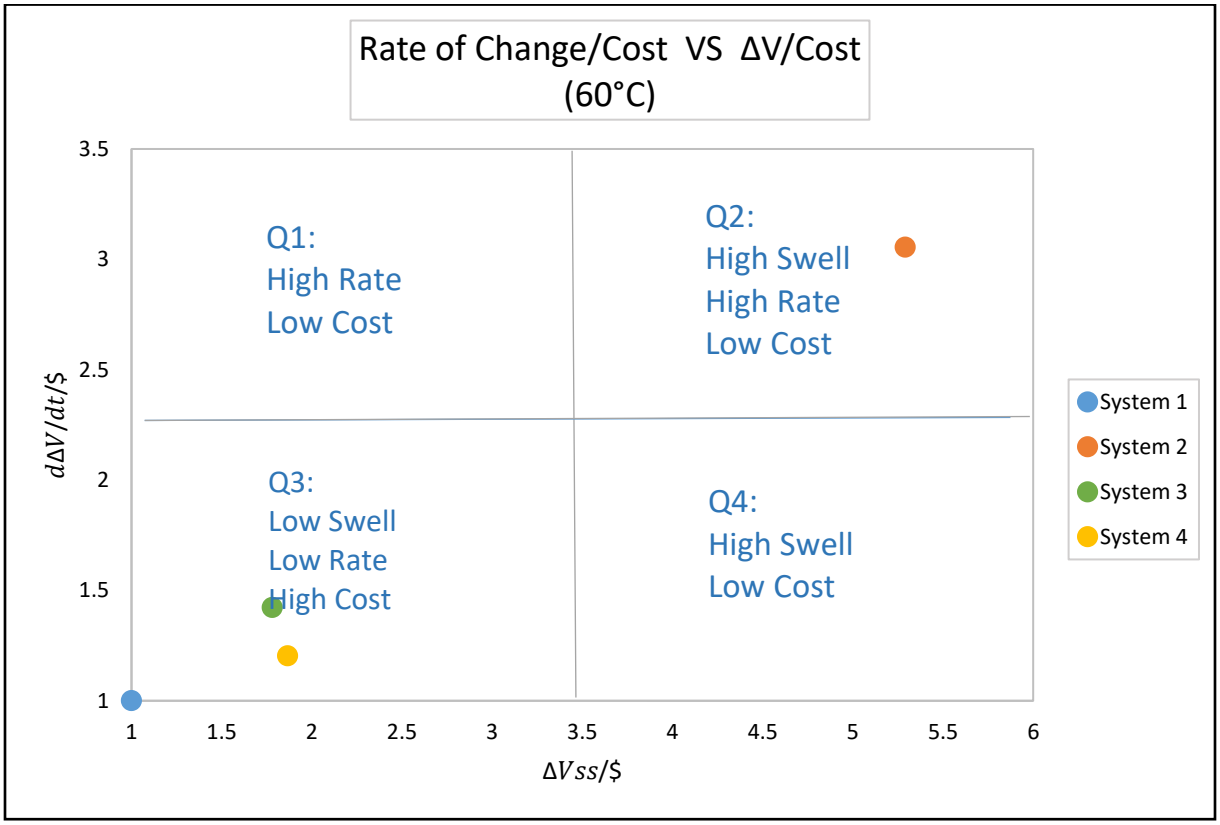

NSA Selection Chart for 80°C

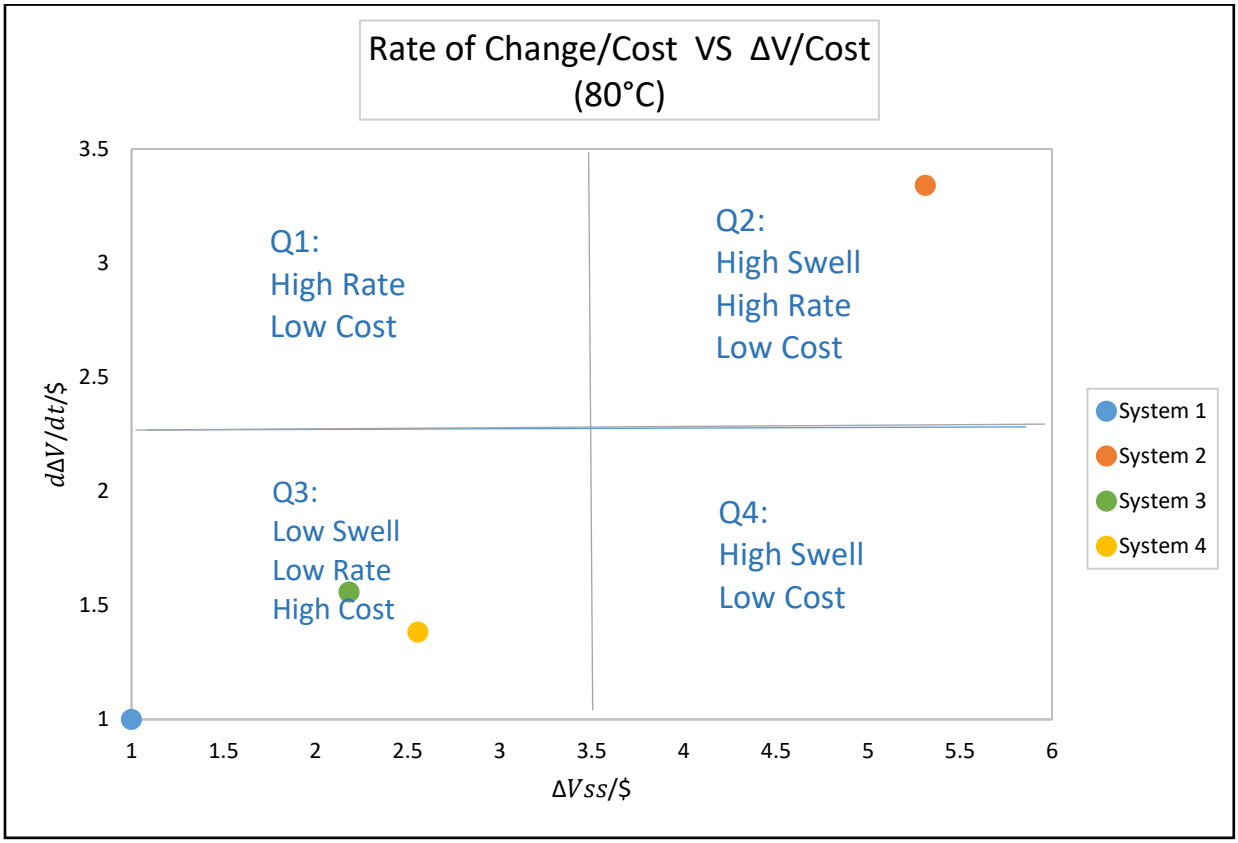

Appendix II

Predictive Modeling for System 1

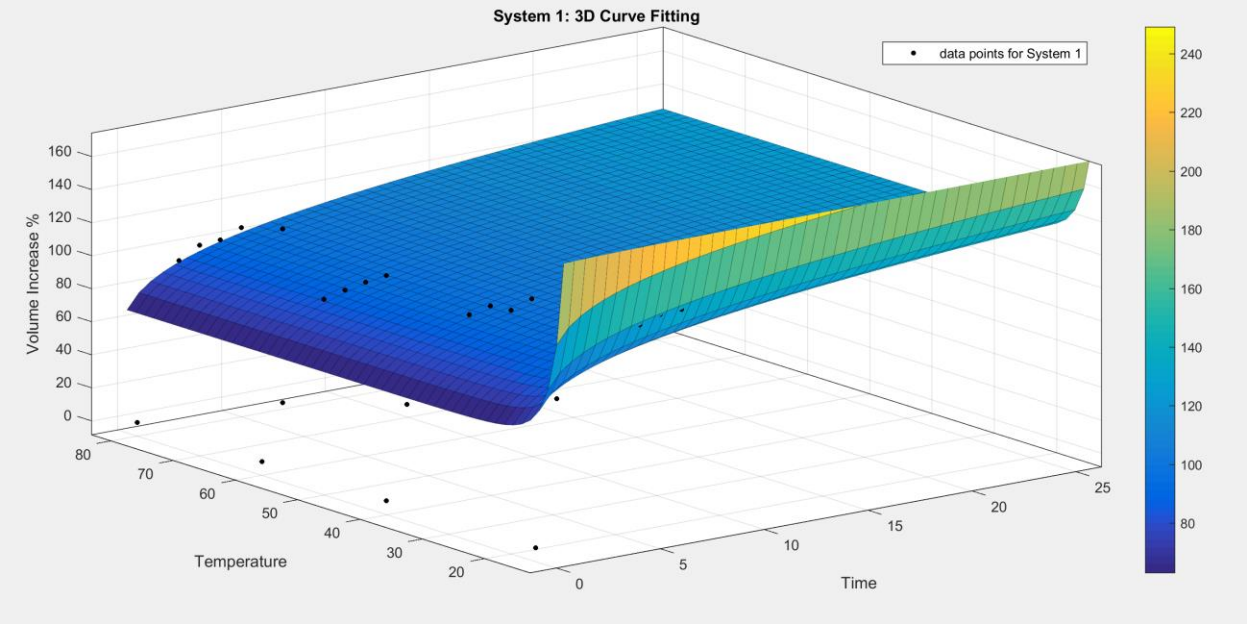

General model:

$\Delta V(t, T) = a*t^b + c*T^d$

Coefficients:

a = 71.73

b = 0.1691

c = 5.06e+09

d = -6.872

R-square: 0.9062

Predictive Modeling for System 2

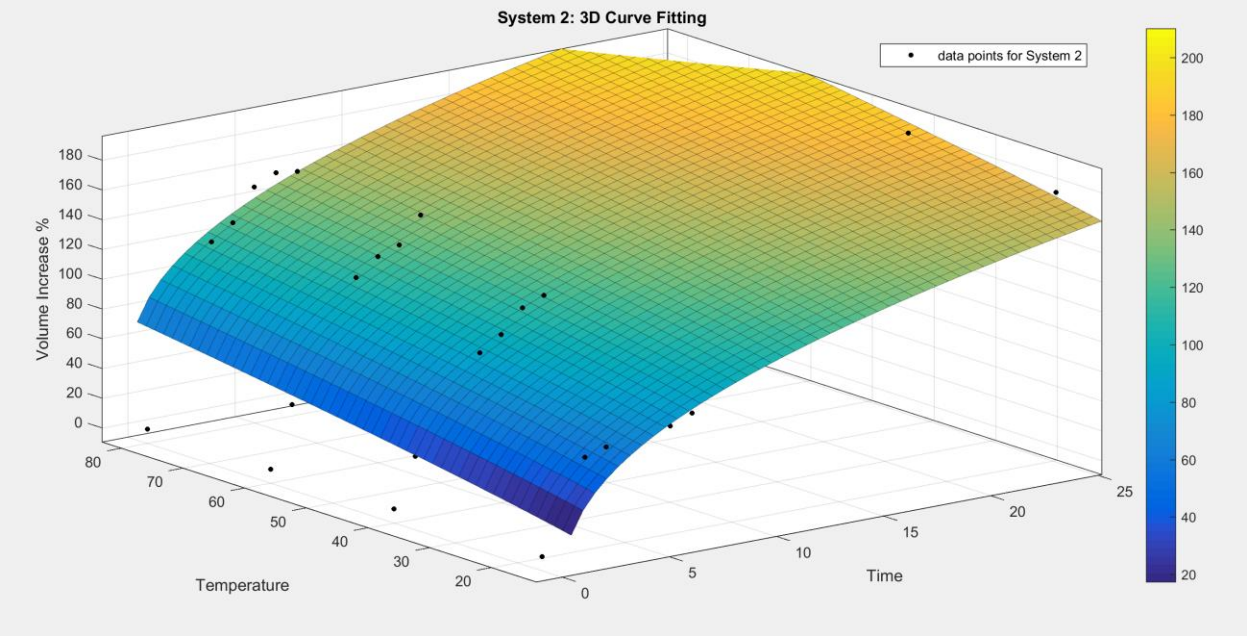

General model:

$\Delta V(t, T) = a*t^b + c*T^d + e$

Coefficients:

a = 62.77

b = 0.3451

c = 2.069

d = 0.7771

e = -45.25

R-square: 0.911

Predictive Modeling for System 3

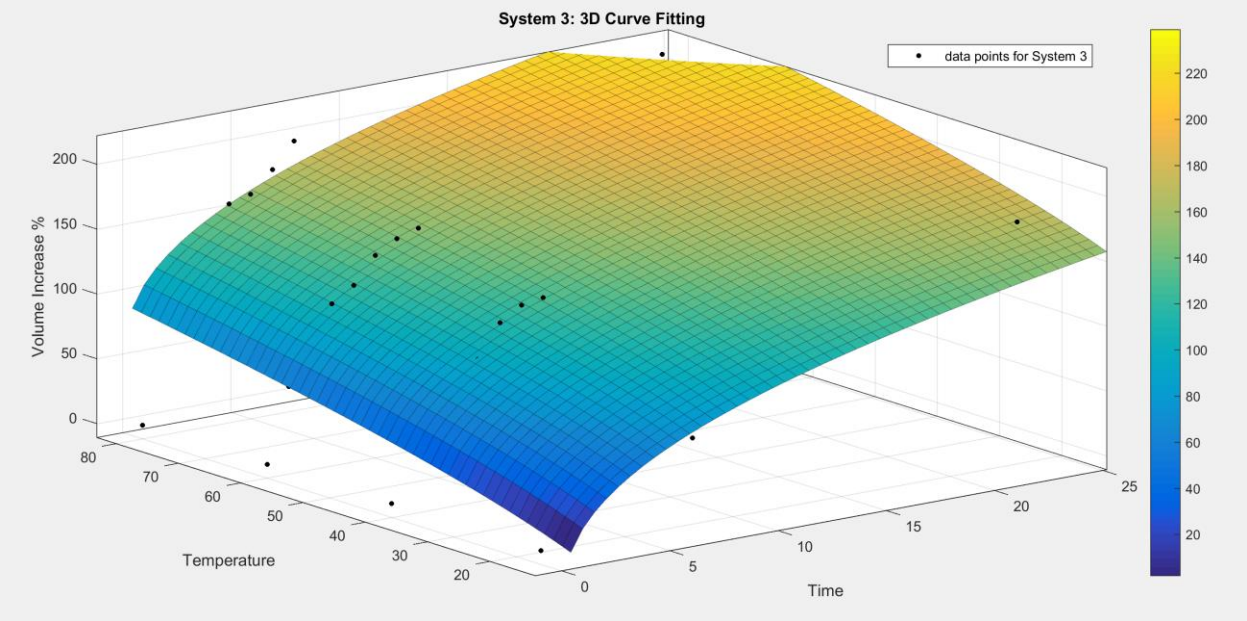

$\Delta V(t, T) = a*t^b + c*T^d + e$

Coefficients:

a = 68.97

b = 0.3417

c = 10.6

d = 0.5595

e = -94.5

R-square:0.903

Appendix III

```
clc
close all
clear all
load Nano_performance_data

%% Initialization.

% Initialize arrays to store fits and goodness-of-fit.
fitresult = cell( 4, 1 );
gof = struct( 'sse', cell( 4, 1 ), ...
    'rsquare', [], 'dfe', [], 'adjrsquare', [], 'rmse', [] );

%% Fit: 'System1'.
[xData, yData, zData] = prepareSurfaceData( Temp1, Time1, dV1 );

% Set up fittype and options.
ft = fittype( 'a*x^-b + c*y^d', 'independent', {'x', 'y'},
'dependent', 'z' );
opts = fitoptions( 'Method', 'NonlinearLeastSquares' );
opts.Display = 'Off';
opts.MaxFunEvals = 6000;
opts.MaxIter = 4000;
opts.StartPoint = [0.853031117721894 0.622055131485066
0.350952380892271 0.513249539867053];

% Fit model to data.
[fitresult{1}, gof(1)] = fit( [xData, yData], zData, ft, opts );

% Plot fit with data.
figure( 'Name', 'System1' );
h = plot( fitresult{1}, [xData, yData], zData );
legend( h, 'System1', 'dV1 vs. Temp1, Time1', 'Location',
'NorthEast' );
% Label axes
xlabel Temp1
ylabel Time1
zlabel dV1
grid on

%% Fit: 'System2'.
[xData, yData, zData] = prepareSurfaceData( Time2, Temp2, dV2 );

% Set up fittype and options.
```

```
ft = fittype( 'a*x^b + c*y^d+e', 'independent', {'x', 'y'},
'dependent', 'z' );
opts = fitoptions( 'Method', 'NonlinearLeastSquares' );
opts.Display = 'Off';
opts.MaxFunEvals = 6000;
opts.MaxIter = 4000;
opts.StartPoint = [0.183907788282417 0.239952525664903
0.41726706908437 0.0496544303257421 0.0838213779969326];

% Fit model to data.
[fitresult{2}, gof(2)] = fit( [xData, yData], zData, ft, opts );

% Plot fit with data.
figure( 'Name', 'System2' );
h = plot( fitresult{2}, [xData, yData], zData );
legend( h, 'System2', 'dV2 vs. Time2, Temp2', 'Location',
'NorthEast' );
% Label axes
xlabel Time2
ylabel Temp2
zlabel dV2
grid on

%% Fit: 'System3'.
[xData, yData, zData] = prepareSurfaceData( Temp3, Time3, dV3 );

% Set up fittype and options.
ft = fittype( 'a*x^b + c*y^d + e', 'independent', {'x', 'y'},
'dependent', 'z' );
opts = fitoptions( 'Method', 'NonlinearLeastSquares' );
opts.Display = 'Off';
opts.MaxFunEvals = 6000;
opts.MaxIter = 4000;
opts.StartPoint = [0.753729094278495 0.380445846975357
0.567821640725221 0.0758542895630636 0.0539501186666072];

% Fit model to data.
[fitresult{3}, gof(3)] = fit( [xData, yData], zData, ft, opts );

% Plot fit with data.
figure( 'Name', 'System3' );
h = plot( fitresult{3}, [xData, yData], zData );
legend( h, 'System3', 'dV3 vs. Temp3, Time3', 'Location',
'NorthEast' );
% Label axes
xlabel Temp3
ylabel Time3
```

```
zlabel dV3
grid on

%% Fit: 'System4'.
[xData, yData, zData] = prepareSurfaceData( Temp4, Time4, dV4 );

% Set up fittype and options.
ft = fittype( 'a*x^b + c*y^d + e', 'independent', {'x', 'y'},
'dependent', 'z' );
opts = fitoptions( 'Method', 'NonlinearLeastSquares' );
opts.Display = 'Off';
opts.MaxFunEvals = 6000;
opts.MaxIter = 4000;
opts.StartPoint    =    [0.469390641058206    0.0119020695012414
0.337122644398882 0.162182308193243 0.794284540683907];

% Fit model to data.
[fitresult{4}, gof(4)] = fit( [xData, yData], zData, ft, opts );

% Plot fit with data.
figure( 'Name', 'System4' );
h = plot( fitresult{4}, [xData, yData], zData );
legend( h, 'System4', 'dV4 vs. Temp4, Time4', 'Location',
'NorthEast' );
% Label axes
xlabel Temp4
ylabel Time4
zlabel dV4
grid on
```